pcim ASIA *Hybrid Platform*

Modular Multilevel Converters Operating Principles and Applications

Prof. Drazen Dujic, Dr. Stefan Milovanovic
Power Electronics Laboratory
Ecole Polytechnique Fédérale de Lausanne

MODULAR MULTILEVEL CONVERTERS - OPERATING PRINCIPLES AND APPLICATIONS - PART 1

Prof. Dražen Dujić, Dr. Stefan Milovanović

École Polytechnique Fédérale de Lausanne (EPFL)
Power Electronics Laboratory (PEL)
Switzerland

TUTORIAL SCHEDULE

Before the virtual coffee break

Part 1) Introduction and motivation

- MMC Applications
- MMC operating principles
- Modeling and control

Part 2) MMC energy control

- Role of circulating currents
- Branch energy control methods
- Performance benchmark

After the virtual coffee break

Part 3) MMC power extension

- MMC scalability
- Branch paralleling
- Energy control

Part 4) MMC research platform

- MMC system level design
- MMC Sub-module development
- MMC RT-HIL development

INTRODUCTION

Non technical one...

Prof. Drazen Dujic

Experience:

2014 – today	École Polytechnique Fédérale de Lausanne (EPFL), Lausanne, Switzerland
2013 – 2014	ABB Medium Voltage Drives, Turgi, Switzerland
2009 – 2013	ABB Corporate Research, Baden-Dättwil, Switzerland
2006 – 2009	Liverpoool John Moores University, Liverpool, United Kingdom
2003 – 2006	University of Novi Sad, Novi Sad, Serbia

Education:

2008	PhD, Liverpoool John Moores University, Liverpool, United Kingdom
2005	M.Sc., University of Novi Sad, Novi Sad, Serbia
2002	Dipl. Ing., University of Novi Sad, Novi Sad, Serbia

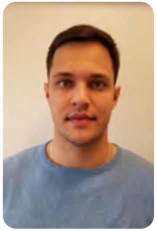

Dr. Stefan Milovanovic

Experience:

2020 – today	École Polytechnique Fédérale de Lausanne (EPFL), Lausanne, Switzerland

Education:

2020	PhD, École Polytechnique Fédérale de Lausanne (EPFL), Lausanne, Switzerland
2016	M.Sc., School of Electrical Engineering, University of Belgrade, Belgrade, Serbia

École Polytechnique Fédérale de Lausanne

School of Engineering

EPFL — STI — IEL — PEL

Institute of Electrical Engineering

- Active since February 2014
- Currently: 14 PhD students, 4 Post Docs, 1 Administrative Ass.
- Funding CH: SNSF, SFOE, Innosuisse
- Funding EU: H2020, S2R JU, ERC CoG
- Funding: Industry OEMs
- `www.epfl.ch/labs/pel/`

ECPE

Competence Centre

▲ Power Electronics Laboratory

PEL RESEARCH FOCUS

MVDC Technologies and Systems

- System Stability
- Protection Coordination
- Power Electronic Converters

MVDC
ENERGY CONVERSION TECHNOLOGIES AND SYSTEMS

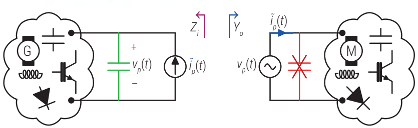

High Power Electronics

- Multilevel Converters
- Solid State Transformers
- Medium Frequency Conversion

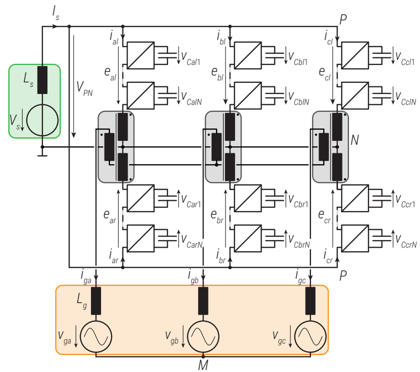

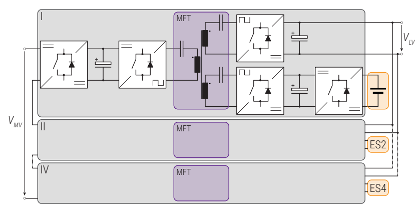

Components

- Semiconductor devices
- Magnetics
- Modeling, Characterization

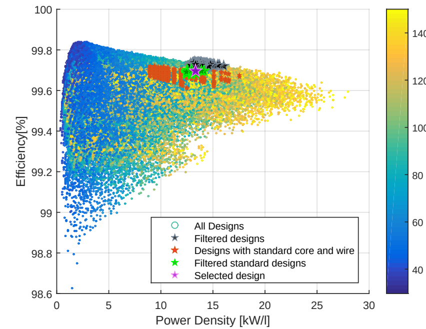

MMC APPLICATIONS

Examples of applications where MMC is already commercialized

HVDC

- Decoupled semiconductor switching frequency from converter apparent switching frequency
- Improved harmonic performance ⇒ less / no filters
- Series-connection of semiconductors still possible
- Fault blocking capability depending on cell type

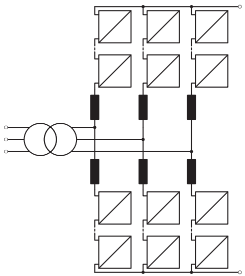

MV Variable Speed Drives

- Monolithic ML topologies (NPC, NPP, FC, ANPC) are not scalable
- Robicon drive ⟶ everyone offers it
- Siemens & Benshaw: MMC drive
- Low $\mathrm{d}v/\mathrm{d}t$ ⇒ motor friendly

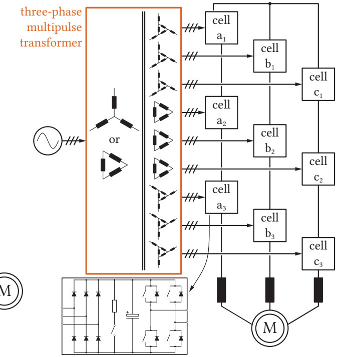

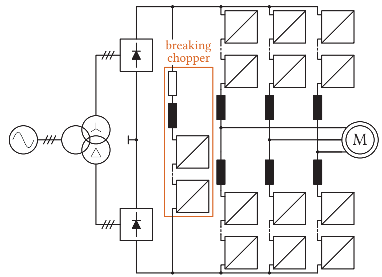

Solid State Transformers (SSTs)

- Power density increase w/ conversion & isolation at higher frequency
- Grid applications / traction transformer w/ different optimization objectives
- MFT design / isolation are the bottlenecks

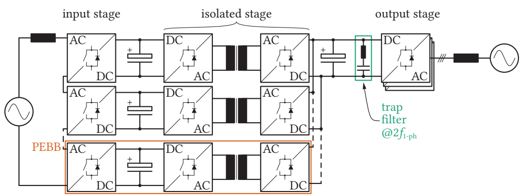

FACTS

- SFC for railway interties (direct catenary connection)
- STATCOM
- BESS (split batteries)

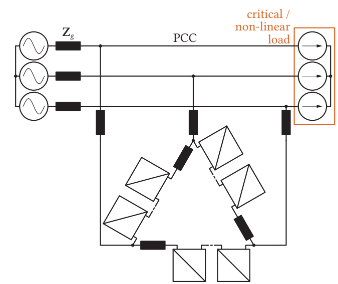

TREND TOWARDS HIGHLY MODULAR CONVERTER TOPOLOGIES

HVDC

- Decoupled semiconductor switching frequency from converter apparent switching frequency
- Improved harmonic performance ⇒ less / no filters
- Series-connection of semiconductors still possible
- Fault blocking capability depending on cell type

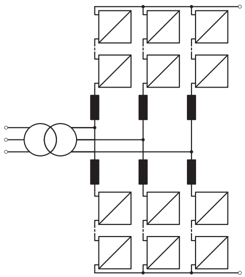

MV Variable Speed Drives

- Monolithic ML topologies (NPC, NPP, FC, ANPC) are not scalable
- Robicon drive ⟶ everyone offers it
- Siemens & Benshaw: MMC drive
- Low $\mathrm{d}v/\mathrm{d}t$ ⇒ motor friendly

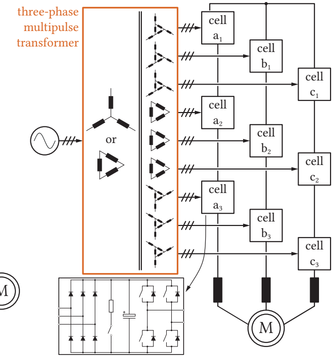

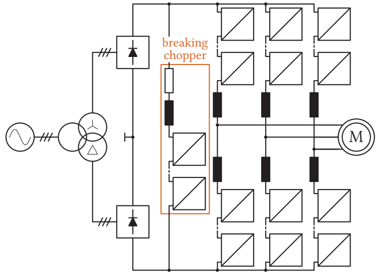

Solid State Transformers (SSTs)

- Power density increase w/ conversion & isolation at higher frequency
- Grid applications / traction transformer w/ different optimization objectives
- MFT design / isolation are the bottlenecks

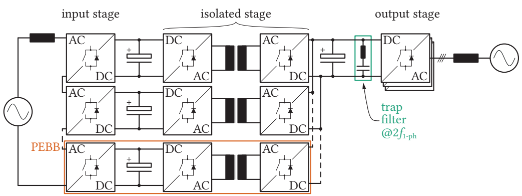

FACTS

- SFC for railway interties (direct catenary connection)
- STATCOM
- BESS (split batteries)

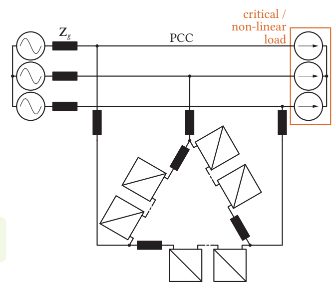

⇒ Modularity provides obvious benefits in high power applications!

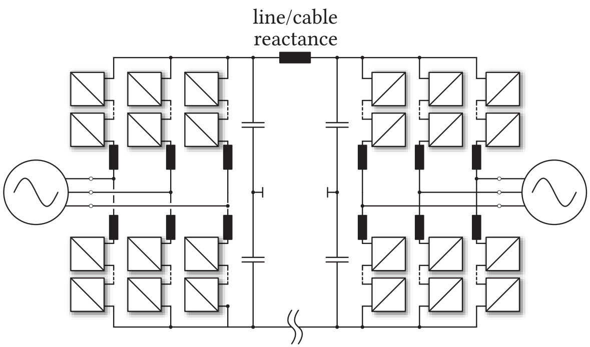

▲ MMC in HVDC (two substations at different locations)

- Modular design using basic sub-module
- Voltage scalability to very high voltage levels
- Low filtering needs on AC side
- Redundancy is easily implemented
- Half-bridge sub-modules are sufficient

▲ SIEMENS MMC-based HVDC PLUS

▲ ABB MMC-based HVDC LIGHT

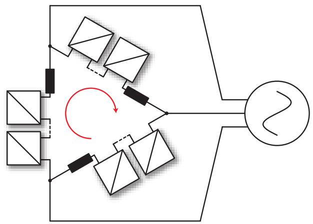

▲ MMC as STATCOM (Delta configuration is shown)

- Transformerless solution
- Double star MMC solution is also possible
- Modular
- Easy voltage scalability (no need for tranasformer)
- Redundancy is easily implemented
- Full-bridge sub-modules

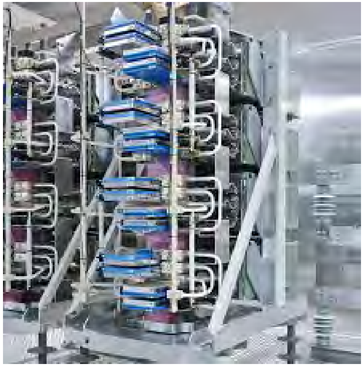

▲ ABB IGBT-based MMC STATCOM

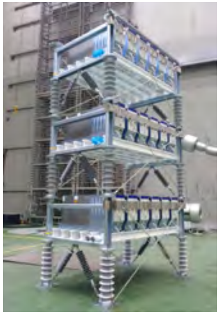

▲ HYOSUNG (left) and LS (right) IGBT-based MMC STATCOMs

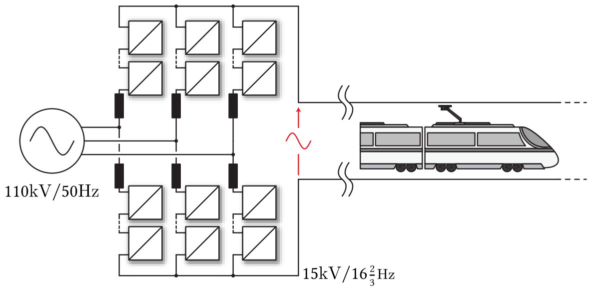

▲ MMC as SFC for Rail Interties (transformer not shown)

- $15kV, 16.7Hz$ or $25kV, 50Hz$ rail networks
- With or without transformer
- Fixed frequencies on both side
- Matrix alike principles of operation
- High efficiency
- Full-bridge sub-modules

▲ SIEMENS IGBT-based MMC for railway interties (SITRAS PLUS)

▲ ABB IGCT-based MMC for railway interties [1]

MMC FOR VARIABLE SPEED DRIVES

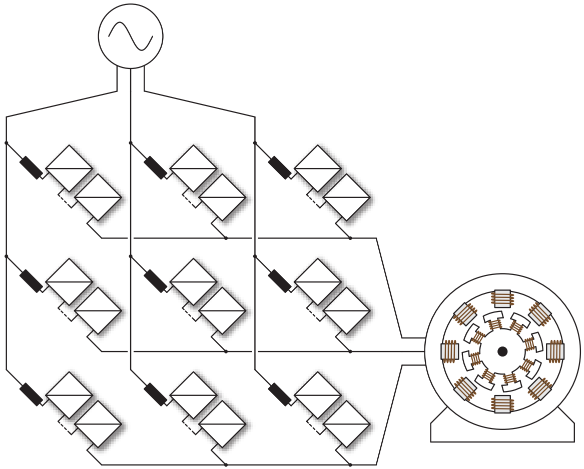

▲ Direct MMC for VSDs (e.g. hydro applications)

- Indirect-MMC: DC-fed MMC inverter (HB SM)
- Direct-MMC: AC-AC Matrix-alike converter (FB SM)
- Low-frequency operation was troublesome
- Power density is an issue
- Hydro applications based on DMMC

Figures: Courtesy of Siemens

▲ SIEMENS MMC VSD GH150

▲ ABB IGCT-based MMC for hydropower applications (one branch only) [2]

MODULAR MULTILEVEL CONVERTER

Modeling and basic operating principles...

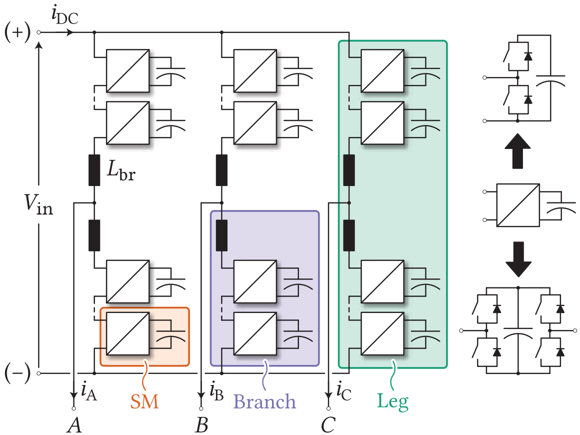

▲ Modular Multilevel Converter

- Stacking of SMs ⇒ reaching high voltage easily
- Semiconductor devices of lower voltage rating
- High-quality waveforms
- Low or almost none filtering requirements
- Redundancy and effortless scalability

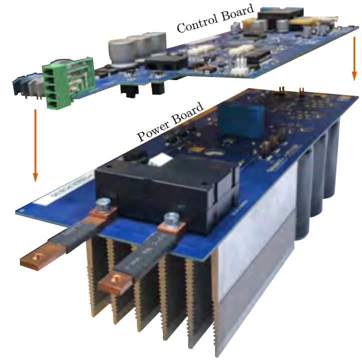

▲ SM developed in PEL

▲ MMC cabinet (hosting ±10kV, 0.5MW converter operating with 96 SMs)

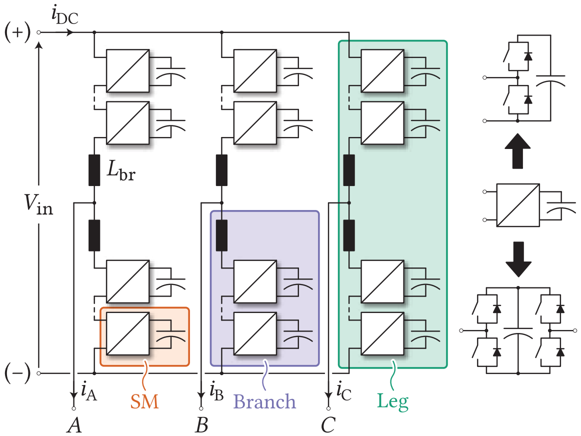

▲ Modular Multilevel Converter

- Stacking of SMs ⇒ reaching high voltage easily
- Semiconductor devices of lower voltage rating
- High-quality waveforms
- Low or almost none filtering requirements
- Redundancy and effortless scalability

⇒ Benefits at the expense of a high number of switching devices and complex control structure

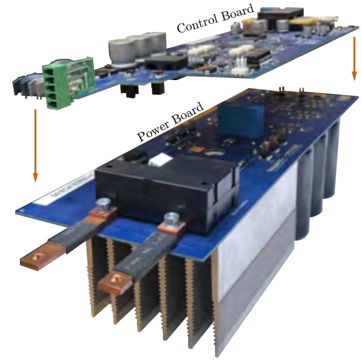

▲ SM developed in PEL

▲ MMC cabinet (hosting ± 10kV, 0.5MW converter operating with 96 SMs)

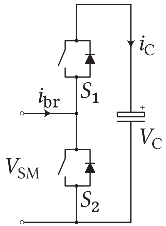

▲ HB SM

S_1	S_2	V_{SM}
1	0	V_C
0	1	0
0	0	$[1+\mathrm{sgn}(i_{br})]V_C/2$
1	1	forbidden

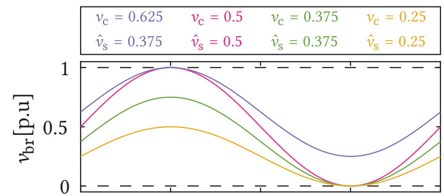

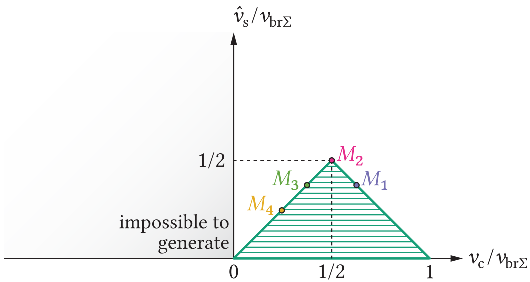

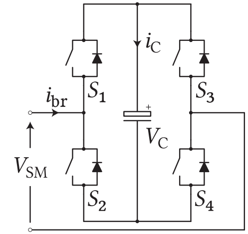

▲ FB SM

S_1	S_2	S_3	S_4	V_{SM}
0	0	0	0	$\mathrm{sgn}(i_{br})V_C$
1	0	0	1	V_C
0	1	1	0	$-V_C$
1	0	1	0	0
0	1	0	1	0
1	1	0	0	
0	0	1	1	forbidden
1	1	1	1	

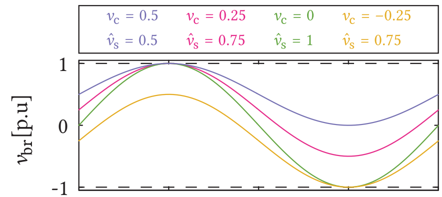

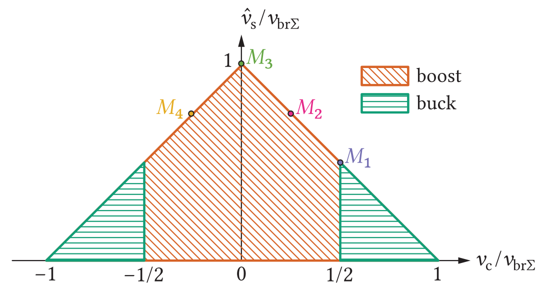

MMC BRANCH MODELING

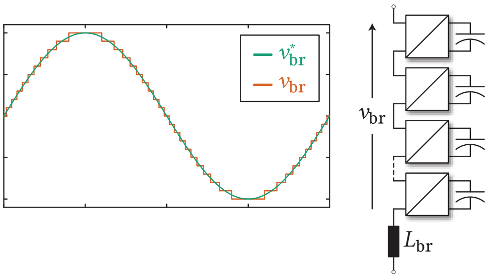

▲ MMC branch voltage example

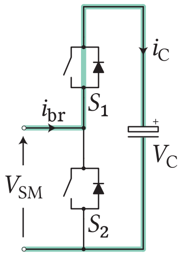

▲ Inserted HB SM ($n_{SM} = 1$)

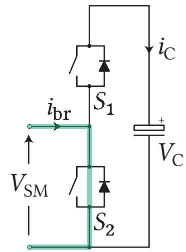

▲ Bypassed HB SM ($n_{SM} = 0$)

SM terminal voltages can be summed, leading to

$$v_{SM,i} = n_{SM} v_{C,i} \qquad \Big/ \sum_{i=1}^{N}$$

Assuming that $v_{C,i} = v_{br\Sigma}/N$ yields

$$v_{br} = \sum_{i=1}^{N} n_{SM} \frac{v_{br\Sigma}}{N} = \underbrace{\frac{\sum_{i=1}^{N} n_{SM}}{N}}_{\substack{\text{insertion index} \\ m(t)}} v_{br\Sigma}$$

Summing the equations set for every individual SM capacitor results in

$$C_{SM} \frac{\mathrm{d}v_{C,i}}{\mathrm{d}t} = n_{SM} i_{br} \qquad \Big/ \sum_{i=1}^{N}$$

$$\underbrace{\frac{C_{SM}}{N}}_{C_{br\Sigma}} \frac{\mathrm{d}v_{br\Sigma}}{\mathrm{d}t} = \underbrace{\frac{\sum_{i=1}^{N} n_{SM}}{N}}_{m(t)} i_{br}$$

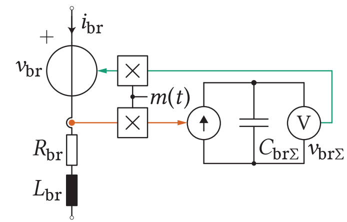

▲ Averaged model of an MMC branch

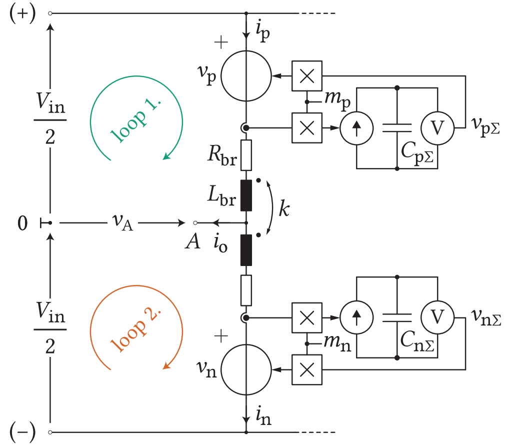

▲ The MMC leg sufficient for basic modeling

Two KVLs can be formed, yielding

$$\text{KVL}_1: \quad \frac{V_{in}}{2} = v_p + L_{br}\frac{di_p}{dt} + R_{br}i_p + kL_{br}\frac{di_n}{dt} + v_A$$

$$\text{KVL}_2: \quad \frac{V_{in}}{2} = v_n + L_{br}\frac{di_n}{dt} + R_{br}i_n + kL_{br}\frac{di_p}{dt} - v_A$$

KVL₁ − KVL₂:

$$(1-k)\frac{L_{br}}{2}\frac{d}{dt}\underbrace{\left(i_p - i_n\right)}_{i_o} + \frac{R_{br}}{2}(i_p - i_n) = \underbrace{\frac{v_n - v_p}{2}}_{v_s} - v_A$$

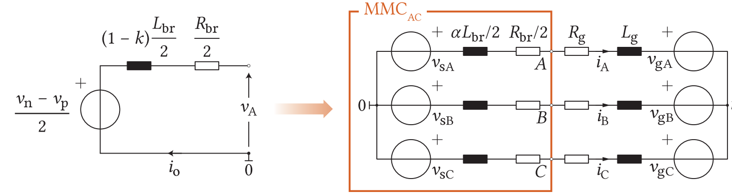

▲ AC equivalent circuit of the observed leg (left); Model of an MMC seen from its AC terminals (right);

KVL₁ + KVL₂:

$$2(1+k)L_{br}\frac{d}{dt}\underbrace{\left(\frac{i_p + i_n}{2}\right)}_{\substack{\text{common-mode} \\ \text{current } (i_c)}} + 2R_{br}\frac{i_p + i_n}{2} = V_{in} - \underbrace{(v_p + v_n)}_{2v_c}$$

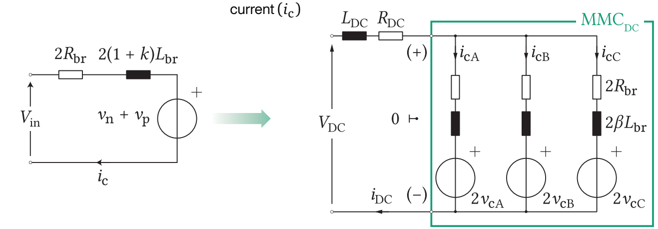

▲ DC equivalent circuit of the observed leg (left); Model of an MMC seen from its DC terminals (right);

Leg AC current ⇒ $i_o = i_p - i_n$

Leg common-mode current ⇒ $i_c = (i_p + i_n)/2$

$$\left.\begin{array}{l} i_o = i_p - i_n \\ i_c = (i_p + i_n)/2 \end{array}\right\} \quad \begin{array}{l} i_p = i_c + i_s/2 \\ i_n = i_c - i_s/2 \end{array}$$

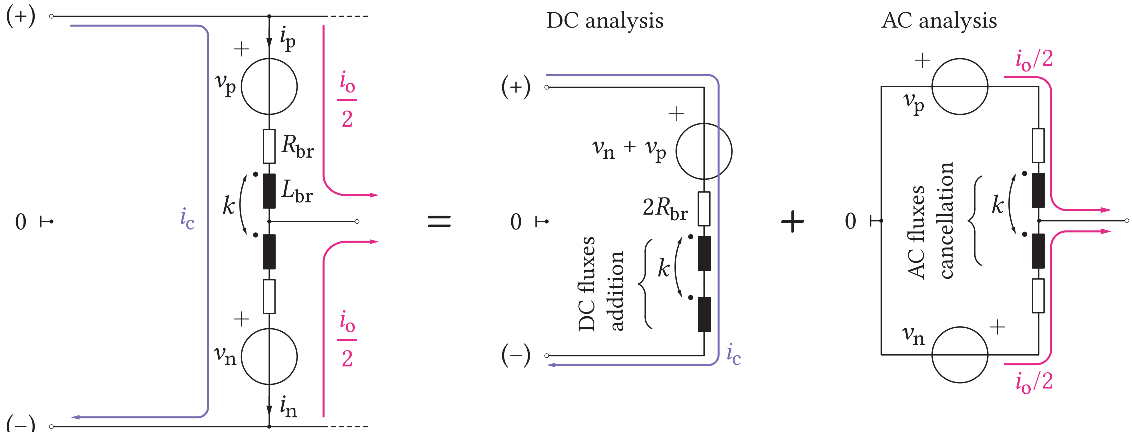

▲ Illustration of the MMC leg current components

⇒ Seen from the DC terminal, two branches operate in series, while the two operate in parallel when observed from the AC terminal

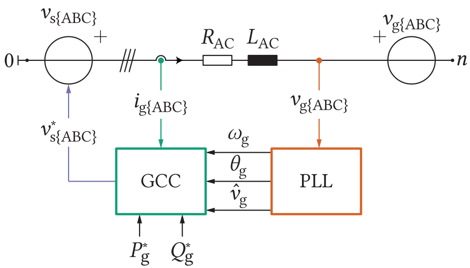

▲ MMC AC side equivalent

Requirements

- Perfect synchronization to the AC grid (PLL)

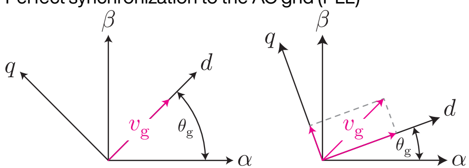

- Sufficiently high voltage reserve (total energy control)

Power control in the dq frame

$$P_g = \frac{3}{2}\left(v_{gd} i_{gd} + \underbrace{v_{gq} i_{gq}}_{=0}\right) = \frac{3}{2} v_{gd} i_{gd}$$

$$Q_g = \frac{3}{2}\left(\underbrace{v_{gq} i_{gd}}_{=0} - v_{gd} i_{gq}\right) = -\frac{3}{2} v_{gd} i_{gq}$$

dq transformation can be performed as

$$\begin{bmatrix} v_d \\ v_q \end{bmatrix} = \underbrace{\frac{2}{3}\begin{bmatrix} \cos(\theta_g) & \cos(\theta_g - 2\pi/3) & \cos(\theta_g - 4\pi/3) \\ -\sin(\theta_g) & -\sin(\theta_g - 2\pi/3) & -\sin(\theta_g - 4\pi/3) \end{bmatrix}}_{K} \begin{bmatrix} v_{gA} \\ v_{gB} \\ v_{gC} \end{bmatrix},$$

while the circuit from the left can be described with the following set of equations:

$$\begin{bmatrix} v_{sA} \\ v_{sB} \\ v_{sC} \end{bmatrix} = \begin{bmatrix} L_{AC} & 0 & 0 \\ 0 & L_{AC} & 0 \\ 0 & 0 & L_{AC} \end{bmatrix} \frac{d}{dt} \begin{bmatrix} i_{gA} \\ i_{gB} \\ i_{gC} \end{bmatrix} + \begin{bmatrix} R_{AC} & 0 & 0 \\ 0 & R_{AC} & 0 \\ 0 & 0 & R_{AC} \end{bmatrix} \begin{bmatrix} i_{gA} \\ i_{gB} \\ i_{gC} \end{bmatrix} + \begin{bmatrix} v_{gA} \\ v_{gB} \\ v_{gC} \end{bmatrix} + v_{n0} \begin{bmatrix} 1 \\ 1 \\ 1 \end{bmatrix},$$

where $L_{AC} = L_g + \alpha L_{br}/2$ and $R_{AC} = R_g + R_{br}/2$.

Multiplying both sides of the above expression with K, leads to

$$v_{sd} = L_{AC}\frac{di_{gd}}{dt} + R_{AC} i_{gd} - \underbrace{\omega_g L_{AC} i_{gq}}_{\text{cross-coupling}} + \underbrace{v_{gd}}_{=\hat{v}_g}$$

$$v_{sq} = L_{AC}\frac{di_{gq}}{dt} + R_{AC} i_{gq} + \underbrace{\omega_g L_{AC} i_{gd}}_{\text{cross-coupling}} + \underbrace{v_{gq}}_{=0}$$

⇒ To achieve decoupled control, cross-coupling terms should be removed

- dq quantities are essentially DC ⇒ PI controllers can be used
- The use feed-forward terms to avoid cross-coupling of the axes

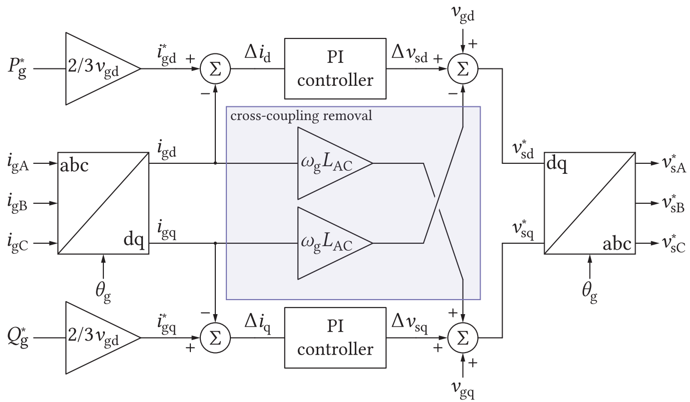

▲ MMC AC current control block diagram

From the control diagram on the left, one can conclude that

$$v_{sd}^* = \Delta v_{sd} + \underbrace{v_{gd} - \omega_g L_{AC} i_{gq}}_{\text{feed-forward}}$$

$$v_{sq}^* = \Delta v_{sq} + \underbrace{v_{gq} + \omega_g L_{AC} i_{gd}}_{\text{feed-forward}}$$

$$\Delta v_{sd} = H_{PI}(i_{gd}^* - i_{gd}) = L_{AC}\frac{di_{gd}}{dt} + R_{AC} i_{gd}$$

$$\Delta v_{sq} = H_{PI}(i_{gq}^* - i_{gq}) = L_{AC}\frac{di_{gq}}{dt} + R_{AC} i_{gq},$$

meaning that **decoupled control** of d and q currents is indeed obtained.

Obtaining the references in the ABC frame can be performed as

$$\begin{bmatrix} v_{sA}^* \\ v_{sB}^* \\ v_{sC}^* \end{bmatrix} = \begin{bmatrix} \cos(\theta_g) & \sin(\theta_g) \\ \cos(\theta_g - 2\pi/3) & \sin(\theta_g - 2\pi/3) \\ \cos(\theta_g + 2\pi/3) & \sin(\theta_g + 2\pi/3) \end{bmatrix} \begin{bmatrix} v_{sd}^* \\ v_{sq}^* \end{bmatrix}$$

AC TERMINAL CURRENT CONTROL (II)

- dq quantities are essentially DC $\Rightarrow$ PI controllers can be used
- The use feed-forward terms to avoid cross-coupling of the axes

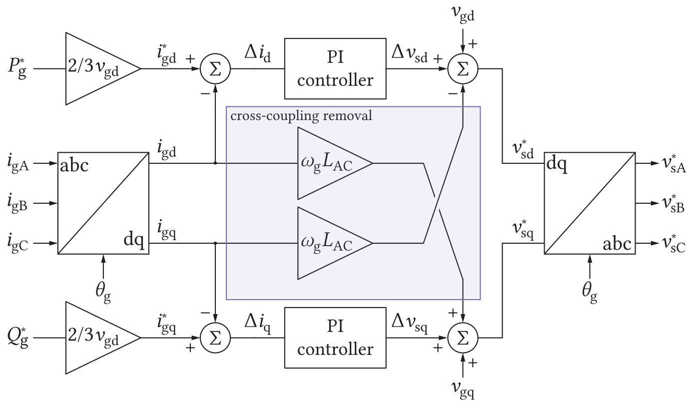

▲ MMC AC current control block diagram

From the control diagram on the left, one can conclude that

$$v_{sd}^* = \Delta v_{sd} + \underbrace{v_{gd} - \omega_g L_{AC} i_{gq}}_{\text{feed-forward}}$$

$$v_{sq}^* = \Delta v_{sq} + \underbrace{v_{gq} + \omega_g L_{AC} i_{gd}}_{\text{feed-forward}}$$

$$\Delta v_{sd} = H_{PI}(i_{gd}^* - i_{gd}) = L_{AC}\frac{di_{gd}}{dt} + R_{AC} i_{gd}$$

$$\Delta v_{sq} = H_{PI}(i_{gq}^* - i_{gq}) = L_{AC}\frac{di_{gq}}{dt} + R_{AC} i_{gq},$$

meaning that **decoupled control** of d and q currents is indeed obtained.

Obtaining the references in the ABC frame can be performed as

$$\begin{bmatrix} v_{sA}^* \\ v_{sB}^* \\ v_{sC}^* \end{bmatrix} = \begin{bmatrix} \cos(\theta_g) & \sin(\theta_g) \\ \cos(\theta_g - 2\pi/3) & \sin(\theta_g - 2\pi/3) \\ \cos(\theta_g + 2\pi/3) & \sin(\theta_g + 2\pi/3) \end{bmatrix} \begin{bmatrix} v_{sd}^* \\ v_{sq}^* \end{bmatrix}$$

⇒ From the AC current control standpoing, the MMC is not different to conventional 2LVL or other mutlilevel converters

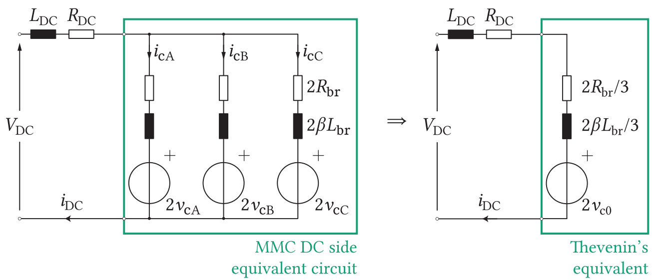

▲ MMC DC side equivalent

If the **inverter operation** is considered, then

$$L_{DC}^{\Sigma}\frac{di_{DC}}{dt}+R_{DC}^{\Sigma}i_{DC}=V_{DC}-2\underbrace{\frac{v_{cA}+v_{cB}+v_{cC}}{3}}_{v_{c0}},$$

where $L_{DC}^{\Sigma}=L_{DC}+2\beta L_{br}/3$ and $R_{DC}^{\Sigma}=R_{DC}+2\beta L_{br}/3$.

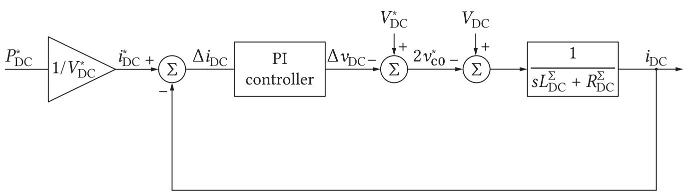

▲ MMC DC current control block diagram

Rectifier operation

- MMC represents a current source
- Some other stage is controlling the current

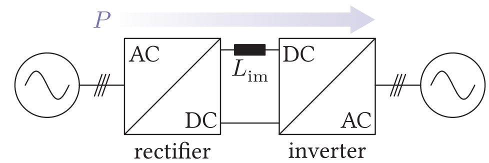

▲ Back-to-Back connection power converters

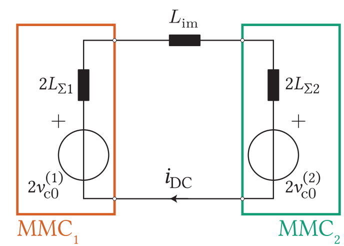

▲ Equivalent circuit describing two B2B connected converters

Control strategy

- MMC_2 controls its current (inverter mode)
- $MMC_1 \Rightarrow 2v_{c0}^{(1)}=V_{DC}^{*}$ followed the **energy control**

Observe the MMC DC equivalent circuit, such that $v_{c,i} = v_{c0}^*$

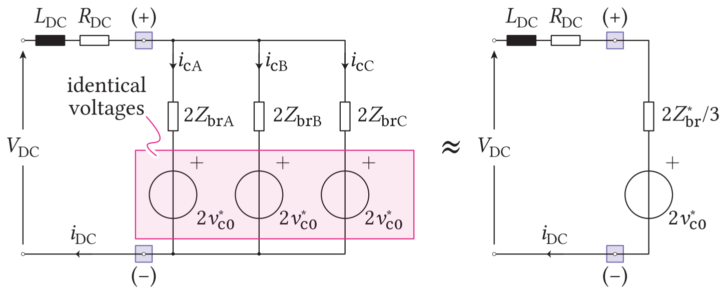

▲ DC equivalent circuit of a 3PH MMC in case $v_{c,i} = v_{c0}^*$

DC terminal current sharing!

$$Z_{brA} \neq Z_{brC} \neq Z_{brC} \Rightarrow i_{cA} \neq i_{cB} \neq i_{cC}$$

Ideally, $i_{c,i} = \frac{i_{DC}}{3}$, however, a more realistic approach implies

$$i_{c,i} = \frac{i_{DC}}{3} + i_{c\Delta,i},$$

where $i_{c,i}$ is referred to as the **circulating current** since

$$\begin{aligned} & i_{cA} + i_{cB} + i_{cC} = i_{DC} \\ \Rightarrow\ & i_{c\Delta A} + i_{c\Delta B} + i_{c\Delta C} = 0 \end{aligned}$$

In case $v_{c,i} = v_{c0}^* + v_{c\Delta,i}$, the circulating currents can be controlled. Without the loss of generality, take phase A as an example:

$$L_{br}\frac{d}{dt}\left(\frac{i_{DC}}{3}\right) + v_{c0}^* = L_{br}\frac{di_{cA}}{dt} + v_{c0}^* + v_{c\Delta A}$$

$$L_{br}\frac{d}{dt}\Big(\underbrace{i_{c\Delta A} - \frac{i_{DC}}{3}}_{i_{c\Delta A}}\Big) = -v_{c\Delta A}$$

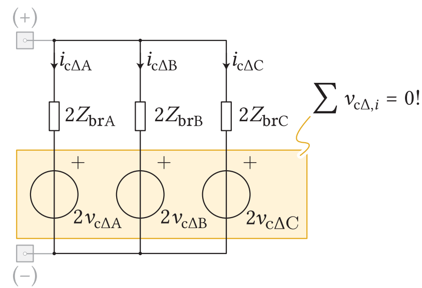

▲ The circuit relevant for circulating current control

$$v_{\pm} = 2v_{c0}^* + \frac{1}{3}\underbrace{\left\{v_{c\Delta A} + v_{c\Delta B} + v_{c\Delta C}\right\}}_{\text{must be equal to 0}}$$

THE CONCEPT OF CIRCULATING CURENTS

Observe the MMC DC equivalent circuit, such that $v_{c,i} = v_{c0}^*$

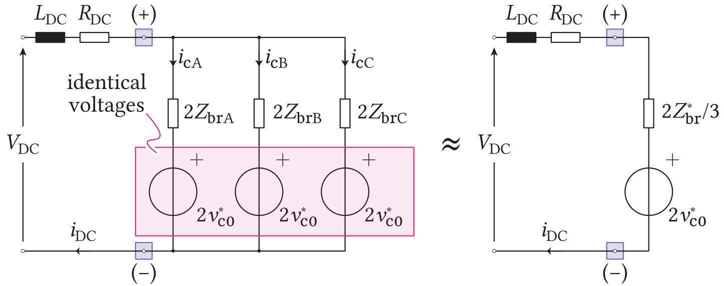

▲ DC equivalent circuit of a 3PH MMC in case $v_{c,i} = v_{c0}^*$

DC terminal current sharing!

$Z_{brA} \neq Z_{brC} \neq Z_{brC} \Rightarrow i_{cA} \neq i_{cB} \neq i_{cC}$

Ideally, $i_{c,i} = \frac{i_{DC}}{3}$, however, a more realistic approach implies

$$i_{c,i} = \frac{i_{DC}}{3} + i_{c\Delta,i},$$

where $i_{c,i}$ is referred to as the **circulating current** since

$$\begin{aligned} & i_{cA} + i_{cB} + i_{cC} = i_{DC} \\ \Rightarrow\ & i_{c\Delta A} + i_{c\Delta B} + i_{c\Delta C} = 0 \end{aligned}$$

In case $v_{c,i} = v_{c0}^* + v_{c\Delta,i}$, the circulating currents can be controlled. Without the loss of generality, take phase A as an example:

$$L_{br}\frac{d}{dt}\left(\frac{i_{DC}}{3}\right) + v_{c0}^* = L_{br}\frac{di_{cA}}{dt} + v_{c0}^* + v_{c\Delta A}$$

$$L_{br}\frac{d}{dt}\underbrace{\left(i_{c\Delta A} - \frac{i_{DC}}{3}\right)}_{i_{c\Delta A}} = -v_{c\Delta A}$$

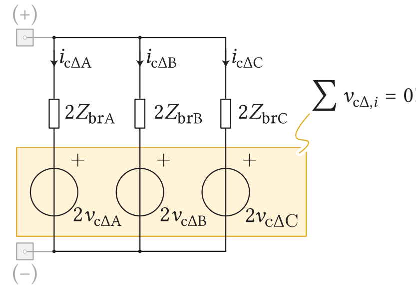

▲ The circuit relevant for circulating current control

$$v_{\pm} = 2v_{c0}^* + \frac{1}{3}\underbrace{\left\{v_{c\Delta A} + v_{c\Delta B} + v_{c\Delta C}\right\}}_{\text{must be equal to 0}}$$

Decoupled control of circulating currents

$$\textstyle\sum_{i=\{A,B,C\}} v_{c\Delta,i} = 0$$

CIRCULATING CURRENTS CONTROL

According to the previous slide

$$\beta L_{\mathrm{br}} \frac{\mathrm{d}i_{\mathrm{c}\Delta}}{\mathrm{d}t} = -v_{\mathrm{c}\Delta\mathrm{A}},$$

allowing for the derivation of control diagram from below.

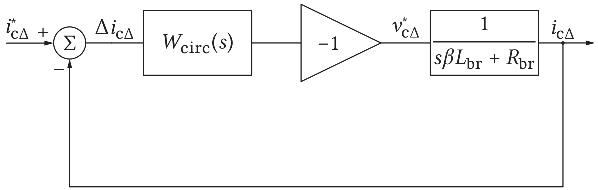

▲ A leg circulating current control block diagram

$$v^*_{\mathrm{c}\Delta\mathrm{A}} + v^*_{\mathrm{c}\Delta\mathrm{B}} + v^*_{\mathrm{c}\Delta\mathrm{C}} = -W_{\mathrm{circ}}(s)\left\{(i^*_{\mathrm{c}\Delta\mathrm{A}} + i^*_{\mathrm{c}\Delta\mathrm{B}} + i^*_{\mathrm{c}\Delta\mathrm{C}}) - \underbrace{(i_{\mathrm{c}\Delta\mathrm{A}} + i_{\mathrm{c}\Delta\mathrm{B}} + i_{\mathrm{c}\Delta\mathrm{C}})}_{=0 \text{ according to the definition}}\right\}$$

Decoupled control of circulating currents

The sum of circ. current references must be zero!

Other possible ways to control the circulating currents:

- $\alpha\beta$ domain (DC components)

$$\beta L_{\mathrm{br}} \frac{\mathrm{d}i^{(\alpha\beta)}_{\mathrm{c}\Delta}}{\mathrm{d}t} = -v^{(\alpha\beta)}_{\mathrm{c}\Delta}$$

- dq frame with positive and negative sequences (as will be seen shortly)

Two modes of operation:

1. Current source mode (also called inverter mode): transferring active power from the dc terminals to the ac terminals
2. Voltage source mode (also called rectifier mode): transferring active power from the ac terminals to the dc terminals

Two sets of state variables:

1. **External** state variables (dc-link voltage, grid currents, etc.): knowledge from VSC control is reused
2. **Internal** state variables (capacitor voltages, circulating currents): specific MMC control

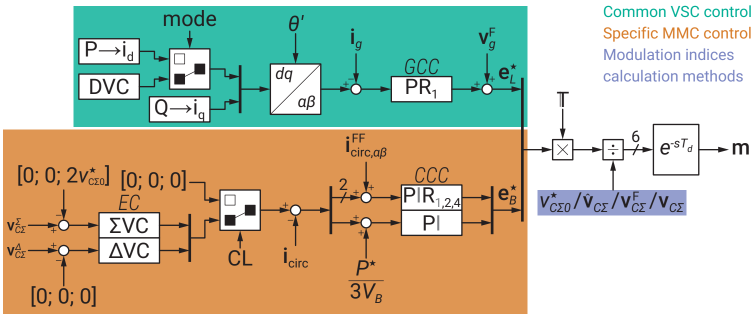

▲ Overall MMC control structure

MODULATION INDEX CALCULATION METHODS

Direct modulation

- The modulation indices are calculated from the *desired* dc average value
- The energy controllers **are disabled**
- The odd harmonics and integrator on dc component in the CCC **are disabled**
- Rely on self balancing of the branch energies [3]

$$m_p = \frac{V_B/2 - e_B^\star/2 - e_L^\star}{v_{C\Sigma 0}^\star}$$

$$m_n = \frac{V_B/2 - e_B^\star/2 + e_L^\star}{v_{C\Sigma 0}^\star}$$

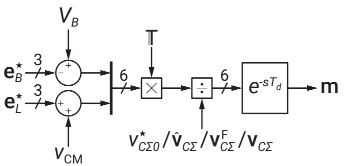

▲ Direct modulation principles

Closed-loop control

- The modulation indices are calculated from the *actual measurements* of the summed branch capacitors
- The energy controllers **are enabled**
- The odd harmonics in the CCC **are enabled**

Open-loop control

- The modulation indices are calculated from *estimates* of the summed branch capacitors in steady-state [4]
- The energy controllers **are disabled**
- The odd harmonics and integrator on dc component in the CCC **are disabled**
- Self energy balance achieved [5]

$$m_p = \frac{V_B/2 - e_B^\star/2 - e_L^\star}{\hat{v}_{C\Sigma p}}$$

$$m_n = \frac{V_B/2 - e_B^\star/2 + e_L^\star}{\hat{v}_{C\Sigma n}}$$

Hybrid voltage control

- The modulation indices are calculated from *filtered values* of the summed branch capacitors measurements
- The energy controllers **are disabled**
- The odd harmonics and integrator on dc component in the CCC **are disabled**
- Self energy balance achieved [6]

$$m_p = \frac{V_B/2 - e_B^\star/2 - e_L^\star}{v_{C\Sigma p}^F}$$

$$m_n = \frac{V_B/2 - e_B^\star/2 + e_L^\star}{v_{C\Sigma n}^F}$$

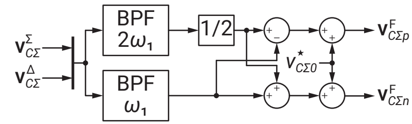

▲ Hybrid voltage control

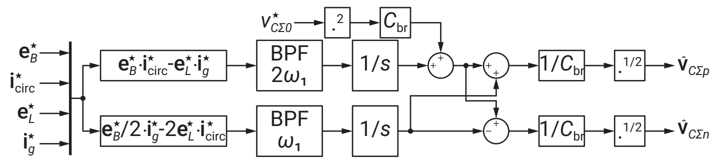

▲ Open-loop control

Branch level modulation

- Each branch handled separately

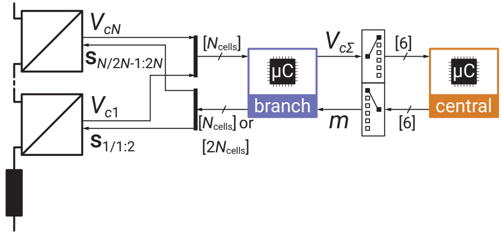

Cell level modulation

- Each cell has its own modulator

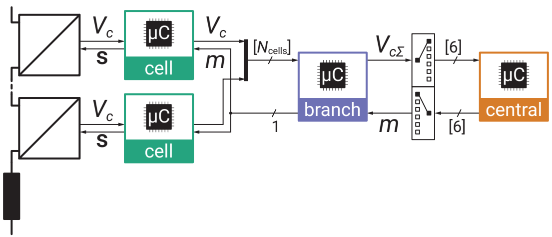

Phase-leg level modulation

- Aim at improving ac-side spectrum and unlocking full modulation method harmonic performance
- Compromises in the circulating current control
- SHE / OPP / SVM with $2N_{\text{cells}} + 1$ modulation

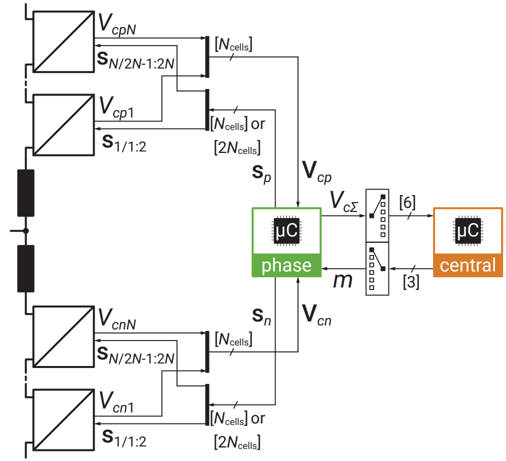

Remark µC denotes either a microcontroller, an FGPA, or a combination of both.

Modular Multilevel Converter

- Modular design easily scalable for higher voltages
- Flexible and adaptable for different conversion needs
- Efficient
- HVDC (early adopters)
- STATCOM, FACTS, RAIL INTERTIES, MV DRIVES
- Can serve MV and HV applications!
- Unlimited research opportunities...[7], [8]

▲ HVDC Light valve hall from ABB.

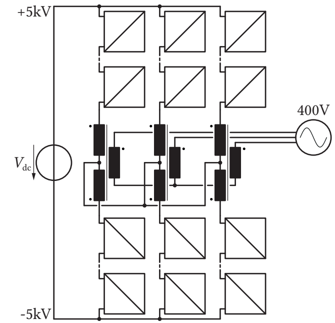

▲ Galvanically Isolated Modular Converter [7]

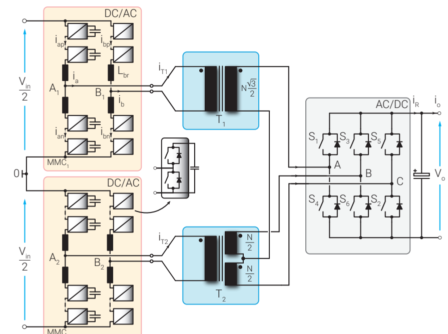

▲ High Power DC-DC Converter Employing Scott Transformer Connection [8]

BIBLIOGRAPHY

[1] D. Weiss et al. "IGCT based Modular Multilevel Converter for an AC-AC Rail Power Supply." *PCIM Europe 2017; International Exhibition and Conference for Power Electronics, Intelligent Motion, Renewable Energy and Energy Management*. 2017, pp. 1–8.

[2] M. Vasiladiotis et al. "IGCT-Based Direct AC/AC Modular Multilevel Converters for Pumped Hydro Storage Plants." *2018 IEEE Energy Conversion Congress and Exposition (ECCE)*. 2018, pp. 4837–4844.

[3] S. Cui et al. "Principles and dynamics of natural arm capacitor voltage balancing of a direct modulated modular multilevel converter." *2015 9th International Conference on Power Electronics and ECCE Asia (ICPE-ECCE Asia)*. June 2015, pp. 259–267.

[4] L. Angquist et al. "Open-Loop Control of Modular Multilevel Converters Using Estimation of Stored Energy." *IEEE Transactions on Industry Applications* 47.6 (Nov. 2011), pp. 2516–2524.

[5] A. Antonopoulos et al. "Global Asymptotic Stability of Modular Multilevel Converters." *IEEE Transactions on Industrial Electronics* 61.2 (Feb. 2014), pp. 603–612.

[6] L. Harnefors et al. "Global Asymptotic Stability of Current-Controlled Modular Multilevel Converters." *IEEE Transactions on Power Electronics* 30.1 (Jan. 2015), pp. 249–258.

[7] A. Christe and D. Dujic. "Galvanically isolated modular converter." *IET Power Electronics* 9.12 (2016), pp. 2318–2328.

[8] S. Milovanovic and D. Dujic. "MMC-Based High Power DC-DC Converter Employing Scott Transformer." *PCIM Europe 2018; International Exhibition and Conference for Power Electronics, Intelligent Motion, Renewable Energy and Energy Management*. June 2018, pp. 1–7.

pcim ASIA Hybrid Platform

Modular Multilevel Converters Operating Principles and Applications

Prof. Drazen Dujic, Dr. Stefan Milovanovic
Power Electronics Laboratory
Ecole Polytechnique Fédérale de Lausanne

MODULAR MULTILEVEL CONVERTERS - OPERATING PRINCIPLES AND APPLICATIONS - PART 2

Prof. Dražen Dujić, Dr. Stefan Milovanović

École Polytechnique Fédérale de Lausanne (EPFL)
Power Electronics Laboratory (PEL)
Switzerland

Before the virtual coffee break

Part 1) Introduction and motivation

- MMC Applications
- MMC operating principles
- Modeling and control

Part 2) MMC energy control

- Role of circulating currents
- Branch energy control methods
- Performance benchmark

After the virtual coffee break

Part 3) MMC power extension

- MMC scalability
- Branch paralleling
- Energy control

Part 4) MMC research platform

- MMC system level design
- MMC Sub-module development
- MMC RT-HIL development

CONTROL OF THE MMC INTERNAL ENERGY

Different methods, properties, comparison...

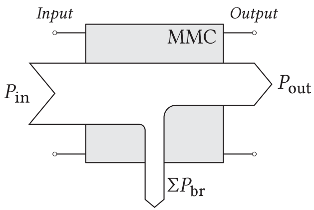

▲ MMC energy flow

Total energy control:

- Inverter ⇒ DC side
- Rectifier ⇒ AC side

? Is total energy control sufficient?

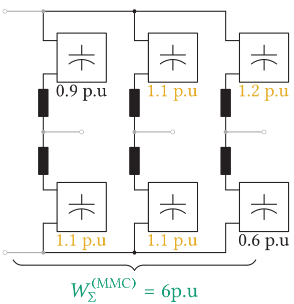

▲ Illustration of the need for additional energy ctrl.

Branch power analysis is conducted on the leg level [1], [2], [3], [4].

$$P_{\mathrm{p}} = \frac{\mathrm{d}W_{\mathrm{p}}}{\mathrm{d}t} = v_{\mathrm{p}} i_{\mathrm{p}} = \left(v_{\mathrm{c}} - v_{\mathrm{s}}\right)\left(i_{\mathrm{c}} + \frac{i_{\mathrm{o}}}{2}\right)$$

$$P_{\mathrm{n}} = \frac{\mathrm{d}W_{\mathrm{n}}}{\mathrm{d}t} = v_{\mathrm{n}} i_{\mathrm{n}} = \left(v_{\mathrm{c}} + v_{\mathrm{s}}\right)\left(i_{\mathrm{c}} - \frac{i_{\mathrm{o}}}{2}\right)$$

Coordinate transformation is performed as

$$\left.\begin{aligned} W_{\Sigma} &= W_{\mathrm{p}} + W_{\mathrm{n}} \\ W_{\Delta} &= W_{\mathrm{p}} - W_{\mathrm{n}} \end{aligned}\right\} \qquad \begin{aligned} \frac{\mathrm{d}W_{\Sigma}}{\mathrm{d}t} &= 2v_{\mathrm{c}} i_{\mathrm{c}} - v_{\mathrm{o}} i_{\mathrm{o}} = \left(v_{\mathrm{c0}} + v_{\mathrm{c}\Delta} - v_{\mathrm{s}}\right)\left(\frac{i_{\mathrm{DC}}}{3} + i_{\mathrm{c}\Delta} + \frac{i_{\mathrm{o}}}{2}\right) \\ \frac{\mathrm{d}W_{\Delta}}{\mathrm{d}t} &= v_{\mathrm{c}} i_{\mathrm{o}} - 2v_{\mathrm{s}} i_{\mathrm{c}} = \left(v_{\mathrm{c0}} + v_{\mathrm{c}\Delta} + v_{\mathrm{s}}\right)\left(\frac{i_{\mathrm{DC}}}{3} + i_{\mathrm{c}\Delta} - \frac{i_{\mathrm{o}}}{2}\right) \end{aligned}$$

Assuming that no circulating currents are generated, while $v_{\mathrm{s}} = \hat{v}_{\mathrm{s}} \cos\left(\omega_g t - \gamma\right)$ and $i_{\mathrm{o}} = \hat{i}_{\mathrm{o}} \cos\left(\omega_g t - \delta\right)$ yields

$$\left.\frac{\mathrm{d}W_{\Sigma}}{\mathrm{d}t}\right|_{\text{no circ.}} = 2v_{\mathrm{c0}} \frac{i_{\mathrm{DC}}}{3} - v_{\mathrm{s}} i_{\mathrm{o}} \approx \underbrace{V_{\mathrm{DC}} \frac{i_{\mathrm{DC}}}{3} - \frac{\hat{v}_{\mathrm{s}} \hat{i}_{\mathrm{o}}}{2} \cos(\gamma - \delta)}_{=0} - \underbrace{\frac{\hat{v}_{\mathrm{s}} \hat{i}_{\mathrm{o}}}{2} \cos\left(2\omega_g t - \gamma - \delta\right)}_{\text{oscillating @}2\omega_g}$$

$$\left.\frac{\mathrm{d}W_{\Delta}}{\mathrm{d}t}\right|_{\text{no circ.}} = \underbrace{-2\hat{v}_{\mathrm{s}} \frac{i_{\mathrm{DC}}}{3} \cos\left(\omega_g t - \gamma\right) + \hat{i}_{\mathrm{o}} v_{\mathrm{c0}} \cos\left(\omega_g t - \delta\right)}_{\text{oscillating @}1\omega_g}$$

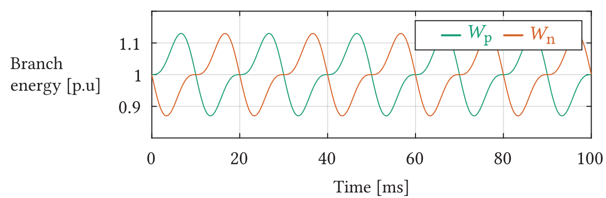

▲ Steady state appearance of the upper and lower branch energies normalized with respect to the branch mean energy.

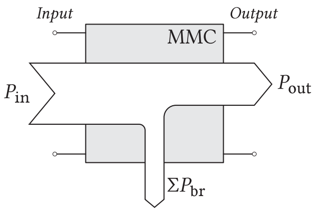

▲ MMC energy flow

Total energy control:

- Inverter ⇒ DC side
- Rectifier ⇒ AC side

? Is total energy control sufficient?

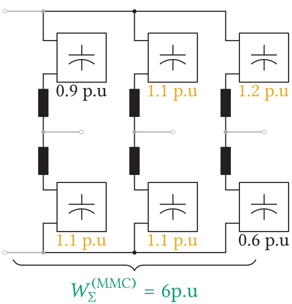

▲ Illustration of the need for additional energy ctrl.

Branch power analysis is conducted on the leg level [1], [2], [3], [4].

$$P_{\mathrm{p}} = \frac{\mathrm{d}W_{\mathrm{p}}}{\mathrm{d}t} = v_{\mathrm{p}} i_{\mathrm{p}} = \left(v_{\mathrm{c}} - v_{\mathrm{s}}\right)\left(i_{\mathrm{c}} + \frac{i_{\mathrm{o}}}{2}\right)$$

$$P_{\mathrm{n}} = \frac{\mathrm{d}W_{\mathrm{n}}}{\mathrm{d}t} = v_{\mathrm{n}} i_{\mathrm{n}} = \left(v_{\mathrm{c}} + v_{\mathrm{s}}\right)\left(i_{\mathrm{c}} - \frac{i_{\mathrm{o}}}{2}\right)$$

Coordinate transformation is performed as

$$\left.\begin{aligned} W_{\Sigma} &= W_{\mathrm{p}} + W_{\mathrm{n}} \\ W_{\Delta} &= W_{\mathrm{p}} - W_{\mathrm{n}} \end{aligned}\right\}$$

$$\frac{\mathrm{d}W_{\Sigma}}{\mathrm{d}t} = 2 v_{\mathrm{c}} i_{\mathrm{c}} - v_{\mathrm{o}} i_{\mathrm{o}} = \left(v_{\mathrm{c}0} + v_{\mathrm{c}\Delta} - v_{\mathrm{s}}\right)\left(\frac{i_{\mathrm{DC}}}{3} + i_{\mathrm{c}\Delta} + \frac{i_{\mathrm{o}}}{2}\right)$$

$$\frac{\mathrm{d}W_{\Delta}}{\mathrm{d}t} = v_{\mathrm{c}} i_{\mathrm{o}} - 2 v_{\mathrm{s}} i_{\mathrm{c}} = \left(v_{\mathrm{c}0} + v_{\mathrm{c}\Delta} + v_{\mathrm{s}}\right)\left(\frac{i_{\mathrm{DC}}}{3} + i_{\mathrm{c}\Delta} - \frac{i_{\mathrm{o}}}{2}\right)$$

Assuming that no circulating currents are ge[...] $v_{\mathrm{s}} = \hat{v}_{\mathrm{s}} \cos\left(\omega_g t - \gamma\right)$ and $i_{\mathrm{o}} = \hat{i}_{\mathrm{o}} \cos\left(\omega_g t - \delta\right)$ yields

$$\left.\frac{\mathrm{d}W_{\Sigma}}{\mathrm{d}t}\right|_{\text{no circ.}} = [\dots]\frac{}{3} - v_{\mathrm{s}} i_{\mathrm{o}} \approx \underbrace{V_{\mathrm{DC}} \frac{i_{\mathrm{DC}}}{3} - \frac{\hat{v}_{\mathrm{s}} \hat{i}_{\mathrm{o}}}{2} \cos(\gamma - \delta)}_{=0} - \underbrace{\frac{\hat{v}_{\mathrm{s}} \hat{i}_{\mathrm{o}}}{2} \cos\left(2\omega_g t - \gamma - \delta\right)}_{\text{oscillating } @2\omega_g}$$

$$\left.\frac{\mathrm{d}W_{\Delta}}{\mathrm{d}t}\right|_{\text{no circ.}} = \underbrace{-2\hat{v}_{\mathrm{s}} \frac{i_{\mathrm{DC}}}{3} \cos\left(\omega_g t - \gamma\right) + \hat{i}_{\mathrm{o}} v_{\mathrm{c}0} \cos\left(\omega_g t - \delta\right)}_{\text{oscillating } @1\omega_g}$$

⚡ In reality, additinal energy controllers are needed

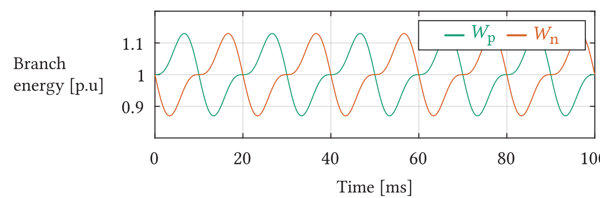

▲ Steady state appearance of the upper and lower branch energies normalized with respect to the branch mean energy.

- Circulating currents can be used to maintain the internal energy balance
- Average values of energies are the only ones of interest

The leg common-mode current can be expressed as

$$i_c = \frac{i_{DC}}{3} + \underbrace{I_{c\Delta}}_{\text{circ. DC}} + \underbrace{\hat{i}^{\sim}_{c\Delta}\cos(\omega_g t - \zeta)}_{\text{circ. AC}},$$

which further leads to

$$\frac{d\overline{W_\Sigma}}{dt} \approx V_{DC} I_{c\Delta} + \underbrace{V_{DC}\frac{i_{DC}}{3} - \frac{\hat{v}_s \hat{i}_o}{2}\cos(\gamma - \delta)}_{=0} + \underbrace{\overline{2v_{c\Delta}\frac{i_{DC}}{3}} + \overline{2v_{c\Delta} i_{c\Delta}}}_{\text{negligible}}$$

$$\frac{d\overline{W_\Delta}}{dt} \approx -\hat{v}_s \hat{i}^{\sim}_{c\Delta}\cos(\gamma - \zeta) + \underbrace{\overline{v_{c\Delta} i_o}}_{\text{negligible}}.$$

If $\gamma = \zeta$ meaning that circ. current AC component is in phase with the leg AC voltage, then

$$\frac{d\overline{W_\Sigma}}{dt} \approx V_{DC} I_{c\Delta}$$
$$\frac{d\overline{W_\Delta}}{dt} \approx -\hat{v}_s \hat{i}^{\sim}_{c\Delta}$$

Two balancing directions can be identified

- **Horizontal direction** (total energy stored in the leg)
- **Vertical direction** (difference of branch energies)

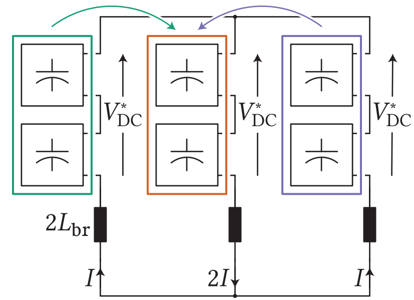

▲ Illustration of the horiz. balancing principle

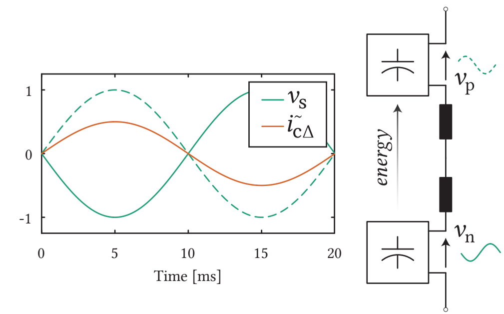

▲ Illustration of the vert. balancing principle

THE BRANCH ENERGY CONTROL (II)

- Circulating currents can be used to maintain the internal energy balance
- Average values of energies are the only ones of interest

The leg common-mode current can be expressed as

$$i_c = \frac{i_{DC}}{3} + \underbrace{I_{c\Delta}}_{\text{circ. DC}} + \underbrace{\hat{i}^{\sim}_{c\Delta}\cos(\omega_g t - \zeta)}_{\text{circ. AC}},$$

which further leads to

$$\frac{d\overline{W_\Sigma}}{dt} \approx V_{DC} I_{c\Delta} + \underbrace{V_{DC}\frac{i_{DC}}{3} - \frac{\hat{v}_s \hat{i}_o}{2}\cos(\gamma - \delta)}_{=0} + \underbrace{\overline{2v_{c\Delta}\frac{i_{DC}}{3}} + \overline{2v_{c\Delta} i_{c\Delta}}}_{\text{negligible}}$$

$$\frac{d\overline{W_\Delta}}{dt} \approx -\hat{v}_s \hat{i}^{\sim}_{c\Delta}\cos(\gamma - \zeta) + \underbrace{\overline{v_{c\Delta} i_o}}_{\text{negligible}}.$$

If $\gamma = \zeta$ meaning that circ. current AC compo... with the leg AC voltage, then

⇒ Circulating currents can be effectively used to obtain the branch energy balance

$$\frac{d\overline{W_\Sigma}}{dt} \approx V_{DC} I_{c\Delta}$$

$$\frac{d\overline{W_\Delta}}{dt} \approx -\hat{v}_s \hat{i}^{\sim}_{c\Delta}$$

Two balancing directions can be identified

- **Horizontal direction** (total energy stored in the leg)
- **Vertical direction** (difference of branch energies)

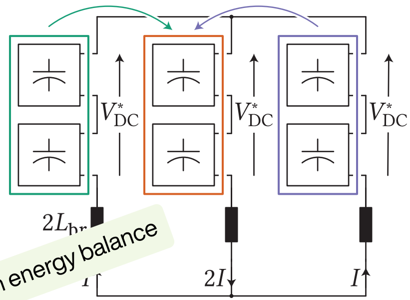

▲ Illustration of the horiz. balancing principle

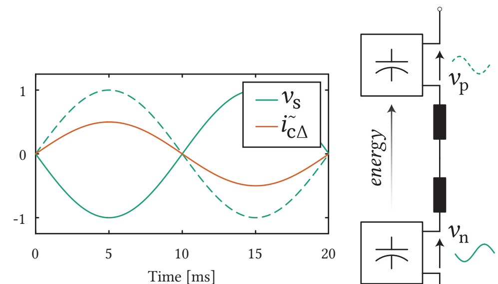

▲ Illustration of the vert. balancing principle

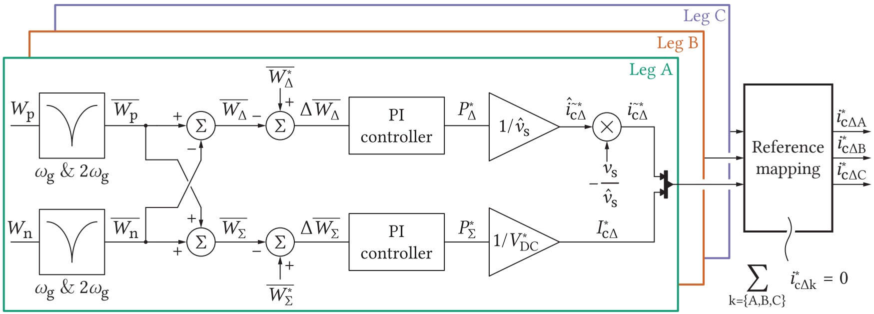

▲ Control block diagram of the MMC energy balancing [4]

An important detail

$\sum \Delta v_{c,i}^* = 0$ must hold at all times!

In other words, an appropriate circulating current reference mapping must be performed, otherwise, the DC link current control becomes influenced by the branch energy balancing.

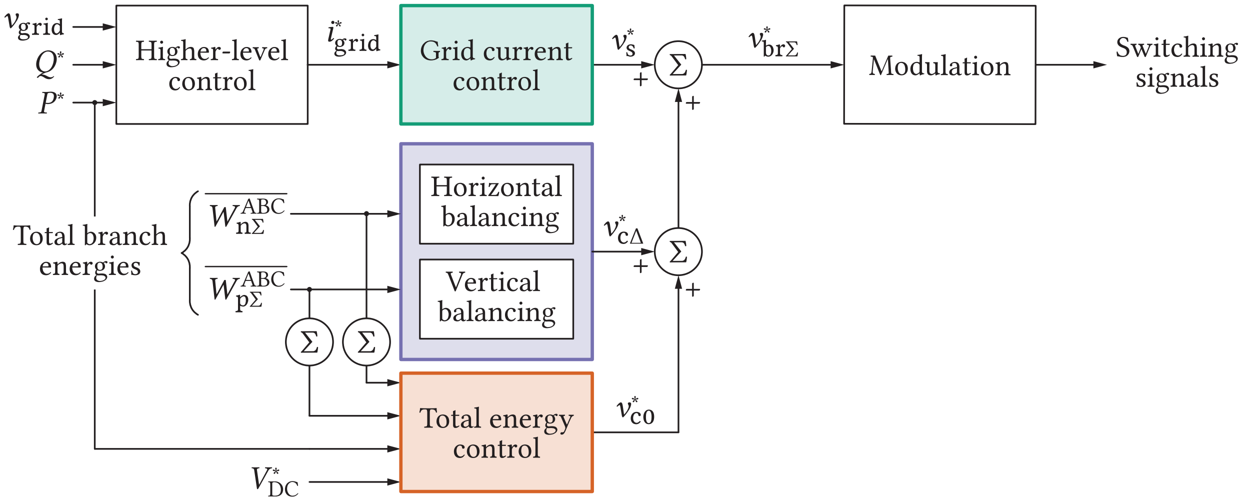

⇒ Suitable choice of variables leads to a complete decoupling among the control layers

COMPARISON OF DIFFERENT ENERGY BALANCING METHODS

What are the approaches reported so far and what do they have in common?

	Method 1 [2]	Method 2 [5]	Method 3 [6]
Horizontal balancing	SVD-based approach	Circ. currents ctrl. in the $\alpha\beta$- domain	Circ. currents ctrl. in the $\alpha\beta$- domain
Vertical balancing	SVD-based approach	Injection of reactive components into circ. currents	Circ. currents +/— sequence control

Important considerations:

- Leg energy balancing is initially done in "per leg" fashion
- Energy unbalances can take any arbitrary values

$\Rightarrow$ The expression $\sum_{i=\{A,B,C\}} i^*_{c\Delta,i} = 0$ **is not necessarily true!**

For the moment, observe an exemplary 1PH MMC, where

$$i^*_{c\Delta A} + i^*_{c\Delta B} \neq 0$$

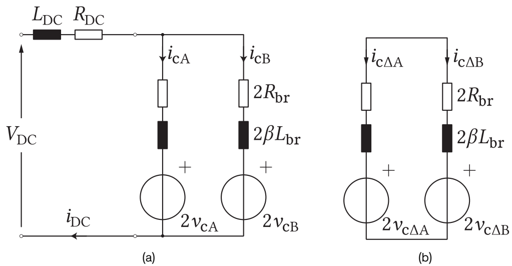

▲ Equivalent circuit of a 1PH-MMC seen from the DC terminals

- Vector notation

$$I^* = \begin{bmatrix} i^*_{c\Delta A} \\ i^*_{c\Delta B} \end{bmatrix}$$

In the observed case, the mathematical formulation of the problem can be expressed as

$$\underbrace{\begin{bmatrix} 1 & 1 \end{bmatrix}}_{T_i} \underbrace{\begin{bmatrix} i^*_{c\Delta A} \\ i^*_{c\Delta B} \end{bmatrix}}_{I_M} = 0$$

All the vectors I_M, satisfying the above requirement, reside in the null-space (kernel) of matrix T_i.

Two core steps:

- Identify the null-space of T_i
- Project the vector I^* onto the $\ker(T_i)$ to obtain I_M

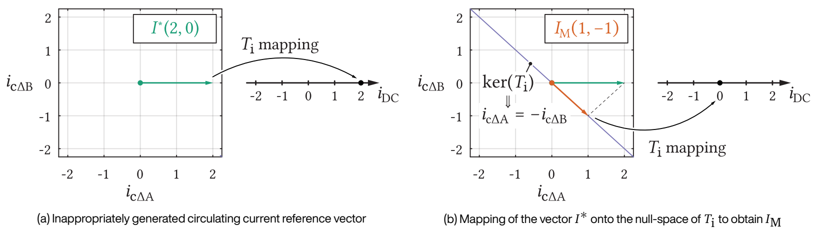

(a) Inappropriately generated circulating current reference vector

(b) Mapping of the vector I^* onto the null-space of T_i to obtain I_M

▲ Circulating current reference mapping procedure

REFERENCE MAPPING AND THE NULL-SPACE CONCEPT (I)

Important considerations:

- Leg energy balancing is initially done in "per leg" fashion
- Energy unbalances can take any arbitrary values

$\Rightarrow$ The expression $\sum_{i=\{A,B,C\}} i^*_{c\Delta,i} = 0$ **is not necessarily true!**

For the moment, observe an exemplary 1PH MMC, where

$$i^*_{c\Delta A} + i^*_{c\Delta B} \neq 0$$

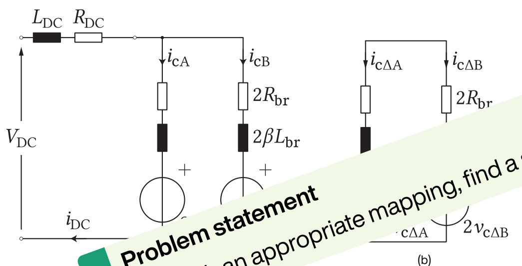

▲ Equivalent ... seen from the DC terminals

- Vector notation

$$I^* = \begin{bmatrix} i^*_{c\Delta A} \\ i^*_{c\Delta B} \end{bmatrix}$$

Problem statement

$\Rightarrow$ Through an appropriate mapping, find a suitable vector I_M such that the sum of its column elements equals zero

In the observed case, the mathematical formulation of the problem can be expressed as

$$\underbrace{\begin{bmatrix} 1 & 1 \end{bmatrix}}_{T_i} \underbrace{\begin{bmatrix} i^*_{c\Delta A} \\ i^*_{c\Delta B} \end{bmatrix}}_{I_M} = 0$$

All the vectors I_M, satisfying the above requirement, reside in the null-space ... matrix T_i.

Two core steps:

- Identify the null-space of T_i
- Project the vector I^* onto th...

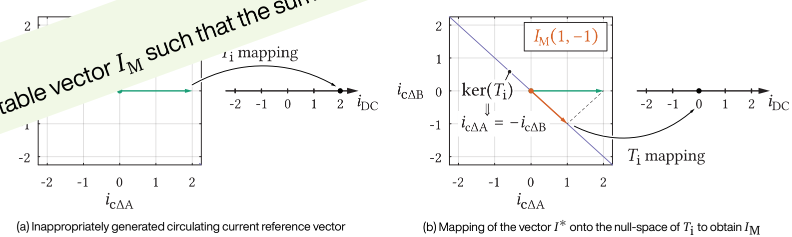

(a) Inappropriately generated circulating current reference vector

(b) Mapping of the vector I^* onto the null-space of T_i to obtain I_M

▲ Circulating current reference mapping procedure

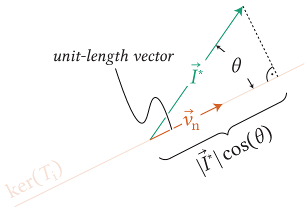

▲ Illustration of the reference maping procedure (2-D problem)

- Vector v_N is referred to as the null-space basis
- Scalar product $\Rightarrow$ projection

In the observed case, it is easy to identify the basis of $\ker(T_i)$ as

$$v_N = \frac{1}{\sqrt{2}}\begin{bmatrix}1\\-1\end{bmatrix}$$

Subsequently, projection of I^* onto $\ker(T_i)$ is obtained as

$$|I_M| = v_N^T I^* = \frac{1}{\sqrt{2}}\begin{bmatrix}1 & -1\end{bmatrix}\begin{bmatrix}2\\0\end{bmatrix} = \sqrt{2}$$

In the final step, assign the direction to the calculated projection

$$I_M = v_N \underbrace{v_N^T I^*}_{|I_M|} = \begin{bmatrix}1\\-1\end{bmatrix}$$

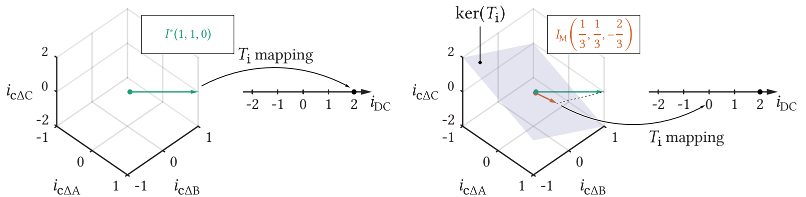

(a) Inappropriately generated circulating current reference vector

(b) Mapping of the vector I^* onto the null-space of T_i to obtain I_M

▲ Illustration of the reference maping procedure (3-D problem)

For the 3PH-MMC, the mapping matrix is $T_i = \begin{bmatrix}1 & 1 & 1\end{bmatrix}$ and $\ker(T_i)$ is a plane.

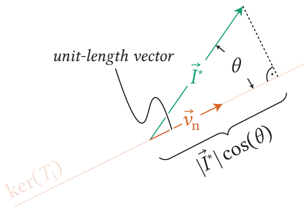

▲ Illustration of the reference maping procedure (2-D problem)

- Vector v_N is referred to as the null-space basis
- Scalar product ⇒ projection

In the observed case, it is easy to identify the basis of $\ker(T_i)$ as

$$v_N = \frac{1}{\sqrt{2}}\begin{bmatrix}1\\-1\end{bmatrix}$$

Subsequently, projection of I^* onto $\ker(T_i)$ is obtained as

$$|I_M| = v_N^T I^* = \frac{1}{\sqrt{2}}\begin{bmatrix}1 & -1\end{bmatrix}\begin{bmatrix}2\\0\end{bmatrix} = \sqrt{2}$$

In the final step, assign the direction to the calculated projection

$$I_M = v_N \underbrace{v_N^T I^*}_{|I_M|} = \begin{bmatrix}1\\-1\end{bmatrix}$$

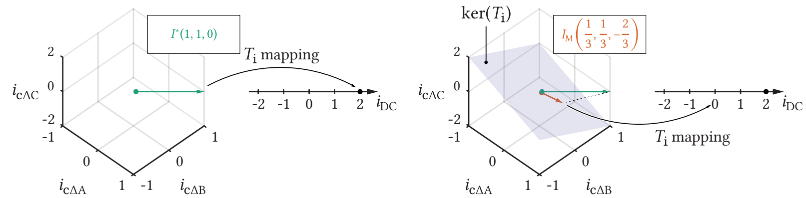

(a) Inappropriately generated circulating current reference vector

(b) Mapping of the vector I^* onto the null-space of T_i to obtain I_M

▲ Illustration of the reference maping procedure (3-D problem)

For the 3PH-MMC, the mapping matrix is $T_i = \begin{bmatrix}1 & 1 & 1\end{bmatrix}$ and $\ker(T_i)$ is a plane.

⇒ **Observation**

If T_i is a $1 \times q$ matrix, where q is the number of MMC phase legs, then $\dim(\ker(T_i)) = q - 1$.

However, it is reasonably to wonder

? How to generalize the reference mapping procedure?

SINGULAR VALUE DECOMPOSITION

- Descriptions in [7], [8]
- Diagonalization of a **non-square** matrix as

$$T_\mathrm{i} = \underbrace{\begin{bmatrix} U_\mathrm{R} & U_\mathrm{N} \end{bmatrix}}_{\substack{U \\ (m\times m)}} \begin{bmatrix} \underset{(r\times r)}{\Sigma} & 0 \\ 0 & 0 \end{bmatrix} \underbrace{\begin{bmatrix} V_\mathrm{R}^T \\ V_\mathrm{N}^T \end{bmatrix}}_{\substack{V^T \\ (n\times n)}}$$

A few important remarks:

- All the vectors from U are linearly independent (orthogonal)
- All the vectors from V are linearly independent (orthogonal)
- All the entries of Σ are real

Let one look for the product

$$T_\mathrm{i} v_{\mathrm{N},i} = U_\mathrm{R} \Sigma \underbrace{V_\mathrm{R}^T v_{\mathrm{N},i}}_{\substack{\text{orthogonal} \\ \text{vectors}}} = 0$$

$\Rightarrow$ Matrix V_N comprises a set of orthonormal bases of $\ker(T_\mathrm{i})$

Relying on the previously presented logic, the reference mapping can be obtained as

$$\boxed{I_\mathrm{M} = V_\mathrm{N} V_\mathrm{N}^T I^*}$$

For the case of the 3PH MMC

$$V_\mathrm{N}^T = \sqrt{\frac{2}{3}} \begin{bmatrix} 1 & -1/2 & -1/2 \\ 0 & \sqrt{3}/2 & -\sqrt{3}/2 \end{bmatrix}$$

Since $T_\mathrm{i} = \begin{bmatrix} 1 \dots 1 \end{bmatrix}_{1\times q}$, it can be shown (detailed description in [4]) that

$$V_\mathrm{N} V_\mathrm{N}^T = \underbrace{\begin{bmatrix} 1 & & \\ & \ddots & \\ & & 1 \end{bmatrix}}_{\substack{\text{identity } q\times q \\ \text{matrix}}} - \frac{1}{q} \begin{bmatrix} 1 & \dots & 1 \\ \vdots & & \vdots \\ 1 & \dots & 1 \end{bmatrix}_{q\times q},$$

no matter how V_N is chosen. Consequently:

$$I_\mathrm{M} = I^* - \underbrace{\frac{1}{q} \sum_{i=1}^{q} I_{i,1}^*}_{\text{average value}}$$

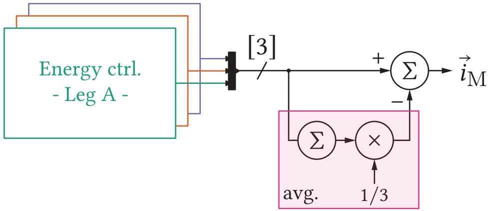

▲ Reference mapping in the 3PH MMC [2], [9]

SINGULAR VALUE DECOMPOSITION

- Descriptions in [7], [8]
- Diagonalization of a **non-square** matrix as

$$T_\mathrm{i} = \underbrace{\begin{bmatrix} U_\mathrm{R} & U_\mathrm{N} \end{bmatrix}}_{\substack{U \\ (m\times m)}} \begin{bmatrix} \underset{(r\times r)}{\Sigma} & 0 \\ 0 & 0 \end{bmatrix} \underbrace{\begin{bmatrix} V_\mathrm{R}^T \\ V_\mathrm{N}^T \end{bmatrix}}_{\substack{V^T \\ (n\times n)}}$$

A few important remarks:

- All the vectors from U are linearly independent (orthogonal)
- All the vectors from V are linearly independent (orthogonal)
- All the entries of Σ are real

Let one look for the product

$$T_\mathrm{i} v_{\mathrm{N},i} = U_\mathrm{R}\Sigma \underbrace{V_\mathrm{R}^T v_{\mathrm{N},i}}_{\text{orth...}} = 0$$

$\Rightarrow$ Matrix V_N comprises a set o... ...onormal bases of $\ker(T_\mathrm{i})$

Relying on the previously presented logic, the reference mapping can be obtained as

$$\boxed{I_\mathrm{M} = V_\mathrm{N} V_\mathrm{N}^T I^*}$$

For the case of the 3PH MMC

$$V_\mathrm{N}^T = \sqrt{\frac{2}{3}} \begin{bmatrix} 1 & -1/2 & -1/2 \\ 0 & \sqrt{3}/2 & -\sqrt{3}/2 \end{bmatrix}$$

Since $T_\mathrm{i} = \begin{bmatrix} 1 \dots 1 \end{bmatrix}_{1\times q}$, it can be shown (detailed description in [4]) that

$$V_\mathrm{N} V_\mathrm{N}^T = \underbrace{\begin{bmatrix} 1 & & \\ & \ddots & \\ & & 1 \end{bmatrix}}_{\substack{\text{identity } q\times q \\ \text{matrix}}} - \frac{1}{q} \begin{bmatrix} 1 & \dots & 1 \\ \vdots & & \vdots \\ 1 & \dots & 1 \end{bmatrix}_{q\times q},$$

no matter how V_N is chose... ...ntly:

$$I_\mathrm{M} = I^* - \underbrace{\frac{1}{q} \sum_{i=1}^{q} I_{i,1}^*}_{\text{average value}}$$

Irrespective of the balancing direction, identical principle can be employed!

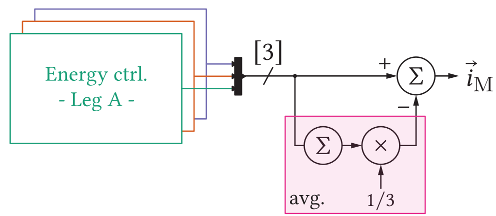

▲ Reference mapping in the 3PH MMC [2], [9]

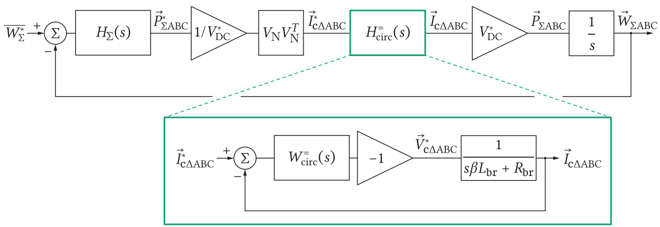

▲ Horizontal balancing control block diagram (SVD method)

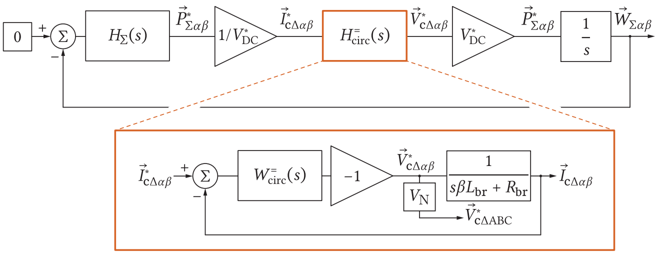

▲ Horizontal balancing control block diagram ($\alpha\beta$ transformation based) [5], [6]

Interestingly, V_N^T actually performs the Clarke transformation!

$$V_\mathrm{N}^T = \sqrt{\frac{2}{3}} \begin{bmatrix} 1 & -1/2 & -1/2 \\ 0 & \sqrt{3}/2 & -\sqrt{3}/2 \end{bmatrix}$$

From here, it is straightforward to show that

$$\vec{V}^*_{\mathrm{c}\Delta} = W^{=}_{\mathrm{circ}}(s)\left(V_\mathrm{N} \frac{H_\Sigma(s)}{V^*_\mathrm{DC}} (\vec{W}^*_{\Sigma\alpha\beta} - \vec{W}_{\Sigma\alpha\beta}) - \vec{I}_{\mathrm{c}\Delta} \right)$$

Multiplying with V_N^T from the left yields

$$\vec{V}^*_{\mathrm{c}\Delta\alpha\beta} = W^{=}_{\mathrm{circ}}(s)\left(\frac{H_\Sigma(s)}{V^*_\mathrm{DC}} (\vec{W}^*_{\Sigma\alpha\beta} - \vec{W}_{\Sigma\mathrm{m}\alpha\beta}) - \vec{I}_{\mathrm{c}\Delta\alpha\beta} \right).$$

APPLICATION OF SVD TO THE VERTICAL BALANCING PROBLEM - METHOD 1

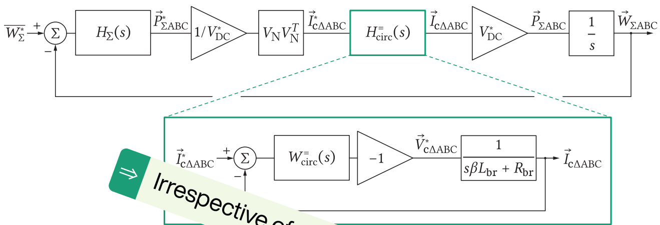

▲ Horizontal balancing control block ... ethod)

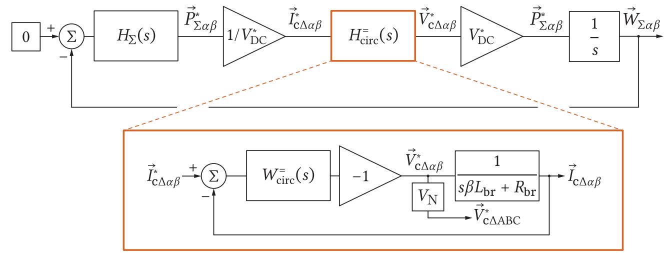

▲ Horizontal balancing control block diagram ($\alpha\beta$ transformation based) [5], [6]

⇛ Irrespective of the reference frame, the same behavior is experienced in terms of horizontal balancing dynamics!

Interestingly, V_N^T actually performs the Clarke tra...

$$V_N^T = \sqrt{\frac{2}{3}} \begin{bmatrix} 1 & -1/2 & -1/2 \\ 0 & \sqrt{3}/2 & -\sqrt{3}/2 \end{bmatrix}$$

From here, it is straightforward to show that

$$\vec{V}^*_{c\Delta} = W^=_{circ}(s)\left(V_N \frac{H_\Sigma(s)}{V^*_{DC}} (\vec{W}^*_{\Sigma\alpha\beta} - \vec{W}_{\Sigma\alpha\beta}) - \vec{I}_{c\Delta} \right)$$

Multiplying with V_N^T from the left yields

$$\vec{V}^*_{c\Delta\alpha\beta} = W^=_{circ}(s)\left(\frac{H_\Sigma(s)}{V^*_{DC}} (\vec{W}^*_{\Sigma\alpha\beta} - \vec{W}_{\Sigma m\alpha\beta}) - \vec{I}_{c\Delta\alpha\beta} \right).$$

APPLICATION OF SVD TO THE VERTICAL BALANCING PROBLEM - METHOD 1

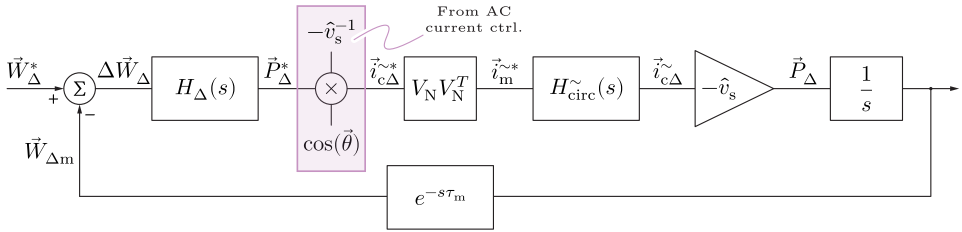

▲ Control block diagram concerning energy balancing in vertical direction (ABC frame)

Method properties:

- Control conducted per every leg individually
- Mapping matrix generated through the SVD utilization
- $H_\Delta(s)$ can be either P- or PI- controller
- Information on voltage v_s is always available in the controller

Observation in the complex domain, leads to

$$\underline{i}^{\sim}_{M} = V_N V_N^T \frac{H_\Delta(s)}{\hat{v}_s} e^{-j\gamma} \underbrace{\begin{bmatrix} 1 & 0 & 0 \\ 0 & a^2 & 0 \\ 0 & 0 & a \end{bmatrix}}_{A} \begin{bmatrix} W_{\Delta A} \\ W_{\Delta B} \\ W_{\Delta C} \end{bmatrix},$$

where $a = e^{j\frac{2\pi}{3}}$. Moreover,

$$V_N V_N^T = \frac{1}{3}\begin{bmatrix} 2 & -1 & -1 \\ -1 & 2 & -1 \\ -1 & -1 & 2 \end{bmatrix}.$$

Fortescue transformation of $\vec{i}^{\sim *}_{M}$ should output only positive and negative sequences.

$$F_{pn0} = \frac{1}{3}\begin{bmatrix} 1 & a & a^2 \\ 1 & a^2 & a \\ 1 & 1 & 1 \end{bmatrix}$$

If $W^*_{\Delta\{A/B/C\}} = 0$, whereas $\tau_m \approx 0$, then

$$\begin{bmatrix} \underline{i}^{\sim}_{m+} \\ \underline{i}^{\sim}_{m-} \\ \underline{i}^{\sim}_{m0} \end{bmatrix} = \frac{H_\Delta(s)}{\hat{v}_s} e^{-j\gamma} \times \begin{bmatrix} \frac{1}{\sqrt{3}} W_{\Delta 0} \\ \frac{1}{\sqrt{6}}\left(W_{\Delta\alpha} + jW_{\Delta\beta}\right) \\ 0 \end{bmatrix},$$

while $\alpha\beta 0$ quantities were obtained by means of the matrix from below.

$$K_{\alpha\beta 0} = \sqrt{\frac{2}{3}}\begin{bmatrix} 1 & -\frac{1}{2} & -\frac{1}{2} \\ 0 & \frac{\sqrt{3}}{2} & -\frac{\sqrt{3}}{2} \\ \frac{1}{\sqrt{2}} & \frac{1}{\sqrt{2}} & \frac{1}{\sqrt{2}} \end{bmatrix}$$

VERTICAL BALANCING - METHOD 2

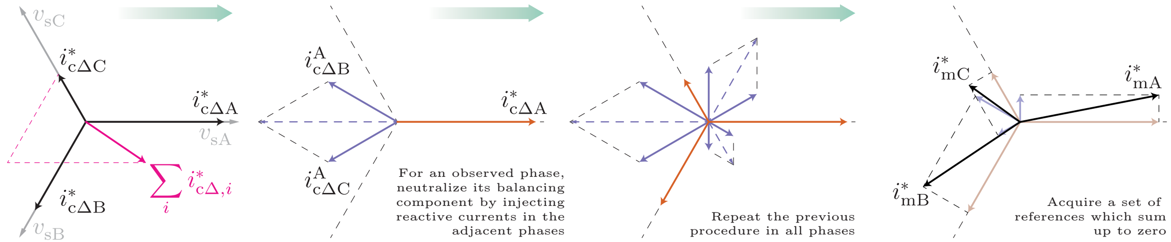

▲ Vert. bal. procedure based on the injection of orthogonal components

- Injection of **reactive** currents
- Sum of circ. current references equal to zero
- Control structure similar to Method 1

Mapping matrix is changed with respect to Method 1.

$$\underline{M}_m = \begin{bmatrix} 1 & j\frac{a}{\sqrt{3}} & -j\frac{a^2}{\sqrt{3}} \\ -j\frac{a^2}{\sqrt{3}} & 1 & j\frac{a}{\sqrt{3}} \\ j\frac{a}{\sqrt{3}} & -j\frac{a^2}{\sqrt{3}} & 1 \end{bmatrix}$$

If $W^*_{\Delta\{A/B/C\}} = 0$, whereas $\tau_m \approx 0$, then

$$\vec{\underline{i}}^{\sim}_{M} = \frac{H_\Delta(s)}{\hat{v}_s} e^{-j\gamma} \underline{M}_m \begin{bmatrix} 1 & 0 & 0 \\ 0 & a^2 & 0 \\ 0 & 0 & a \end{bmatrix} \begin{bmatrix} W_{\Delta A} \\ W_{\Delta B} \\ W_{\Delta C} \end{bmatrix} \xrightarrow[K_{\alpha\beta 0}]{F_{pn0}} \begin{bmatrix} \underline{i}^{\sim}_{m+} \\ \underline{i}^{\sim}_{m-} \\ \underline{i}^{\sim}_{m0} \end{bmatrix} = \frac{H_\Delta(s)}{\hat{v}_s} e^{-j\gamma} \times \begin{bmatrix} \frac{1}{\sqrt{3}} W_{\Delta 0} \\ \frac{2}{\sqrt{6}} \left(W_{\Delta\alpha} + j W_{\Delta\beta} \right) \\ 0 \end{bmatrix}$$

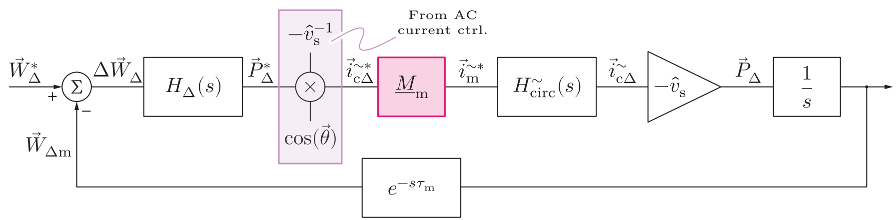

▲ Control block associated to the balancing method described above

- Direct control of the energy unbalances in the $\alpha\beta 0$ domain ($V_N^T = K_{\alpha\beta}$)
- The use of $+/-$ circ. current sequences (similar approach followed in [10], [11])

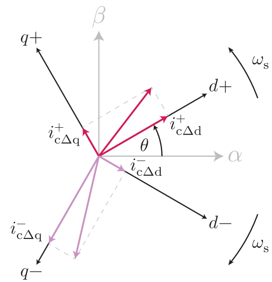

▲ Positive and negative seq.

Circ. currents in the ABC frame can be obtained as

$$\begin{bmatrix} i_{c\Delta A} \\ i_{c\Delta B} \\ i_{c\Delta C} \end{bmatrix} = K_{\alpha\beta}^T \underbrace{\begin{bmatrix} \cos(\theta) & -\sin(\theta) \\ \sin(\theta) & \cos(\theta) \end{bmatrix}}_{\text{counterclockwise rotation}} \begin{bmatrix} i^+_{c\Delta d} \\ i^+_{c\Delta q} \end{bmatrix} + K_{\alpha\beta}^T \underbrace{\begin{bmatrix} \cos(\theta) & \sin(\theta) \\ -\sin(\theta) & \cos(\theta) \end{bmatrix}}_{\text{clockwise rotation}} \begin{bmatrix} i^-_{c\Delta d} \\ i^-_{c\Delta q} \end{bmatrix}.$$

According to [6], the following expressions can be established:

$$P_{\Delta\alpha} = -\frac{2}{\sqrt{6}}\hat{v}_s i^-_{c\Delta d} \qquad P_{\Delta\beta} = +\frac{2}{\sqrt{6}}\hat{v}_s i^-_{c\Delta q} \qquad P_{\Delta 0} = -\frac{2}{\sqrt{3}}\hat{v}_s i^+_{c\Delta d}$$

$\Rightarrow$ Decoupled control of relevant energy components

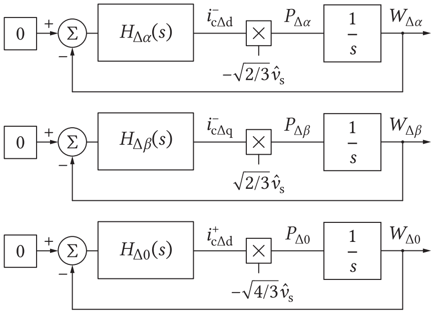

▲ Block diagram derived according to the equations on the left

- Controllers $H_{\Delta\{\alpha/\beta/0\}}(s)$ can be tuned independently!
- $i^+_{c\Delta q}$ can be controlled to zero
- For simplicity reasons assume that $H_{\Delta\{\alpha/\beta/0\}}(s) = H_\Delta(s)$

$$F_{pn0}\begin{bmatrix} i_{c\Delta A} \\ i_{c\Delta B} \\ i_{c\Delta C} \end{bmatrix} = \begin{bmatrix} \tilde{i}_{m+} \\ \tilde{i}_{m-} \\ \tilde{i}_{m0} \end{bmatrix} = \frac{H_\Delta(s)}{\hat{v}_s} e^{-j\gamma} \times \begin{bmatrix} \frac{1}{\sqrt{2}} W_{\Delta 0} \\ W_{\Delta\alpha} + jW_{\Delta\beta} \\ 0 \end{bmatrix}$$

- Direct control of the energy unbalances in the $\alpha\beta 0$ domain ($V_{\mathrm{N}}^{T} = K_{\alpha\beta}$)
- The use of $+/-$ circ. current sequences (similar approach followed in [10], [11])

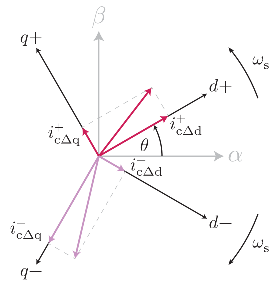

▲ Positive and negative seq.

Circ. currents in the ABC frame can be obtained as

$$\begin{bmatrix} i_{\mathrm{c\Delta A}} \\ i_{\mathrm{c\Delta B}} \\ i_{\mathrm{c\Delta C}} \end{bmatrix} = K_{\alpha\beta}^{T} \underbrace{\begin{bmatrix} \cos(\theta) & -\sin(\theta) \\ \sin(\theta) & \cos(\theta) \end{bmatrix}}_{\text{counterclockwise rotation}} \begin{bmatrix} i^{+}_{\mathrm{c\Delta d}} \\ i^{+}_{\mathrm{c\Delta q}} \end{bmatrix} + K_{\alpha\beta}^{T} \underbrace{\begin{bmatrix} \cos(\theta) & \sin(\theta) \\ -\sin(\theta) & \cos(\theta) \end{bmatrix}}_{\text{clockwise rotation}} \begin{bmatrix} i^{-}_{\mathrm{c\Delta d}} \\ i^{-}_{\mathrm{c\Delta q}} \end{bmatrix}.$$

According to [6], the following expressions can be established:

$$P_{\Delta\alpha} = -\frac{2}{\sqrt{6}} \hat{v}_{\mathrm{s}} i^{-}_{\mathrm{c\Delta d}} \qquad P_{\Delta\beta} = +\frac{2}{\sqrt{6}} \hat{v}_{\mathrm{s}} i^{-}_{\mathrm{c\Delta q}} \qquad P_{\Delta 0} = -\frac{2}{\sqrt{3}} \hat{v}_{\mathrm{s}} i^{+}_{\mathrm{c\Delta d}}$$

⇒ Decoupled control of relevant energy components

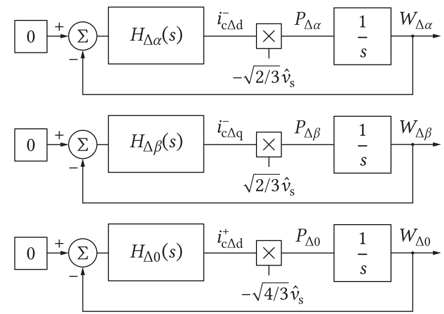

▲ Block diagram derived according to the equations on the left

- Controllers $H_{\Delta\{\alpha/\beta/0\}}(s)$ can be tuned independently!
- $i^{+}_{\mathrm{c\Delta q}}$ can be controlled to zero
- For simplicity reasons assume that $H_{\Delta\{\alpha/\beta/0\}}(s) = H_{\Delta}(s)$

$$F_{\mathrm{pn0}} \begin{bmatrix} i_{\mathrm{c\Delta A}} \\ i_{\mathrm{c\Delta B}} \\ i_{\mathrm{c\Delta C}} \end{bmatrix} = \begin{bmatrix} \tilde{i}_{\mathrm{m+}} \\ \tilde{i}_{\mathrm{m-}} \\ \tilde{i}_{\mathrm{m0}} \end{bmatrix} = \frac{H_{\Delta}(s)}{\hat{v}_{\mathrm{s}}} e^{-j\gamma} \times \begin{bmatrix} \frac{1}{\sqrt{2}} W_{\Delta 0} \\ W_{\Delta\alpha} + jW_{\Delta\beta} \\ 0 \end{bmatrix}$$

Problem statement

? How to compare the vertical balancing methods presented so far?

VERTICAL BALANCING METHODS COMPARISON (I)

Method 1

$$\begin{bmatrix} \underline{i}_{\mathrm{m}+}^{\sim} \\ \underline{i}_{\mathrm{m}-}^{\sim} \\ \underline{i}_{\mathrm{m}0}^{\sim} \end{bmatrix} = \frac{H_{\Delta}(s)}{\hat{v}_s} e^{-j\gamma} \times \begin{bmatrix} \frac{1}{\sqrt{3}} W_{\Delta 0} \\ \frac{1}{\sqrt{6}} (W_{\Delta\alpha} + jW_{\Delta\beta}) \\ 0 \end{bmatrix}$$

Method 2

$$\begin{bmatrix} \underline{i}_{\mathrm{m}+}^{\sim} \\ \underline{i}_{\mathrm{m}-}^{\sim} \\ \underline{i}_{\mathrm{m}0}^{\sim} \end{bmatrix} = \frac{H_{\Delta}(s)}{\hat{v}_s} e^{-j\gamma} \times \begin{bmatrix} \frac{1}{\sqrt{3}} W_{\Delta 0} \\ \frac{2}{\sqrt{6}} (W_{\Delta\alpha} + jW_{\Delta\beta}) \\ 0 \end{bmatrix}$$

Method 3

$$\begin{bmatrix} \underline{i}_{\mathrm{m}+}^{\sim} \\ \underline{i}_{\mathrm{m}-}^{\sim} \\ \underline{i}_{\mathrm{m}0}^{\sim} \end{bmatrix} = \frac{H_{\Delta}(s)}{\hat{v}_s} e^{-j\gamma} \times \begin{bmatrix} \frac{1}{\sqrt{2}} W_{\Delta 0} \\ 1 (W_{\Delta\alpha} + jW_{\Delta\beta}) \\ 0 \end{bmatrix}$$

Circ. current $+/-$ sequences can be expressed as

$$\underline{i}_{\mathrm{m}+}^{\sim} = \frac{H_{\Delta}(s)}{\hat{v}_s} e^{-j\gamma} \times k_+ W_{\Delta 0}$$

$$\underline{i}_{\mathrm{m}-}^{\sim} = \frac{H_{\Delta}(s)}{\hat{v}_s} e^{-j\gamma} \times k_- (W_{\Delta\alpha} + jW_{\Delta\beta}),$$

allowing for the representation in a tabular form

	Method 1	Method 2	Method 3
k_+	$\frac{1}{\sqrt{3}}$	$\frac{1}{\sqrt{3}}$	$\frac{1}{\sqrt{2}}$
k_-	$\frac{1}{\sqrt{6}}$	$\frac{2}{\sqrt{6}}$	1

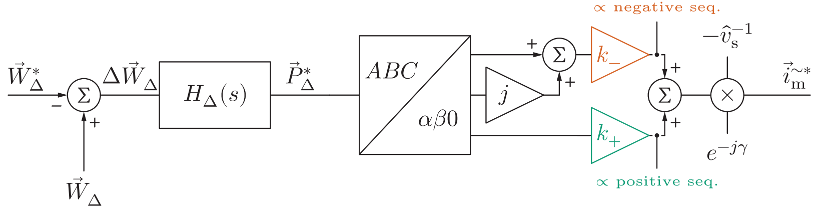

▲ An alternative way of generating circulating current references achieving the energy balance in vertical direction

In general, the expressions

$$i_{\mathrm{c}\Delta\mathrm{d}}^{+} = \Re\left(\sqrt{\frac{3}{2}} e^{j\gamma} \underline{i}_{\mathrm{m}+}^{\sim}\right) \quad i_{\mathrm{c}\Delta\mathrm{q}}^{+} = \Im\left(\sqrt{\frac{3}{2}} e^{j\gamma} \underline{i}_{\mathrm{m}+}^{\sim}\right) \quad i_{\mathrm{c}\Delta\mathrm{d}}^{-} = \Re\left(\sqrt{\frac{3}{2}} e^{j\gamma} \underline{i}_{\mathrm{m}-}^{\sim}\right) \quad i_{\mathrm{c}\Delta\mathrm{q}}^{-} = -\Im\left(\sqrt{\frac{3}{2}} e^{j\gamma} \underline{i}_{\mathrm{m}-}^{\sim}\right)$$

hold, while $i_{\mathrm{c}\Delta\mathrm{q}}^{+} = 0$. From here, one can obtain system of equations provided below.

$$i_{\mathrm{c}\Delta\mathrm{d}}^{+} = \sqrt{\frac{3}{2}} k_+ \frac{H_{\Delta}}{\hat{v}_s} W_{\Delta 0} \qquad i_{\mathrm{c}\Delta\mathrm{d}}^{-} = \sqrt{\frac{3}{2}} k_- \frac{H_{\Delta}}{\hat{v}_s} W_{\Delta\alpha} \qquad i_{\mathrm{c}\Delta\mathrm{q}}^{-} = -\sqrt{\frac{3}{2}} k_- \frac{H_{\Delta}}{\hat{v}_s} W_{\Delta\beta}.$$

Combining the above system with

$$P_{\Delta\alpha} = -\frac{2}{\sqrt{6}} \hat{v}_s i_{\mathrm{c}\Delta\mathrm{d}}^{-} \qquad P_{\Delta\beta} = +\frac{2}{\sqrt{6}} \hat{v}_s i_{\mathrm{c}\Delta\mathrm{q}}^{-} \qquad P_{\Delta 0} = -\frac{2}{\sqrt{3}} \hat{v}_s i_{\mathrm{c}\Delta\mathrm{d}}^{+}$$

yields

$$\begin{aligned} P_{\Delta\alpha} &= -k_- H_{\Delta} W_{\Delta\alpha} &&= -k_{1\alpha} H_{\Delta} W_{\Delta\alpha} \\ P_{\Delta\beta} &= -k_- H_{\Delta} W_{\Delta\beta} &&= -k_{1\beta} H_{\Delta} W_{\Delta\beta} \\ P_{\Delta 0} &= -\sqrt{2} k_+ H_{\Delta} W_{\Delta 0} &&= -k_{10} H_{\Delta} W_{\Delta 0}. \end{aligned}$$

VERTICAL BALANCING METHODS COMPARISON (II)

According to previous derivations, the expression

$$\boxed{P_{\Delta\{\alpha/\beta/0\}} = -k_{1\{\alpha/\beta/0\}} H_\Delta W_{\Delta\{\alpha/\beta/0\}}}$$

can be established, whereas

Coefficient	Method 1	Method 2	Method 3
$k_{1\alpha}$	$\frac{1}{2}\sqrt{\frac{2}{3}}$	$\sqrt{\frac{2}{3}}$	1
$k_{1\beta}$	$\frac{1}{2}\sqrt{\frac{2}{3}}$	$\sqrt{\frac{2}{3}}$	1
k_{10}	$\sqrt{\frac{2}{3}}$	$\sqrt{\frac{2}{3}}$	1

Furthermore, the relationship from below can be obtained.

$$\boxed{P_{\Delta\{\alpha/\beta/0\}} = k_{2\{\alpha/\beta/0\}} \hat{v}_s i_{c\Delta\{d-/q-/d+\}}}$$

$k_{20} = -2/\sqrt{3}$ and $k_{2\{\alpha/\beta\}} = \mp 2/\sqrt{6}$

⇒ Generalized control block diagram

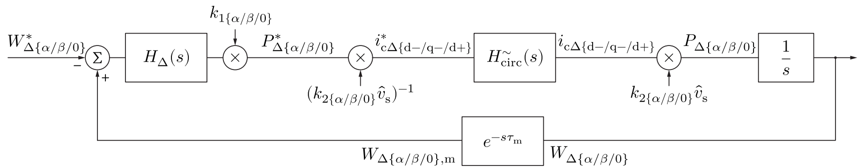

▲ A general control block diagram concerning vertical balancing of the MMC energies.

To commence the comparison, once can assume that

$$H^{\sim}_{circ}(s) = \frac{1}{1+s\tau_c} \qquad H_{mf}(s) = e^{-s\tau_m} \approx \frac{1-s\frac{\tau_m}{2}}{1+s\frac{\tau_m}{2}} \qquad H_\Delta(s) = k_{p\Delta}.$$

Establishing the function $G(s)$ allows for a straightforward analysis throught the root-locus method.

$$G(s) = \frac{H^{\sim}_{circ}(s)H_{mf}(s)}{s} = \frac{N(s)}{D(s)} \xRightarrow{\text{All the poles can be identifed by solving}} D(s) + k_{p\Delta}k_{1\{\alpha/\beta/0\}}N(s) = 0.$$

For the moment, assume the $W_{\Delta 0}$ component is analyzed. Hence, $k_{10} = 1$.

If $k_{p\Delta} \to 0$, zeros$[D(s)]$⇒poles$[W_{\Delta 0}/W^*_{\Delta 0}]$

$$\sigma_1 = 0$$
$$\sigma_2 = -\frac{2}{\tau_m}$$
$$\sigma_3 = -\frac{1}{\tau_c}$$

If $k_{p\Delta} \to \infty$, zeros$[N(s)]$⇒poles$[W_{\Delta 0}/W^*_{\Delta 0}]$

$$n_1 = \frac{2}{\tau_m}$$

According to previous derivations, the expression

$$\boxed{P_{\Delta\{\alpha/\beta/0\}} = -k_{1\{\alpha/\beta/0\}} H_{\Delta} W_{\Delta\{\alpha/\beta/0\}}}$$

can be established, whereas

Coefficient	Method 1	Method 2	Method 3
$k_{1\alpha}$	$\frac{1}{2}\sqrt{\frac{2}{3}}$	$\sqrt{\frac{2}{3}}$	1
$k_{1\beta}$	$\frac{1}{2}\sqrt{\frac{2}{3}}$	[illegible]	1
k_{10}	$\sqrt{\frac{2}{3}}$	$\sqrt{\frac{?}{3}}$	[illegible]

Furthermore, the relationship from below can be obtai...

$$\boxed{P_{\Delta\{\alpha/\beta/0\}} = k_{2\{\alpha/\beta/0\}} \hat{v}_s i_{c\Delta\{d^-/q^-/d^+\}}}$$

$k_{20} = -2/\sqrt{3}$ and $k_{2\{\alpha/\beta\}} = \mp 2/\sqrt{6}$

⇒ Generalized control block diagram

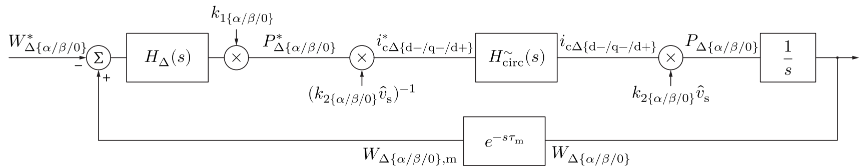

▲ A general control block diagram concerning vertical balancing of the MMC energies.

To commence the comparison, once can assume that

$$H^{\sim}_{circ}(s) = \frac{1}{1+s\tau_c} \qquad H_{mf}(s) = e^{-s\tau_m} \approx \frac{1-s\frac{\tau_m}{2}}{1+s\frac{\tau_m}{2}} \qquad H_\Delta(s) = k_{p\Delta}.$$

Est... ...nction $G(s)$ allows for a straightforward analysis throught the root-locus method.

$$G(s) = \frac{H_{circ} \ldots N(s)}{s} \xrightarrow{\text{All the poles can be identifed by solving}} D(s) + k_{p\Delta} k_{1\{\alpha/\beta/0\}} N(s) = 0.$$

For the moment, assume the $W_{\Delta 0}$ com... ...zed. Hence, $k_{10} = 1$.

Time constants τ_c and τ_m can stand in any arbitrary order ⇒ An example is required

If $k_{p\Delta} \to 0$, zeros$[D(s)]$⇒poles$[W_{\Delta 0}/W^*_{\Delta 0}]$

$$\sigma_1 = 0$$

$$\sigma_2 = -\frac{2}{\tau_m}$$

$$\sigma_3 = -\frac{1}{\tau_c}$$

If $k_{p\Delta} \to \infty$, ze... $N(s)$]⇒poles$[W_{\Delta 0}/W^*_{\Delta 0}]$

$$n_1 = \frac{2}{\tau_m}$$

VERTICAL BALANCING METHODS COMPARISON (III)

▲ Parameters of the converter used for further analyses

Rated power (S^*)	Output voltage (V_{DC})	Grid voltage (v_g)	Number of SMs per branch (N)	Nominal SM voltage (V_{SM})	SM capacitance (C_{SM})	Branch inductance (L_{br})	Branch resistance (R_{br})	PWM carrier frequency (f_c)	Fundamental frequency (f_o)
1.25MVA	5kV	3.3kV	6	1kV	3.36mF	2.5mH	60mΩ	1kHz	60Hz

In the setup used to verify the results presented henceforward

$$\tau_m \approx 375\mu s \qquad \text{and} \qquad \tau_c \approx \frac{1}{f_{bw}^{circ}} = 1\text{ms},$$

resulting in the diagram presented bellow.

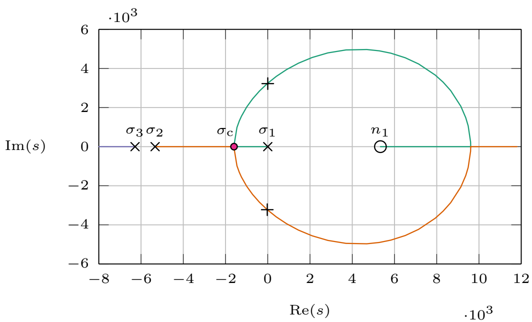

▲ Root locus constructed based on the function $G(s)$

Apparently, there exists an optimal gain $k^*_{p\Delta}$ guaranteeing the fastest and strictly aperiodic response! To calculate $k^*_{p\Delta}$, one should substitute the solution of

$$\frac{dD(s)}{ds}N(s) - \frac{dN(s)}{ds}D(s) = 0,$$

which is actually $s = \sigma_c$, into

$$k^*_{p\Delta} = -\frac{D(\sigma_c)}{N(\sigma_c)}.$$

In the analyzed example, $k^*_{p\Delta} \approx 642$!

▲ Parameters of the converter used for further analyses

Rated power (S^*)	Output voltage (V_{DC})	Grid voltage (v_g)	Number of SMs per branch (N)	Nominal SM voltage (V_{SM})	SM capacitance (C_{SM})	Branch inductance (L_{br})	Branch resistance (R_{br})	PWM carrier frequency (f_c)	Fundamental frequency (f_o)
1.25MVA	5kV	3.3kV	6	1kV	3.36mF	2.5mH	60mΩ	1kHz	60Hz

In the setup used to verify the results presented henceforward

$$\tau_m \approx 375\mu s \qquad \text{and} \qquad \tau_c \approx \frac{1}{f_{bw}^{circ}} = 1\text{ms},$$

resulting in the diagram presented bellow.

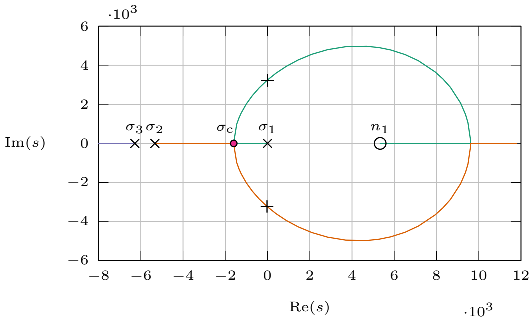

▲ Root locus constructed based on the function $G(s)$

Apparently, there exists an optimal gain $k^*_{p\Delta}$ guaranteeing the fastest and strictly aperiodic response! To calculate $k^*_{p\Delta}$, one should substitute the solution of

$$\frac{dD(s)}{ds}N(s) - \frac{dN(s)}{ds}D(s) = 0,$$

which is actually $s = \sigma_c$, into

$$k^*_{p\Delta} = -\frac{D(\sigma_c)}{N(\sigma_c)}.$$

In the analyzed example, $k^*_{p\Delta} \approx 642$!

? Is this gain realistic?

Assuming that $\Delta W_0 = 0.1 W^*_{br}$, where $W^*_{br} \approx C_{SM} V^{*2}_{br\Sigma}/(2N)$, one can realize that

$$\hat{i}_{c\Delta 0} = k_{p\Delta}\frac{0.1\sqrt{3}W^*_{br}}{2\hat{v}_s} \approx 210\text{A},$$

which is approximately 70% of the converter nominal AC current amplitude!

▲ Parameters of the converter used for further analyses

Rated power (S^*)	Output voltage (V_{DC})	Grid voltage (v_g)	Number of SMs per branch (N)	Nominal SM voltage (V_{SM})	SM capacitance (C_{SM})	Branch inductance (L_{br})	Branch resistance (R_{br})	PWM carrier frequency (f_c)	Fundamental frequency (f_o)
1.25MVA	5kV	3.3kV	6	1kV	3.36mF	2.5mH	60mΩ	1kHz	60Hz

In the setup used to verify the results presented henceforward

$$\tau_m \approx 375\mu s \qquad \text{and} \qquad \tau_c \approx \frac{1}{f_{bw}^{circ}} = 1\text{ms},$$

resulting in the diagram presented bellow.

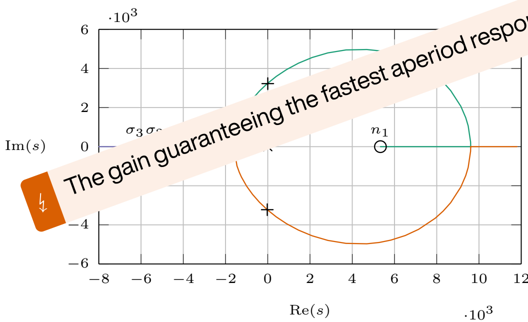

▲ Root locus constructed based on the function $G(s)$

Apparently, there exists an optimal gain $k^*_{p\Delta}$ guara… and strictly aperiodic response! To calculate $k^*_{p\Delta}$, one should s… of

$$\ldots N(s) - \frac{dN(s)}{ds} D(s) = 0,$$

which is …

$$k^*_{p\Delta} = -\frac{D(\sigma_c)}{N(\sigma_c)}.$$

In the analyzed example, $k^*_{p\Delta} \approx 642$!

The gain guaranteeing the fastest aperiod response is not practical from neither hardware nor control viewpoint. Hence $k_{p\Delta} \ll k^*_{p\Delta}$

? Is this gain realistic?

Assuming that $\Delta W_0 = 0.1 W^*_{br}$, where $W^*_{br} \approx C_{SM} V^{*2}_{br\Sigma}/(2N)$, one can realize that

$$\hat{i}_{c\Delta 0} = k_{p\Delta} \frac{0.1\sqrt{3} W^*_{br}}{2\hat{v}_s} \approx 210\text{A},$$

which is approximately 70% of the converter nominal AC current amplitude!

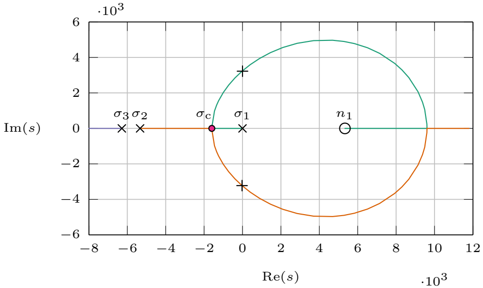

▲ Root locus constructed based on the function $G(s)$

Since $k_{\mathrm{p}\Delta} \ll k^{*}_{\mathrm{p}\Delta}$ one can conclude that $\sigma_1 \gg \sigma_{\mathrm{c}}$. From the equation

$$D(s) + \underbrace{k_{\mathrm{p}\Delta} k_{1\{\alpha/\beta/0\}}}_{k'_{\mathrm{p}}} N(s) = 0,$$

the following observations can be made

- The higher k'_{p} the further the pole σ_1 from the imaginary axis
- For fixed $k_{\mathrm{p}\Delta}$, the system dynamics depends on $k_{1\{\alpha/\beta/0\}}$

▲ Reminder - values of coefficients determining the balancing dynamics of energy components $W_{\Delta\alpha}$, $W_{\Delta\beta}$ and $W_{\Delta 0}$, respectively.

Coefficient	Method 1	Method 2	Method 3
$k_{1\alpha}$	$\frac{1}{2}\sqrt{\frac{2}{3}}$	$\sqrt{\frac{2}{3}}$	1
$k_{1\beta}$	$\frac{1}{2}\sqrt{\frac{2}{3}}$	$\sqrt{\frac{2}{3}}$	1
k_{10}	$\sqrt{\frac{2}{3}}$	$\sqrt{\frac{2}{3}}$	1

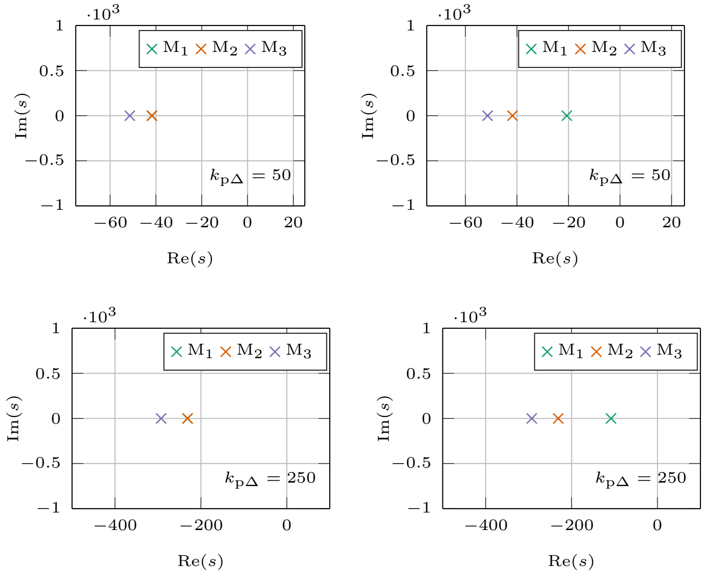

▲ Position of poles in the closed loop function $W_{\Delta\{\alpha/\beta/0\}}/W^{*}_{\Delta\{\alpha/\beta/0\}}$ for two different gains $k_{\mathrm{p}\Delta}$

VERTICAL BALANCING METHODS COMPARISON (IV)

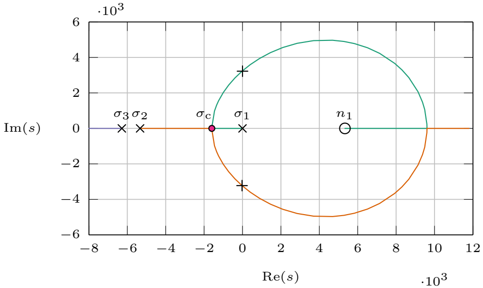

▲ Root locus constructed based on the function $G(s)$

Since $k_{p\Delta} \ll k^*_{p\Delta}$ one can conclude that $\sigma_1 \gg \sigma_c$. From the equation

$$D(s) + \underbrace{k_{p\Delta} k_{1\{\alpha/\beta/0\}}}_{k'_p} N(s) = 0,$$

the following observations can be m

- The higher k'_p the f ... om the imaginary axis
- For fix ... ynamics depends on $k_{1\{\alpha/\beta/0\}}$

⇒ Moving from Method 1 to 3 increases the gain k'_p ⇒ Method 3 is supposed to provide the fastest response if the gain $k_{p\Delta}$ is fixed!

▲ Re ... values of coefficients determining the balancing dynamics of energy components $W_{\Delta\alpha}$, $W_{\Delta\beta}$ and $W_{\Delta 0}$, respectively.

Coefficient	Method 1	Method 2	Method 3
$k_{1\alpha}$	$\frac{1}{2}\sqrt{\frac{2}{3}}$	$\sqrt{\frac{2}{3}}$	1
$k_{1\beta}$	$\frac{1}{2}\sqrt{\frac{2}{3}}$	$\sqrt{\frac{2}{3}}$	1
k_{10}	$\sqrt{\frac{2}{3}}$	$\sqrt{\frac{2}{3}}$	1

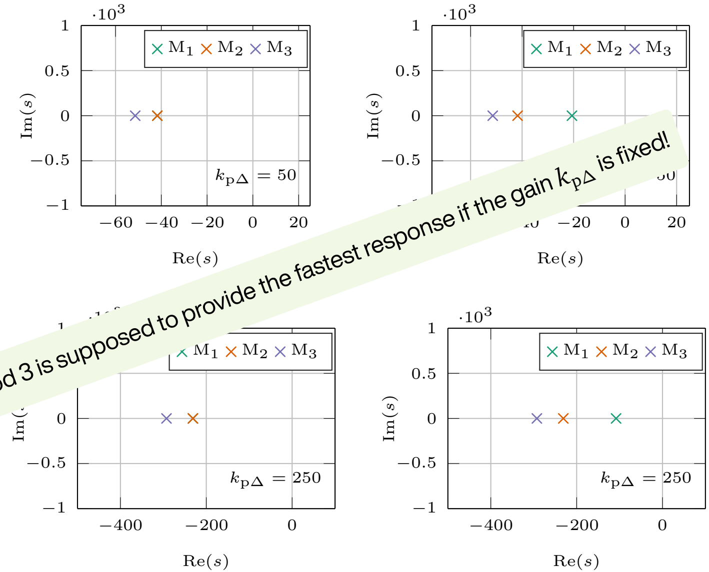

▲ Position of poles in the closed loop function $W_{\Delta\{\alpha/\beta/0\}}/W^*_{\Delta\{\alpha/\beta/0\}}$ for two different gains $k_{p\Delta}$

VERTICAL BALANCING METHODS COMPARISON - IMPORTANT REMARKS

- Controllers in the $\alpha\beta 0$ domain (Method 3) do not have to be identically tuned
- For Methods 1 and 2, every leg has its own controller, however, controllers are tuned identically
- The gain $k_{\mathrm{p}\Delta}$ does not have to be fixed
- Methods 1 and 2 can be derived from Method 3 if

$$H_{\mathrm{c}\Delta 0}^{\text{(method 3)}} = H_{\Delta}^{\text{(method 1/2)}} \times \frac{k_{10}^{\text{(method 1/2)}}}{k_{10}^{\text{(method 3)}}}$$

$$H_{\mathrm{c}\Delta\{\alpha/\beta\}}^{\text{(method 3)}} = H_{\Delta}^{\text{(method 1/2)}} \times \frac{k_{1\{\alpha/\beta\}}^{\text{(method 1/2)}}}{k_{1\{\alpha/\beta\}}^{\text{(method 3)}}}$$

- Method 3 can be derived from Method 2 if the gains are increased by the factor $\sqrt{\frac{3}{2}}$ (if $H_{\Delta\{\alpha/\beta/0\}}(s) = H_{\Delta}(s)$).
- Method 3 cannot be derived from Method 1
- Average energies response was considered (for branch voltage ripple optimization, please refer to [12], [10], [1], [13])

▲ Reminder - values of coefficients determining the balancing dynamics of energy components $W_{\Delta\alpha}$, $W_{\Delta\beta}$ and $W_{\Delta 0}$, respectively.

Coefficient	Method 1	Method 2	Method 3
$k_{1\alpha}$	$\frac{1}{2}\sqrt{\frac{2}{3}}$	$\sqrt{\frac{2}{3}}$	1
$k_{1\beta}$	$\frac{1}{2}\sqrt{\frac{2}{3}}$	$\sqrt{\frac{2}{3}}$	1
k_{10}	$\sqrt{\frac{2}{3}}$	$\sqrt{\frac{2}{3}}$	1

▲ Parameters of the converter used for further analyses

Rated power (S^*)	Output voltage (V_{DC})	Grid voltage (v_g)	Number of SMs per branch (N)	Nominal SM voltage (V_{SM})	SM capacitance (C_{SM})	Branch inductance (L_{br})	Branch resistance (R_{br})	PWM carrier frequency (f_c)	Fundamental frequency (f_o)
1.25MVA	5kV	3.3kV	6	1kV	3.36mF	2.5mH	60mΩ	1kHz	60Hz

- Converter with parameters provided above (identical to [14])
- Real industrial ABB PEC800 controller
  - Master & Slave PECs (flexibility in reconfiguration)
  - PECMI (v/i measurements)
  - Control HUB (SM signals aggregation and reference processing)
  - COMBIO (Realays/Switches/Monitoring)
  - **More details in Part 4.**
- Identical gains $k_{p\Sigma} = k_{p\Delta} = 50$

⇒ Control structure identical to the real prototype

(a) Front view

(b) Rear view

▲ HIL system used for result verification purposes

HIL VERIFICATION - HORIZONTAL BALANCING

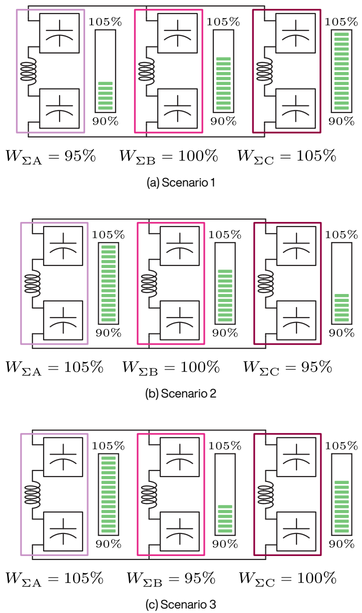

▲ Unbalance scenarios used for results verification purpose

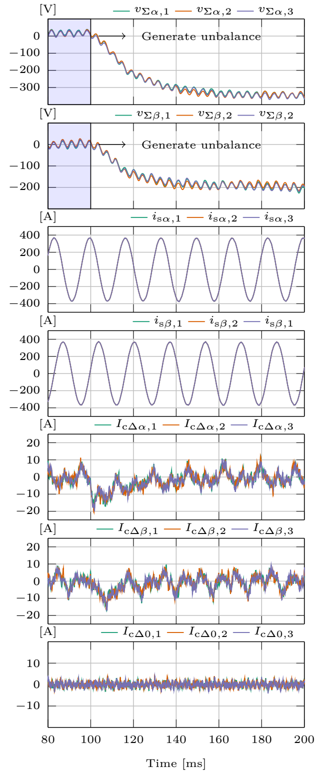

▲ Response under the unbalance scenario 1

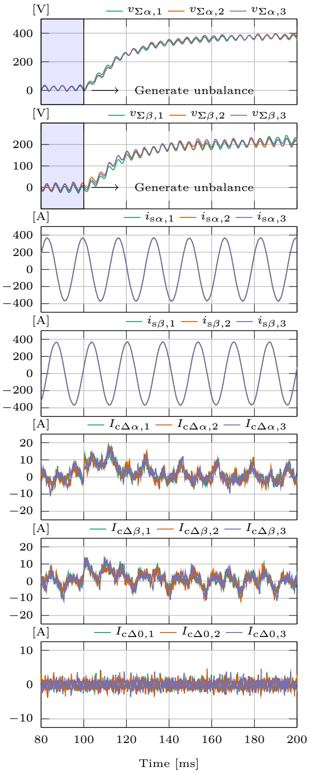

▲ Response under the unbalance scenario 2

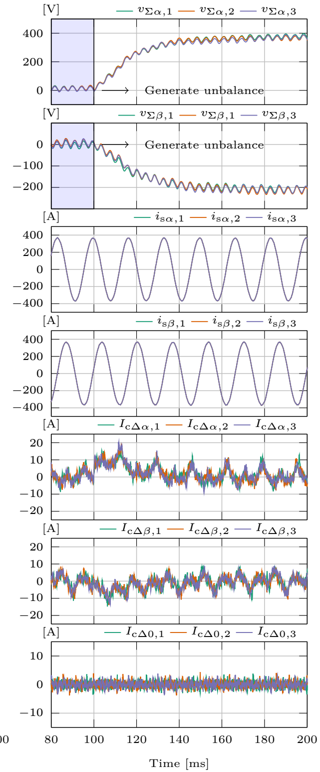

▲ Response under the unbalance scenario 2

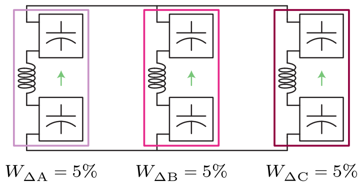

(a) Scenario 1

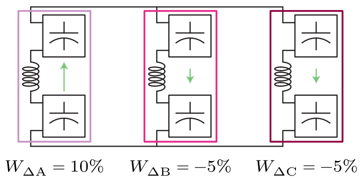

(b) Scenario 2

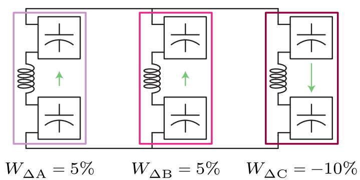

(c) Scenario 3

▲ Unbalance scenarios used for results verification purpose

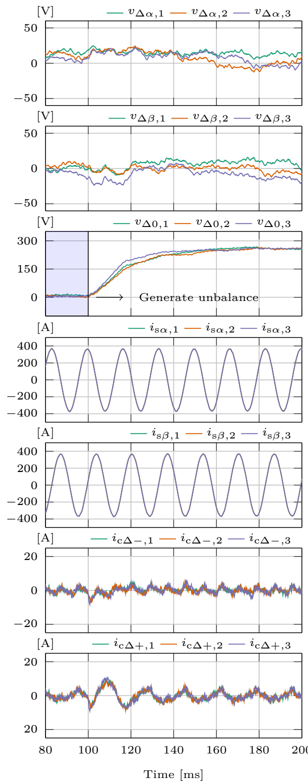

▲ Response under the unbalance scenario 1

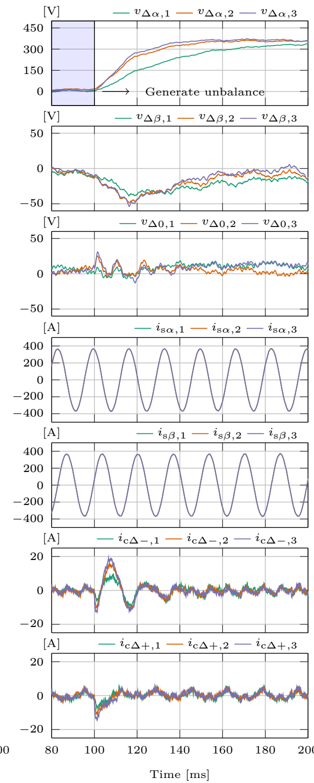

▲ Response under the unbalance scenario 2

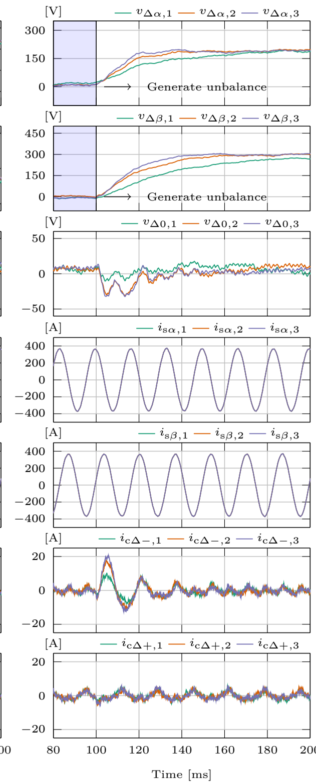

▲ Response under the unbalance scenario 2

- Control of average energies
- Three **decoupled** layers of balancing
  - Total energy control
  - Horizontal balancing
  - Vertical balancing
- Different options with regards to the choice of bal. methods
- Chosen approach **affects the energy balancing dynamics**

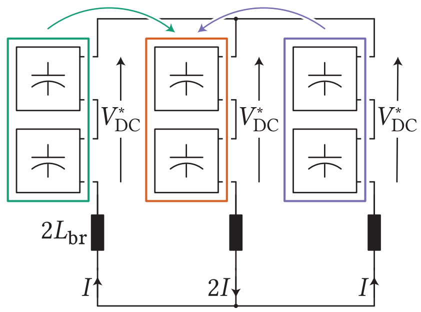

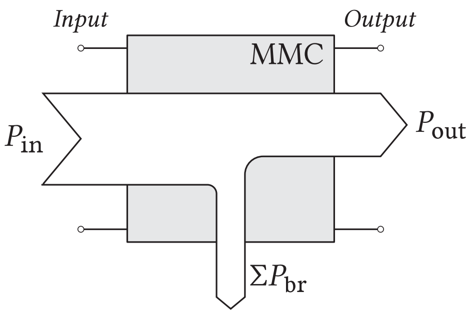

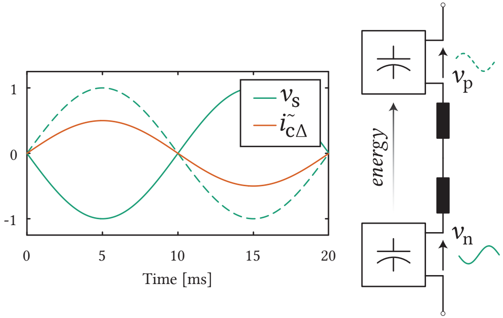

BIBLIOGRAPHY

[1] A. J. Korn, M. Winkelnkemper, and P. Steimer. “Low output frequency operation of the Modular Multi-Level Converter.” *2010 IEEE Energy Conversion Congress and Exposition*. 2010, pp. 3993–3997.

[2] A. J. Korn et al. “Capacitor voltage balancing in modular multilevel converters.” *6th IET Int. Conf. on Power Electronics, Machines and Drives (PEMD 2012)*. Mar. 2012, pp. 1–5.

[3] Kamran Sharifabadi et al. *Design, control, and application of modular multilevel converters for HVDC transmission systems*. John Wiley & Sons, 2016.

[4] Stefan Milovanovic. “MMC-based conversion for MVDC applications.” (2020), p. 268. URL: `http://infoscience.epfl.ch/record/277121`.

[5] P. Münch et al. “Integrated current control, energy control and energy balancing of Modular Multilevel Converters.” *IECON 2010 - 36th Annual Conf. on IEEE Industrial Electronics Society*. Nov. 2010, pp. 150–155.

[6] J. Kolb et al. “Cascaded Control System of the Modular Multilevel Converter for Feeding Variable-Speed Drives.” 30.1 (2015), pp. 349–357.

[7] Gilbert Strang. “Linear algebra and its applications, Thomson Learning.” *Inc., London* (1988).

[8] M. Basić, S. Milovanović, and D. Dujić. “Comparison of two Modular Multilevel Converter Internal Energy Balancing Methods.” *2019 20th International Symposium on Power Electronics (Ee)*. 2019, pp. 1–8.

[9] Kosei Shinoda et al. “Energy difference controllers for MMC without DC current perturbations.” *The 2nd International Conference on HVDC (HVDC2016)*. 2016.

[10] G. Bergna et al. “An Energy-Based Controller for HVDC Modular Multilevel Converter in Decoupled Double Synchronous Reference Frame for Voltage Oscillation Reduction.” 60.6 (2013), pp. 2360–2371.

[11] S. Cui et al. “A comprehensive cell capacitor energy control strategy of a modular multilevel converter (MMC) without a stiff DC bus voltage source.” *2014 IEEE Applied Power Electronics Conference and Exposition - APEC 2014*. 2014, pp. 602–609.

[12] A. Rasic et al. “Optimization of the modular multilevel converters performance using the second harmonic of the module current.” *2009 13th European Conf. on Power Electronics and Appl.* Sept. 2009, pp. 1–10.

[13] J. Pou et al. “Circulating Current Injection Methods Based on Instantaneous Information for the Modular Multilevel Converter.” 62.2 (2015), pp. 777–788.

[14] M. M. Steurer et al. “Multifunctional Megawatt-Scale Medium Voltage DC Test Bed Based on Modular Multilevel Converter Technology.” 2.4 (Dec. 2016), pp. 597–606.

pcim ASIA Hybrid Platform

Modular Multilevel Converters Operating Principles and Applications

Prof. Drazen Dujic, Dr. Stefan Milovanovic
Power Electronics Laboratory
Ecole Polytechnique Fédérale de Lausanne

MODULAR MULTILEVEL CONVERTERS - OPERATING PRINCIPLES AND APPLICATIONS - PART 3

Prof. Dražen Dujić, Dr. Stefan Milovanović

École Polytechnique Fédérale de Lausanne (EPFL)
Power Electronics Laboratory (PEL)
Switzerland

TUTORIAL SCHEDULE

Before the virtual coffee break

Part 1) Introduction and motivation

- MMC Applications
- MMC operating principles
- Modeling and control

Part 2) MMC energy control

- Role of circulating currents
- Branch energy control methods
- Performance benchmark

After the virtual coffee break

Part 3) MMC power extension

- MMC scalability
- Branch paralleling
- Energy control

Part 4) MMC research platform

- MMC system level design
- MMC Sub-module development
- MMC RT-HIL development

MMC POWER CAPACITY EXTENSION

Boosting the power through branch paralleling...

MODULAR MULTILEVEL CONVERTER POWER SCALING

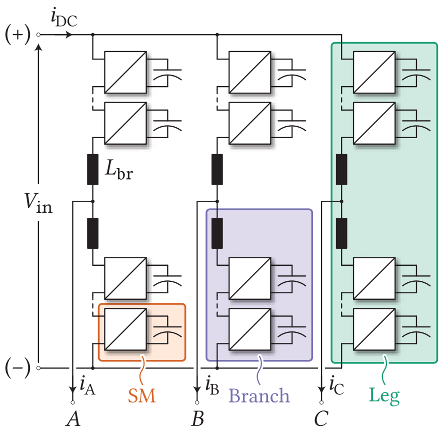

▲ Conventional 3PH MMC

- Series connection of SMs
- Extremely flexible in terms of voltage scaling
- Convenient if application voltage is freely selected

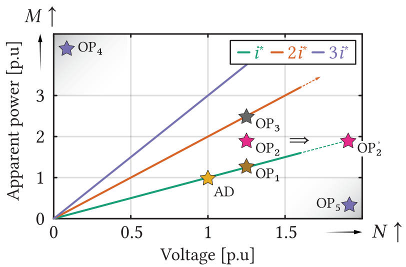

▲ MMC power scaling [1], [2], [3]

- Existing SM design is assumed
- Linear $S = f(V)$ change **for a given current rating**
- Current capacity ↑ ⇒ new characteristics

▲ SM designed at PEL

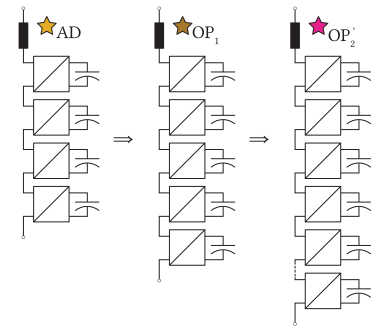

▲ MMC branch voltage scaling

MODULAR MULTILEVEL CONVERTER POWER SCALING

⇒ Increasing the MMC power capacity at fixed operating voltage requires its current handling capabilities boost!

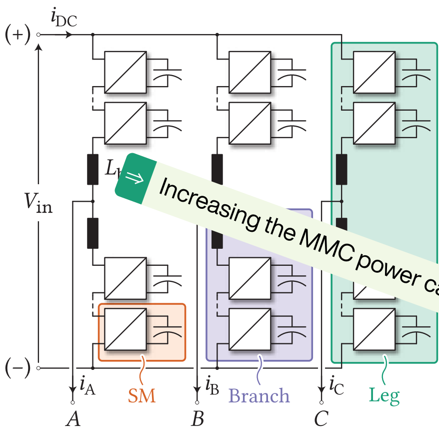

▲ Conventional 3PH MMC

- Series connection of SMs
- Extremely flexible in terms of voltage scaling
- Convenient if application voltage is freely selected

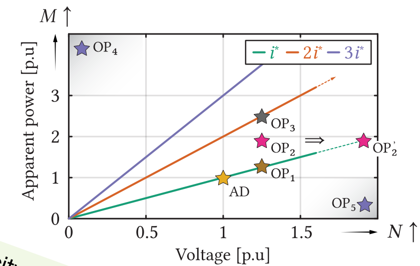

▲ MMC powe... [2]

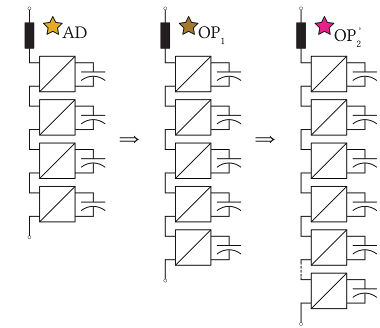

▲ MMC branch voltage scaling

- Existing SM design is assu...
- **Linear** $S = f(V)$ change **for a given** ...
- Current capacity ↑ ⇒ new characteristics

▲ SM designed at PEL

COMMON MMC CURRENT CAPACITY INCREASE METHODS

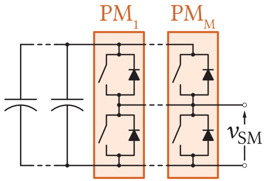

▲ Paralleling semiconductor modules [4], [5]

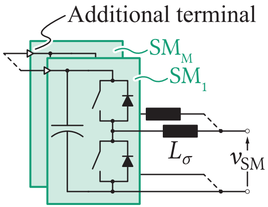

▲ Paralleling SMs [6], [7]

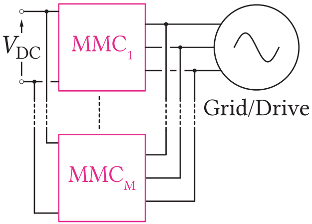

▲ Paralleling converters [8], [9], [10]

COMMON MMC CURRENT CAPACITY INCREASE METHODS

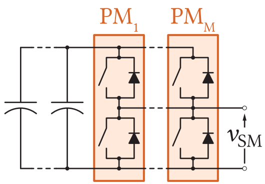

▲ Paralleling semiconductor modules [4], [5]

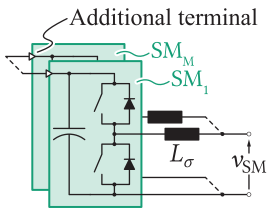

▲ Paralleling SMs [6], [7]

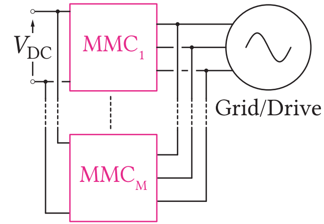

▲ Paralleling converters [8], [9], [10]

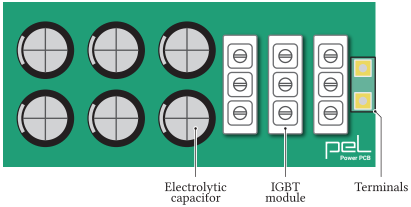

▲ Exemplary cell design; Current capacity - $3I_{\text{rated}}$

COMMON MMC CURRENT CAPACITY INCREASE METHODS

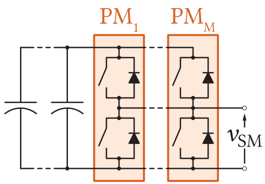

▲ Paralleling semiconductor modules [4], [5]

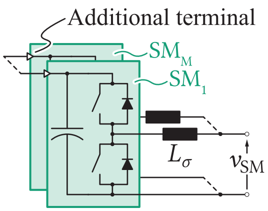

▲ Paralleling SMs [6], [7]

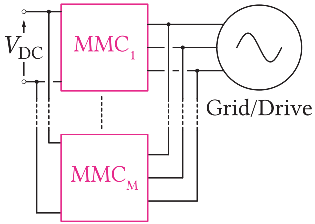

▲ Paralleling converters [8], [9], [10]

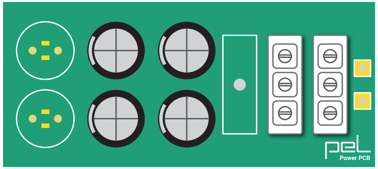

▲ Exemplary cell design; Current capacity - $2I_{\text{rated}}$

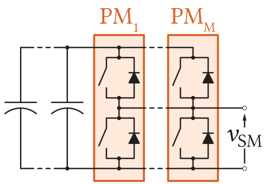

▲ Paralleling semiconductor modules [4], [5]

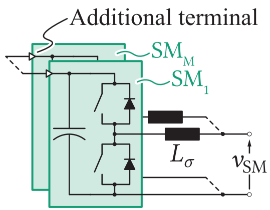

▲ Paralleling SMs [6], [7]

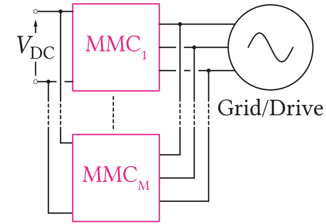

▲ Paralleling converters [8], [9], [10]

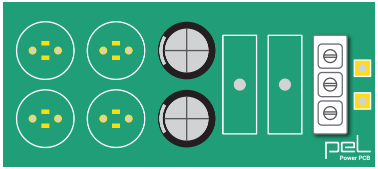

▲ Exemplary cell design; Current capacity - I_{rated}

- Special design considerations
- Cell frame size does not change
- Possible heat sink oversizing?

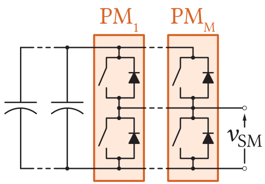

▲ Paralleling semiconductor modules [4], [5]

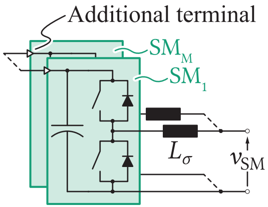

▲ Paralleling SMs [6], [7]

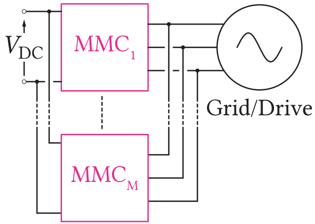

▲ Paralleling converters [8], [9], [10]

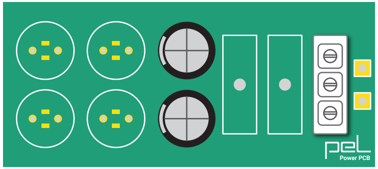

▲ Exemplary cell design; Current capacity - I_{rated}

- ► Special design considerations
- ► Cell frame size does not change
- ► Possible heat sink oversizing?

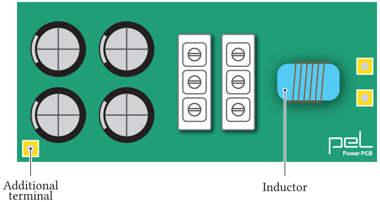

▲ Cell designed for paralleling

- ► Additional inductor is needed
- ► Additional terminal for the capacitors
- ► Special gate driver structure

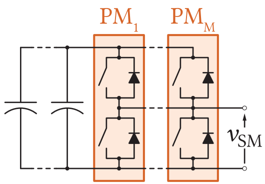

▲ Paralleling semiconductor modules [4], [5]

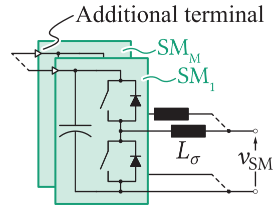

▲ Paralleling SMs [6], [7]

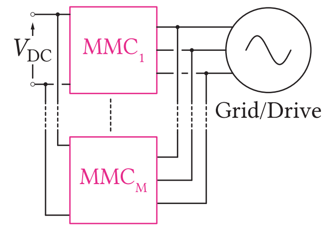

▲ Paralleling converters [8], [9], [10]

- Well known principle
- Problem is shifted to the control domain

Paralleled MMC branches⇒ System simplification

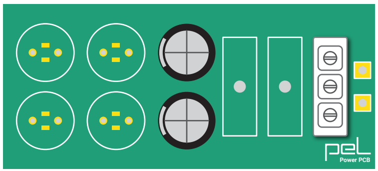

▲ Exemplary cell design; Current capacity - I_{rated}

- Special design considerations
- Cell frame size does not change
- Possible heat sink oversizing?

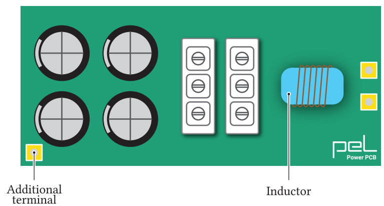

▲ Cell designed for paralleling

- Additional inductor is needed
- Additional terminal for the capacitors
- Special gate driver structure

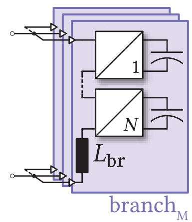

▲ Paralleling branches [2], [3], [11]

COMMON MMC CURRENT CAPACITY INCREASE METHODS

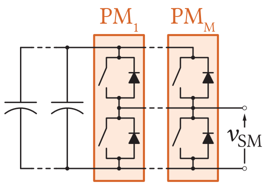

▲ Paralleling semiconductor modules [4], [5]

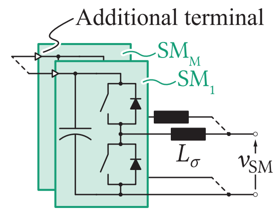

▲ Paralleling SMs [6], [7]

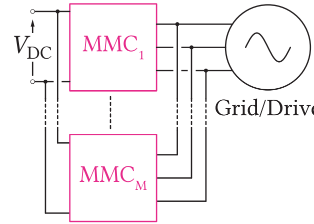

▲ Paralleling converters [8], [9], [10]

- Well known principle
- Problem is shifted to the control domain

Paralleled MMC branches⇒ System simplification

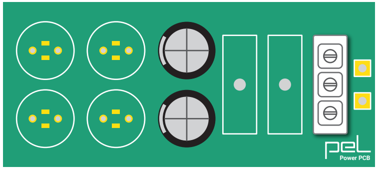

▲ Exemplary cell design; Current capacity - I_{rated}

- Special design considerations
- Cell frame size does not change
- Possible heat sink oversizing?

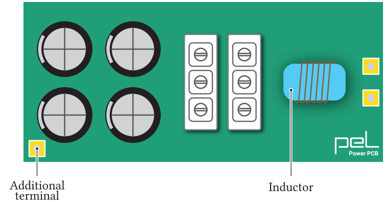

▲ Cell designed for paralleling

- Additional inductor is needed
- Additional terminal for the capacitors
- Special gate driver structure

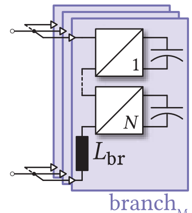

▲ Paralleling branches [2], [3], [11]

⇒ If the branches are paralleled, there is no need to go through a new design process to accomplish the MMC power extension

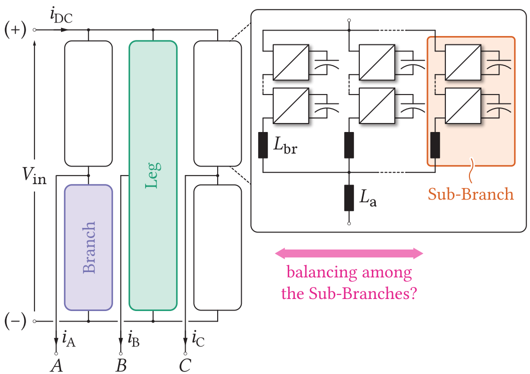

▲ MMC with paralleled (sub)branches

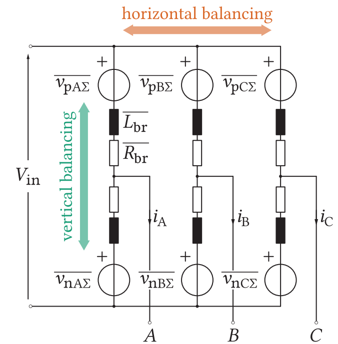

▲ Equivalent circuit of the converter operating with parallel (sub)branches

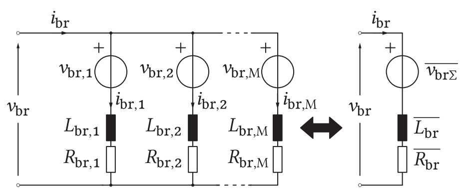

▲ Branch equivalent circuit

$$\overline{v_{br\Sigma}} = \frac{1}{M}\sum_{i=1}^{M} v_{br,i} \quad \text{and} \quad \frac{1}{\overline{Z_{br}}} = \frac{1}{Z_{br,1}} + \frac{1}{Z_{br,2}} + \cdots + \frac{1}{Z_{br,M}}$$

- Equivalent circuit ≡ Conventional MMC
- All state of the art control considerations still hold
- New layers of control to be added?
  - Unequal SBR parameters
  - SBR energy balance
  - SBR current balance
- Voltage quality improvement due to paralleling

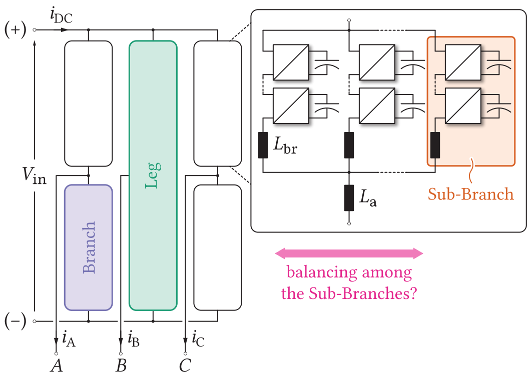

▲ MMC with paralleled (sub)branches

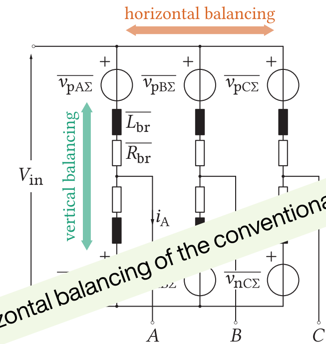

▲ ... of the converter operating with parallel (sub)branches

The SBR energy balancing problem is somewhat similar to the horizontal balancing of the conventional MMC

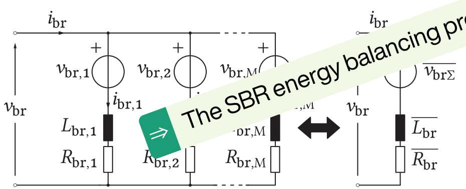

▲ Branch equivalent circuit

$$\overline{v_{br\Sigma}} = \frac{1}{M}\sum_{i=1}^{M} v_{br,i} \quad \text{and} \quad \frac{1}{\overline{\overline{Z_{br}}}} = \frac{1}{Z_{br,1}} + \frac{1}{Z_{br,2}} + \cdots + \frac{1}{Z_{br,M}}$$

- Equivalent circuit ≡ Conventional MMC
- All state of the art control considerations still hold
- New layers of control to be added?
  - Unequal SBR parameters
  - SBR energy balance
  - SBR current balance
- Voltage quality improvement due to paralleling

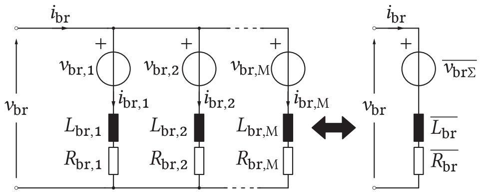

$$\boxed{Z_{br,1} \neq \ldots \neq Z_{br,M} \implies i_{br,1} \neq \ldots \neq i_{br,M}}$$

▲ Equivalent circuit of the branch

$$L_{br}\frac{\mathrm{d}}{\mathrm{d}t}\Big(\underbrace{i_{br,i} - \frac{i_{br}}{M}}_{\Delta i_{br,i}}\Big) + R_{br}\Big(i_{br,i} - \frac{i_{br}}{M}\Big) = \overline{v_{br\Sigma}} - v_{br,i}$$

Should $v_{br,i}$ be chosen like: $v_{br,i} = \overline{v^*_{br\Sigma}} + \Delta v_{br,i}$

$$L_{br}\frac{\mathrm{d}}{\mathrm{d}t}\Delta i_{br,i} + R_{br}\Delta i_{br,i} = -\Delta v_{br,i}$$

- Equal current sharing obtained by means of $\Delta v_{br,i}$
- Total branch voltage must not be corrupted!

$$\boxed{\sum_{i=1}^{M} \Delta v_{br,i} = 0}$$

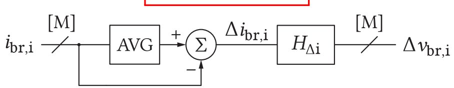

▲ SBR current balancing controller

Energy vs. current sharing ⇒ an important aspect to consider!

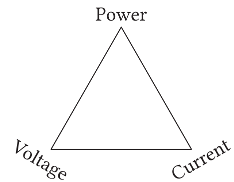

▲ Power extension triangle

Current sharing	YES	NO	NO
Voltage sharing	NO	YES	NO
Power sharing	NO	NO	YES

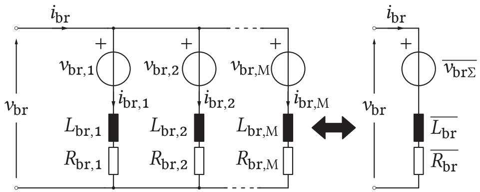

$$\boxed{Z_{\text{br},1} \neq \ldots \neq Z_{\text{br,M}} \implies i_{\text{br},1} \neq \ldots \neq i_{\text{br,M}}}$$

▲ Equivalent circuit of the branch

$$L_{\text{br}} \frac{\mathrm{d}}{\mathrm{d}t} \underbrace{\left(i_{\text{br},i} - \frac{i_{\text{br}}}{M} \right)}_{\Delta i_{\text{br},i}} + R_{\text{br}} \left(i_{\text{br},i} - \frac{i_{\text{br}}}{M} \right) = \overline{v_{\text{br}\Sigma}} - v_{\text{br},i}$$

Should $v_{\text{br,i}}$ be chosen like: $v_{\text{br,i}} = \overline{v^*_{\text{br}\Sigma}} + \Delta v_{\text{br,i}}$

$$L_{\text{br}} \frac{\mathrm{d}}{\mathrm{d}t} \Delta i_{\text{br},i} + R_{\text{br}} \Delta i_{\text{br},i} = -\Delta v_{\text{br},i}$$

- Equal current sharing obtained by means of $\Delta v_{\text{br,i}}$
- Total branch voltage must not be corrupted!

$$\boxed{\textstyle\sum_{i=1}^{M} \Delta v_{\text{br},i} = 0}$$

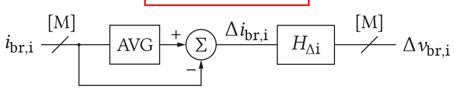

▲ SBR current balancing controller

Energy vs. current sharing ⇒ an important aspect to consider!

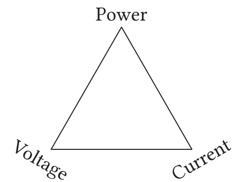

▲ Power extension triangle

Current sharing	YES	NO	NO
Voltage sharing	NO	YES	NO
Power sharing	NO	NO	YES

Current balancing is not enough!

SBR powers are different ⇒ capacitor energy (voltage) divergence

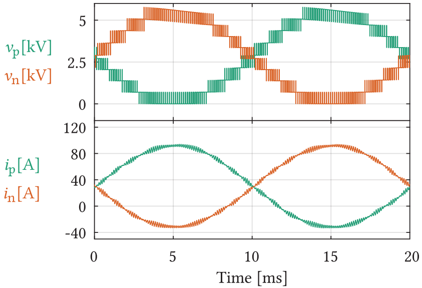

▲ Typical voltage/current waveforms of an SBR

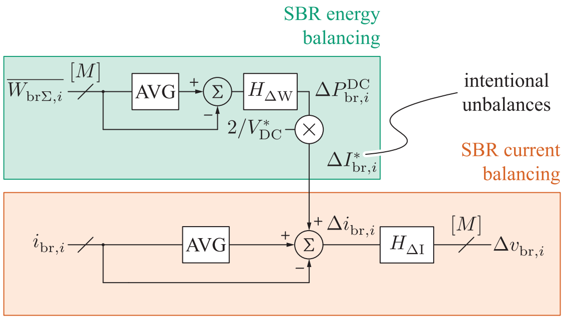

▲ SBR energy controller

(Sub)branch power equation

$$P_{sbr} = \overline{v_{sbr} i_{sbr}}$$
$$= V_{sbr}^{DC} I_{sbr}^{DC} + \overline{v_{sbr}^{\sim} i_{sbr}^{\sim}}$$

Taylor series expansion

$$P_{sbr} = P_{sbr}^{nom} + \underbrace{\Delta P_{sbr}^{DC}}_{\approx \frac{1}{2} V_{DC}^* \Delta I_{sbr}^{DC}} + \underbrace{\Delta P_{sbr}^{AC}}_{\text{depends on } \Delta L_{br}}$$

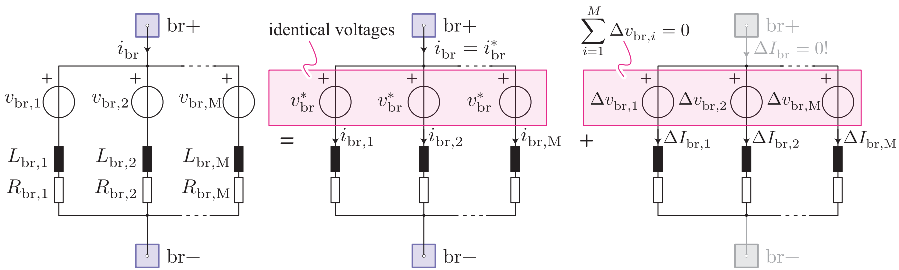

▲ The branch voltage components represented through the superposition principle

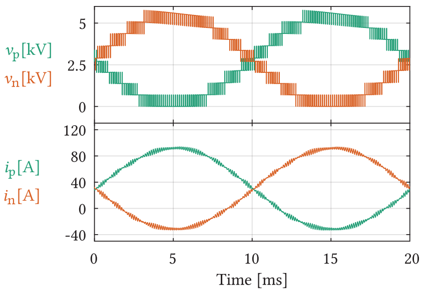

▲ Typical voltage/current waveforms of an SBR

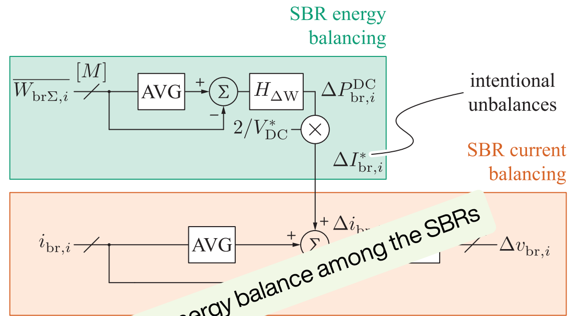

▲ SBR energy controller

Additional control layer included in order to ensure the energy balance among the SBRs

(Sub)branch power equation

$$P_{\mathrm{sbr}} = \overline{v_{\mathrm{sbr}} i_{\mathrm{sbr}}}$$
$$= V^{\mathrm{DC}}_{\mathrm{sbr}} I^{\mathrm{DC}}_{\mathrm{sbr}} + \overline{v^{\sim}_{\mathrm{sbr}} i^{\sim}_{\mathrm{sbr}}}$$

Taylor series expansion

$$P_{\mathrm{sbr}} = P^{\mathrm{nom}}_{\mathrm{sbr}} + \underbrace{\Delta P^{\mathrm{DC}}_{\mathrm{sbr}}}_{\approx \frac{1}{2} V^*_{\mathrm{DC}} \Delta I^{\mathrm{DC}}_{\mathrm{sbr}}} + \underbrace{\Delta P^{\mathrm{AC}}_{\mathrm{sbr}}}_{\text{depends on } \Delta L_{\mathrm{br}}}$$

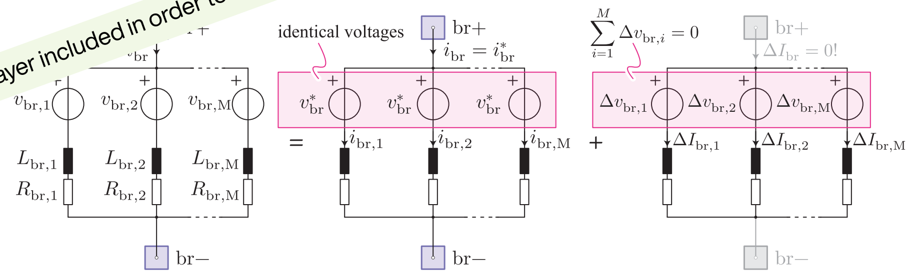

▲ The branch voltage components represented through the superposition principle

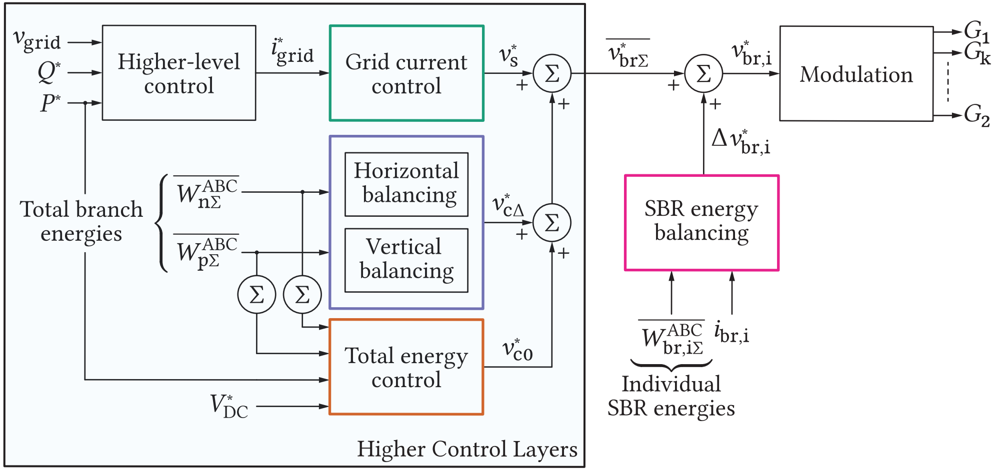

▲ Converter control layers

- Additional control layer (conventional MMC control is retained as can be seen on the left-hand side)
- Decoupling from the higher control levels ensured by means of $\sum_{i=1}^{M} \Delta v_{br,i} = 0$
- Independent on the number of paralleled SBRs (the same approach for both odd and even M)
- Power scalability depending solely upon the control system limitations

SIMULATION RESULTS

	Rated power (P)	Input voltage (V_{in})	No. of cells/SBR (N)	Cell rated voltage (V_{cell})	Cell capacitance (C_{cell})	No. of paralleled SBRs (M)	SBR inductance (L_{br})	SBR resistance (R_{br})	Sw. frequency (f_{sw})
Left	1MW	5kV	5	1kV	0.83mF	2	5mH	60mΩ	999Hz
Right	1.5MW	5kV	5	1kV	0.83mF	3	7.5mH	60mΩ	999Hz

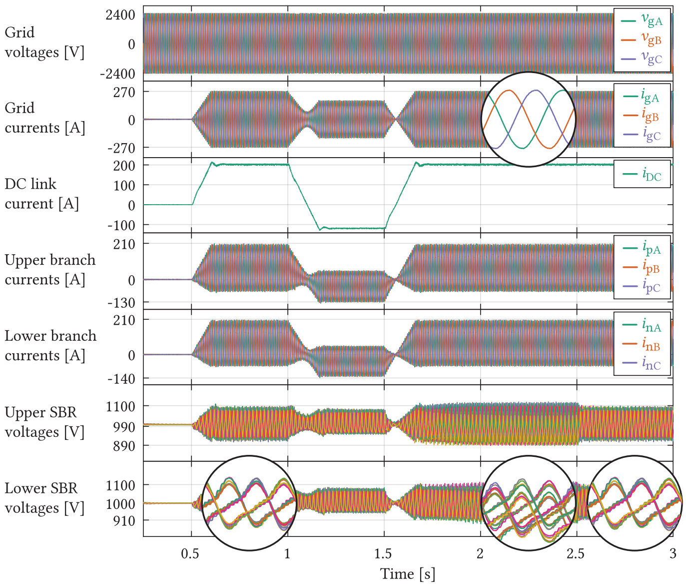

▲ Simulation results in case $M = 2$

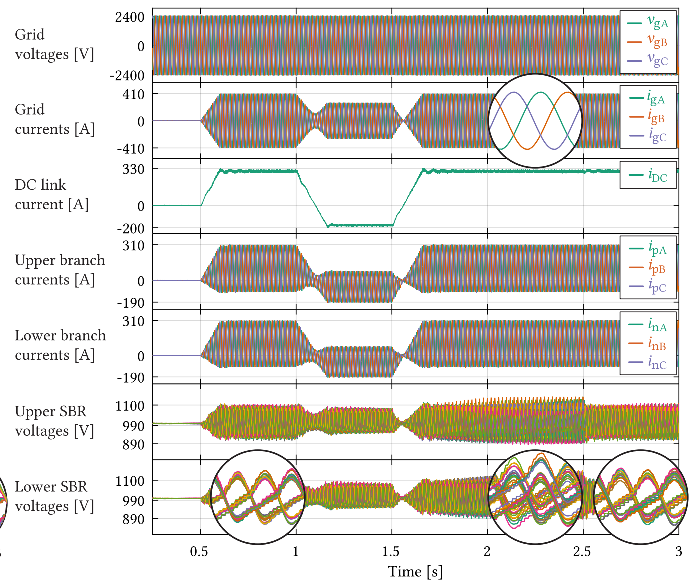

▲ Simulation results in case $M = 3$

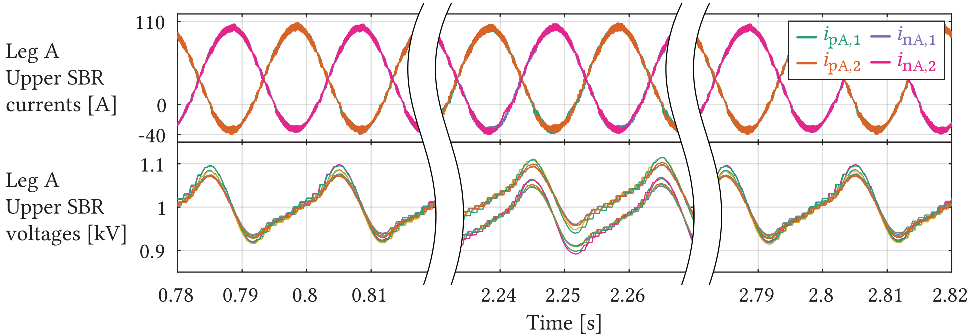

▲ Leg A upper and lower SBR currents (top) along with SBR voltages (bottom) in case $M = 2$

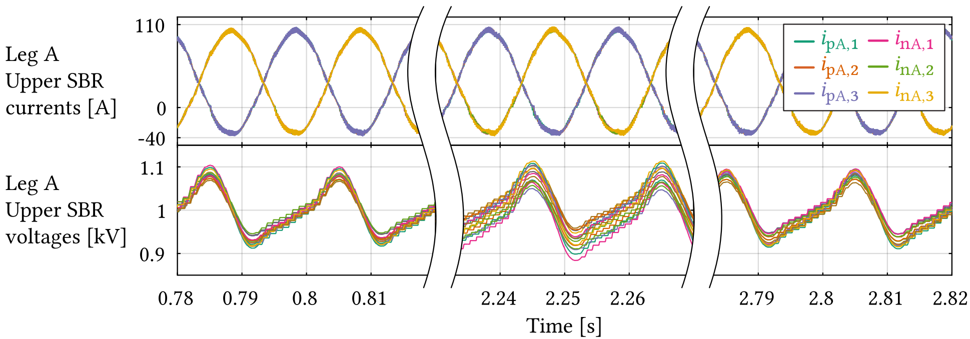

▲ Leg A upper and lower SBR currents (top) along with SBR voltages (bottom) in case $M = 3$

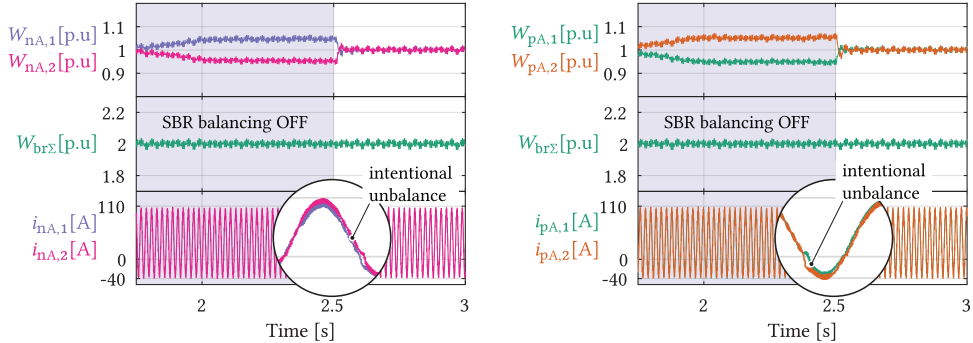

▲ Leg A lower (left) and upper (right) SBR currents and energies in case $M = 2$

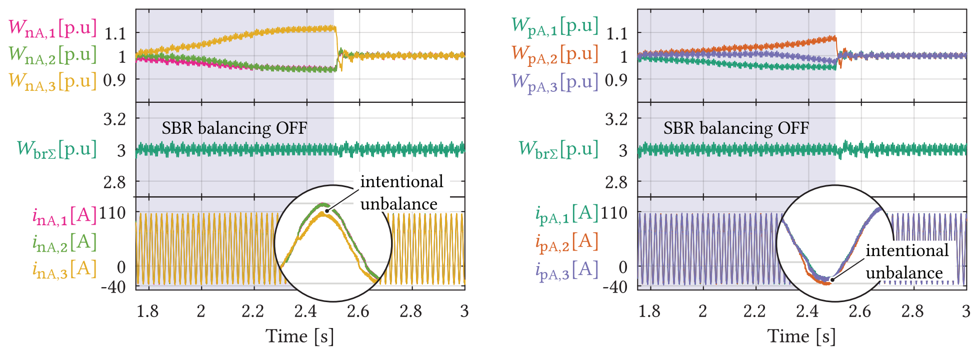

▲ Leg A lower (left) and upper (right) SBR currents and energies in case $M = 3$

SIMULATION RESULTS

There are two relevant questions one might ask:

- How aggressive is the SBR energy balancing controller?
- Should current rating of the SMs be increased owing to the presence of SBR energy balancing?

$$\Delta I^*_{\mathrm{br,i}} = \underbrace{\Delta W_{\mathrm{br,i}\Sigma}}_{\text{Energy error}} \cdot \underbrace{H_{\Delta W}}_{\text{Controller TF}} \cdot \underbrace{\frac{2}{V^*_{\mathrm{DC}}}}_{\text{several kV}}$$

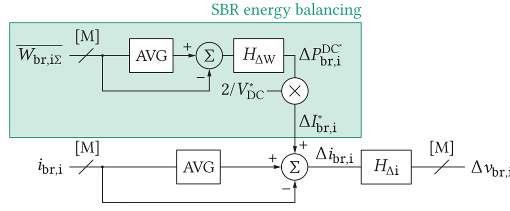

▲ SBR energy control (recap)

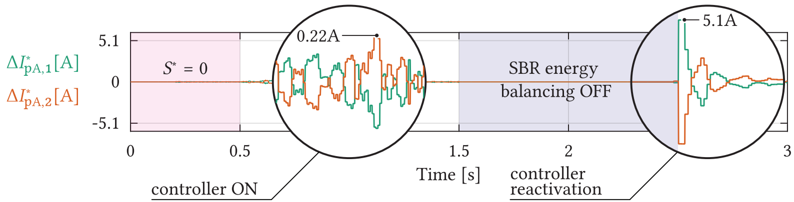

▲ References provided by the SBR energy balancing controller ($M = 2$)

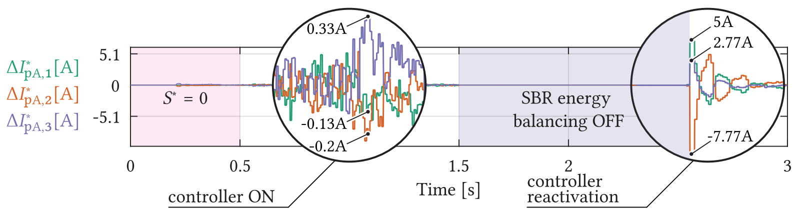

▲ References provided by the SBR energy balancing controller ($M = 3$)

- $\Delta I^*_{\mathrm{br,i}} < 10\%\ \hat{i}_{\mathrm{br}}$ **(Modest response!)**
- $\sum_{i=1}^{M} \Delta I^*_{\mathrm{br,i}} = 0$
- $\sum_{i=1}^{M} \Delta v^*_{\mathrm{br,i}} = 0 \Rightarrow$ no interference with higher control loops

SIMULATION RESULTS

There are two relevant questions one might ask:

- How aggressive is the SBR energy balancing controller?
- Should current rating of the SMs be increased owing to the presence of SBR energy balancing?

$$\Delta I^*_{\mathrm{br,i}} = \underbrace{\Delta W_{\mathrm{br,i}\Sigma}}_{\text{Energy error}} \cdot \underbrace{H_{\Delta \mathrm{W}}}_{\text{Controller TF}} \cdot \underbrace{\frac{2}{V^*_{\mathrm{DC}}}}_{\text{several kV}}$$

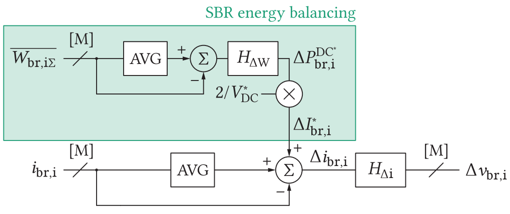

▲ SBR energy control (recap)

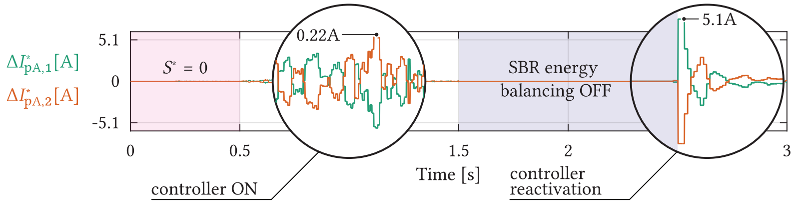

▲ References provided by the SBR energy balancing controller ($M = 2$)

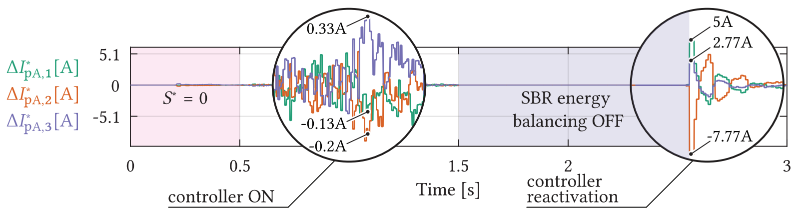

▲ References provided by the SBR energy balancing controller ($M = 3$)

- $\Delta I^*_{\mathrm{br,i}} < 10\%\ \hat{i}_{\mathrm{br}}$ **(Modest response!)**
- $\sum_{i=1}^{M} \Delta I^*_{\mathrm{br,i}} = 0$
- $\sum_{i=1}^{M} \Delta v^*_{\mathrm{br,i}} = 0 \Rightarrow$ no interference with higher control loops

⇒ No need for SM current rating upgrade!

SUMMARY

- **MMC power extension** as a main motivation
- **Simple and cheap** (no need for major redesign of the converter parts)
- The challenge is shifted to the **control domain**
- State of the art control methods + **Additional loops**
- Possible AC **voltage quality improvement**

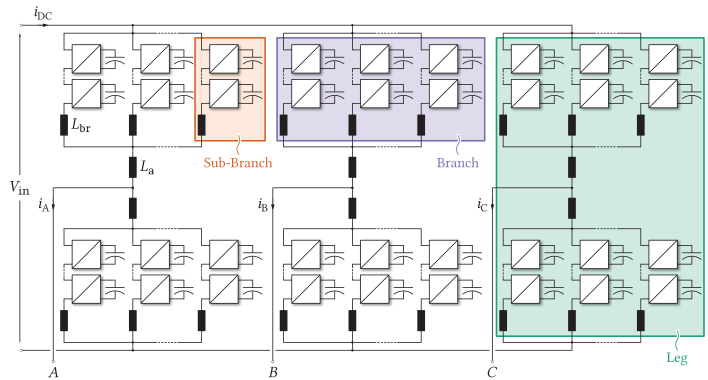

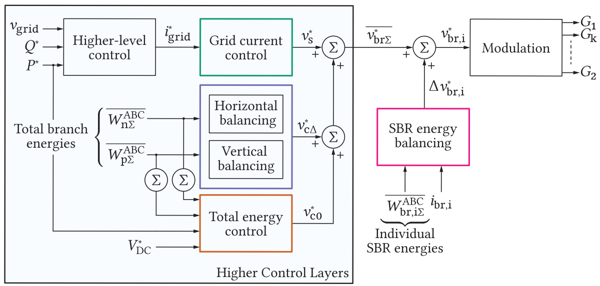

BIBLIOGRAPHY

[1] Miodrag Basic, Pedro CO Silva, and Drazen Dujic. “High Power Electronics Innovation Perspectives for Pumped Storage Power Plants.” (2018).

[2] S. Milovanović and D. Dujić. “On Facilitating the Modular Multilevel Converter Power Scalability Through Branch Paralleling.” *2019 IEEE Energy Conversion Congress and Exposition (ECCE)*. Sept. 2019.

[3] Stefan Milovanovic. “MMC-based conversion for MVDC applications.” (2020), p. 268. URL: `http://infoscience.epfl.ch/record/277121`.

[4] Andreas Volke, Jost Wendt, and Michael Hornkamp. *IGBT modules: technologies, driver and application*. Infineon, 2012.

[5] R. Hermann et al. “Parallel Connection of Integrated Gate Commutated Thyristors (IGCTs) and Diodes.” 24.9 (Sept. 2009), pp. 2159–2170.

[6] R. Grinberg et al. “Study of overcurrent protection for modular multilevel converter.” *2014 IEEE Energy Conversion Congress and Exposition (ECCE)*. Sept. 2014, pp. 3401–3407.

[7] M. M. Steurer et al. “Multifunctional Megawatt-Scale Medium Voltage DC Test Bed Based on Modular Multilevel Converter Technology.” 2.4 (Dec. 2016), pp. 597–606.

[8] Josep Pou et al. “Current balancing strategy for interleaved voltage source inverters.” *EPE Journal* 21.1 (2011), pp. 29–34.

[9] J. Pou et al. “Control strategy to balance operation of parallel connected legs of modular multilevel converters.” *2013 IEEE International Symposium on Industrial Electronics*. 2013, pp. 1–7.

[10] F. Gao et al. “Control of Parallel-Connected Modular Multilevel Converters.” *IEEE Transactions on Power Electronics* 30.1 (2015), pp. 372–386.

[11] S. Milovanovic and D. Dujic. “On Power Scalability of Modular Multilevel Converters: Increasing Current Ratings Through Branch Paralleling.” *IEEE Power Electronics Magazine* 7.2 (2020), pp. 53–63.

Modular Multilevel Converters Operating Principles and Applications

Prof. Drazen Dujic, Dr. Stefan Milovanovic
Power Electronics Laboratory
Ecole Polytechnique Fédérale de Lausanne

MODULAR MULTILEVEL CONVERTERS - OPERATING PRINCIPLES AND APPLICATIONS - PART 4

Prof. Dražen Dujić, Dr. Stefan Milovanović

École Polytechnique Fédérale de Lausanne (EPFL)
Power Electronics Laboratory (PEL)
Switzerland

Before the virtual coffee break

Part 1) Introduction and motivation
- MMC Applications
- MMC operating principles
- Modeling and control

Part 2) MMC energy control
- Role of circulating currents
- Branch energy control methods
- Performance benchmark

After the virtual coffee break

Part 3) MMC power extension
- MMC scalability
- Branch paralleling
- Energy control

Part 4) MMC research platform
- MMC system level design
- MMC Sub-module development
- MMC RT-HIL development

MMC RESEARCH PLATFORM

High power university lab prototype and versatile HIL system

ONGOING MMC RELATED ACTIVITIES

Pump Hydro Storage Research Platform

- MMC based AC/AC converter
- Interface between SG and local AC grid

▲ MMC-Based AC/AC Converter for Pump Hydro Applications

Flexible DC Source (FlexDCS)

- MMC Based DC Source rated at 0.5 MVA
- Reconfiguration unit allows series/parallel operation
- Four quadrant operation
- Flexible voltage source in a range ±10 kV DC
- Flexible current source in a range ±100 A DC

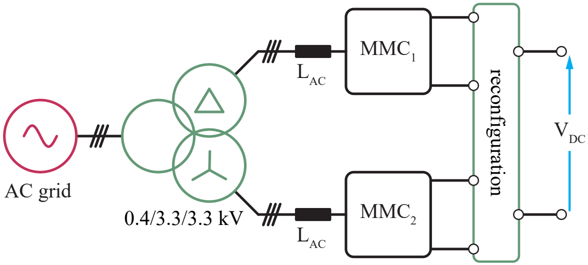

▲ Flexible DC Source Topology [1]

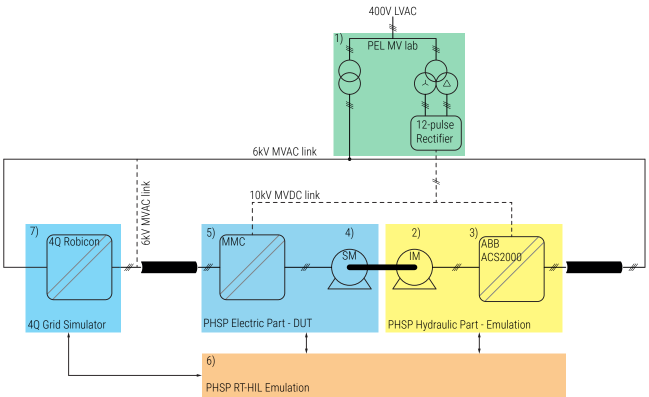

▲ Pumped Hydro Storage Plants - Research Platform

MMC – CONVERTER LAYOUT

MMC demonstrator ratings are:

- 500 kVA
- 10 $kV_{dc} \longleftrightarrow 400\ V_{ac}$ or $6.6\ kV_{ac}$
- 16 low voltage cells per branch ⇒ 32 cells per phase (cabinet) ⇒ 96 cells in total
- Industrial central controller and communication (ABB AC PEC 800)

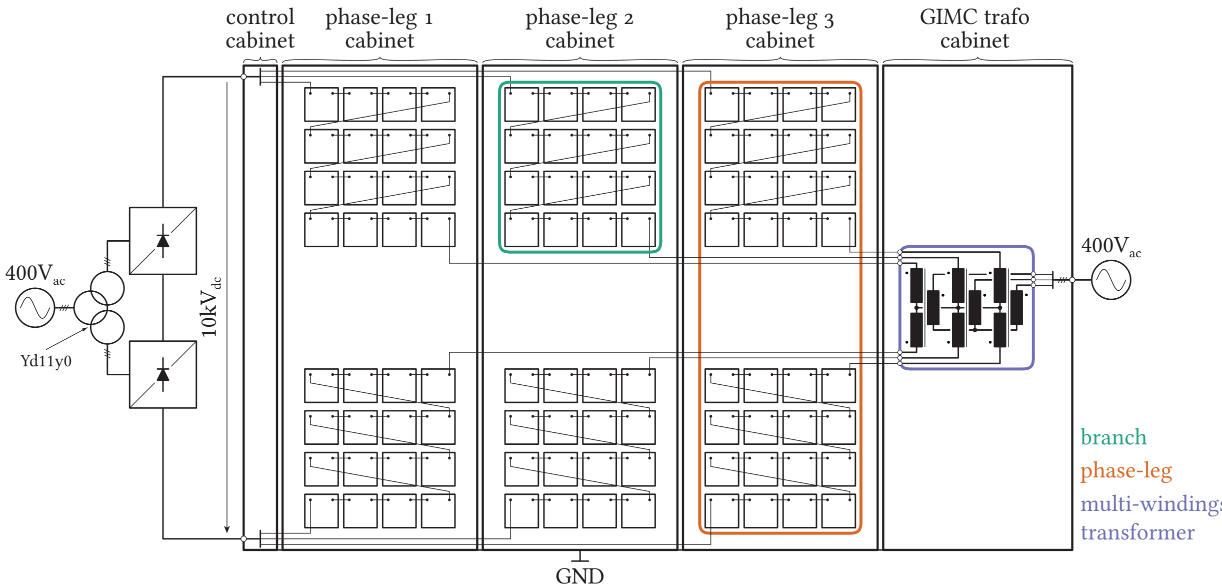

▲ DC/3-AC MMC Converter Layout [2]

MMC – SUBMODULE OPTIMIZATION

Submodule

- 1.2 kV / 50 A full-bridge IGBT module
- $C_{cell} = 2.25\,\text{mF}$

Thermal design

- Cell level: detailed FEM
- Cabinet level: simplified FEM

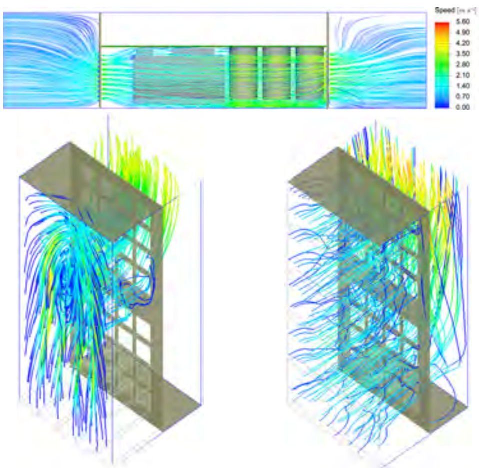

▲ CFD simulations

Semiconductor losses

- Virtual Submodule concept has been utilized [3]
- Closed-loop waveforms are approached by analytical waveforms

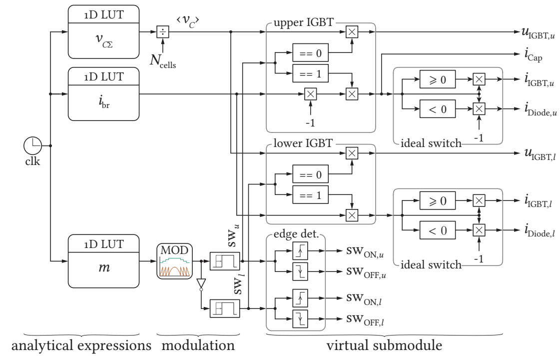

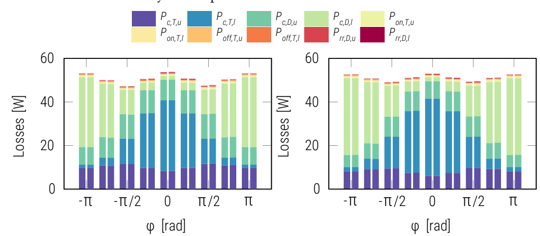

▲ PS-PWM, DC circ

▲ PS-PWM, DC+2nd circ

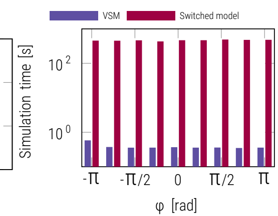

▲ Time benchmark

INSULATION COORDINATION (I)

System partitioning

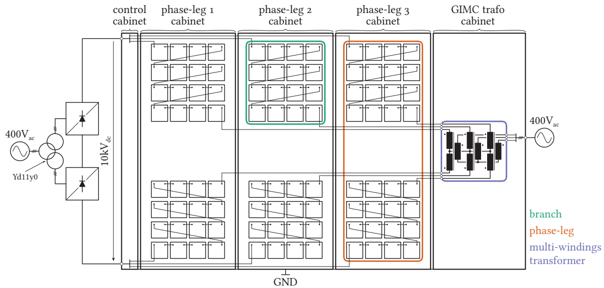

Zones definition [4]

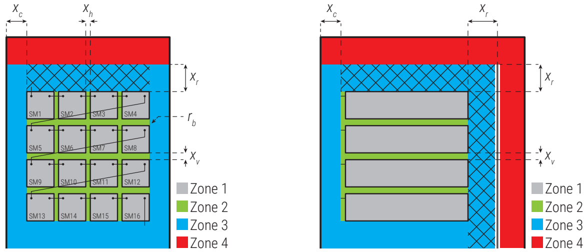

Zone 1 (ins. coord. inside a SM's enclosure) system voltage: 1 kV_{ac}

Zone 2 (ins. coord. branch)

- Horizontal system voltage: 1 kV_{ac}
- Vertical system voltage: 3.6 kV_{ac}

Zone 3 (ins. coord. branch - cabinet (at GND)) system voltage: 6.6 kV_{ac}

Zone 4 (ins. coord. for LV circuits) system voltage: 0.4 kV_{ac}

Standards

- UL840 for cell PCB (< 1 kV)
- IEC61800-5-1 (AC motor drives)
  - Pollution degree 2: "Normally, only non-conductive pollution occurs. Occasionally, however, a temporary conductivity caused by condensation is to be expected, when the PDS is out of operation."
  - Overvoltage category II: "Equipment not permanently connected to the fixed installation. Examples are appliances, portable tools and other plug-connected equipment."

Zone 2

- Box at dc- cell's potential (floating)
- Box corner radius: 3 mm
- MKHP (high CTI material) drawer holding 4 cells

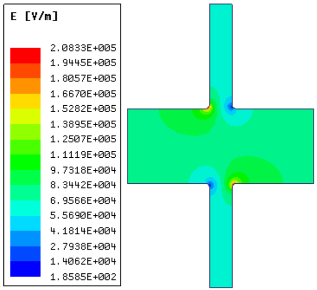

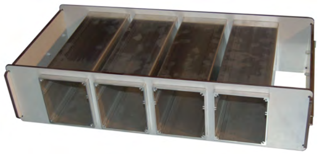

▲ E-field FEM simulations for drawer design

INSULATION COORDINATION (II)

- √ MV MMC converter laboratory prototype layout compliant with:
  - UL840 (for cell)
  - IEC 61800-5-1
- √ Complete AC dielectric withstand tests on real prototype [4]

▲ Cabinet of one phase-leg (32 cells) in Faraday cage during insulation coordination testing

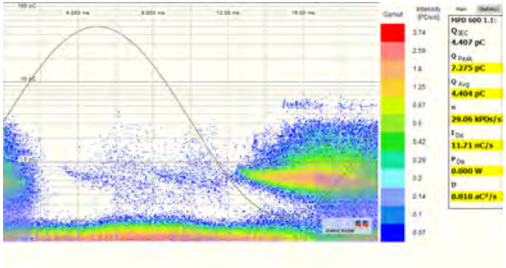

▲ AC dielectric withstand test result

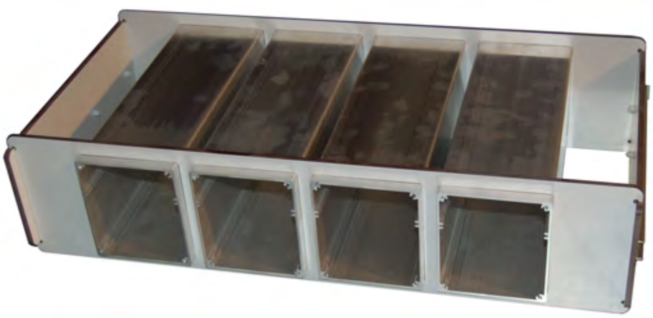

▲ Drawer holding 4 cell (MKHP material)

MMC – CONVERTER LAYOUT

MMC demonstrator ratings are:

- 500 kVA (2 x 250 kVA)
- $\pm$ 10 $kV_{dc} \longleftrightarrow$ 2 x 3.3 kV_{ac}
- 8 low voltage cells per branch $\Rightarrow$ 16 cells per MMC phase $\Rightarrow$ 58 cells in total - per MMC
- Industrial central controller and communication (ABB AC PEC 800)

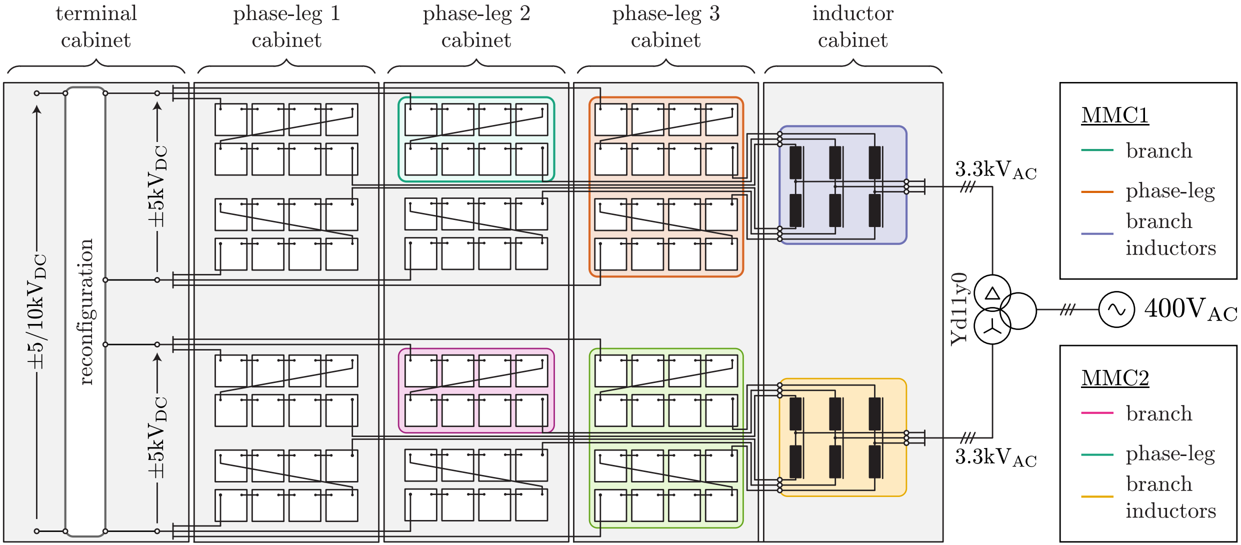

▲ Flexible DC Source Converter Layout

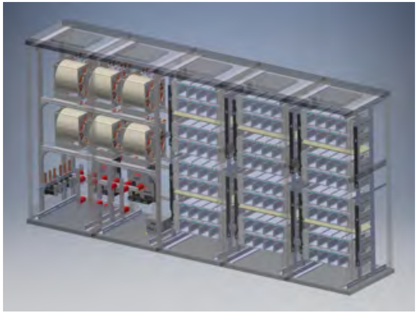

▲ MMC CAD development

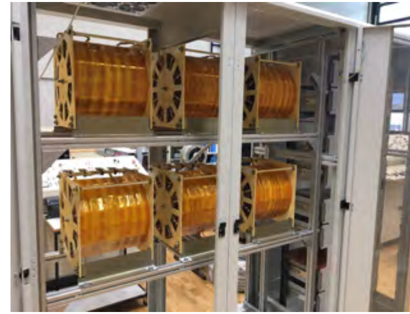

▲ MMC coupled air-core branch inductors

▲ MMC - Actual mechanical assembly

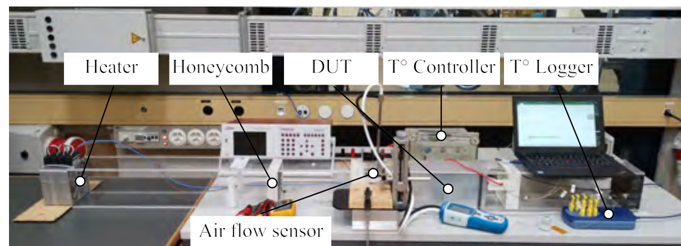

▲ MMC Submodule thermal heat-run test setup [5]

MMC SUB-MODULE

Low voltage based sub-module including cell controller

MMC SUB-MODULE – STRUCTURE

Key Features

- Low voltage power components
- Full-bridge sub-module structure
- Sub-module rated voltage - 625 V
- Sub-module insulation coordination - 900 V
- Two interconnected PCBs: **Power PCB** and **Control PCB**

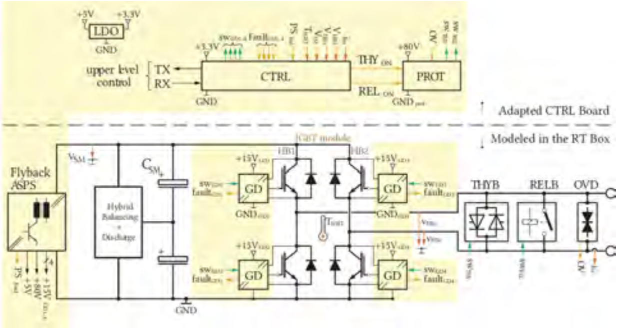

▲ MMC Sub-module Structure: Yellow parts - Control PCB

▲ Developed MMC FB sub-module based on the 1.2kV IGBTs

MMC SUB-MODULE – POWER PCB

- Power processing part
- Semikron full-bridge IGBT module 1.2 kV/50 A
- Bank of electrolytic capacitors $C_{sm} = 2.25$ mF
- Protection devices: Bypass thyristor, relay and OVD
- Current and voltage measurements
- Hybrid balancing circuitry
- Hardware reconfiguration (HR)

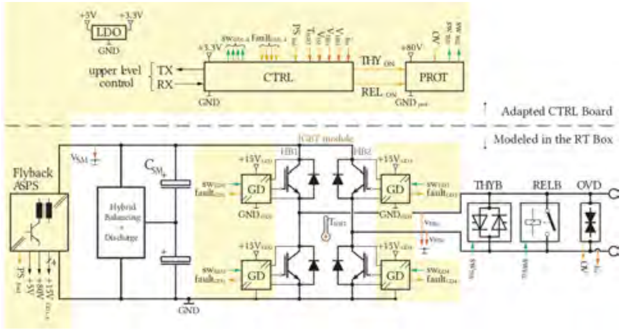

▲ MMC Sub-module Structure: Yellow parts - Control PCB

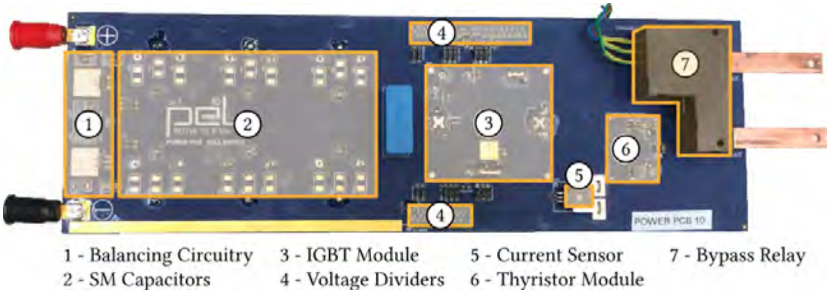

▲ Overview of the Power PCB

MMC SUB-MODULE – CONTROL PCB

- Flyback based auxiliary power supply
  - +5V Output, used as a control feedback
  - +80V Protection supply
  - +15V Gate drivers supplies
  - +15V Self-supply output
- DSP based main SM Controller
  - Communication with upper level control
  - Voltage and current measurements
  - Monitoring the SM condition
  - Decentralized modulation
- Gate drivers
- Protection logic
  - Protection activation from upper level control
  - Protection activation from DSP
  - Protection activation by overvoltage detection
- Fiber-optical communication link

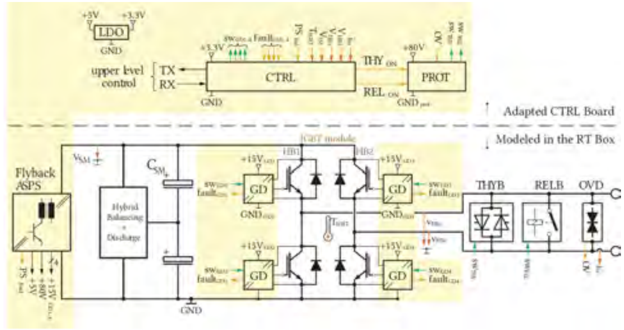

▲ MMC Sub-module Structure: Yellow parts- Control PCB

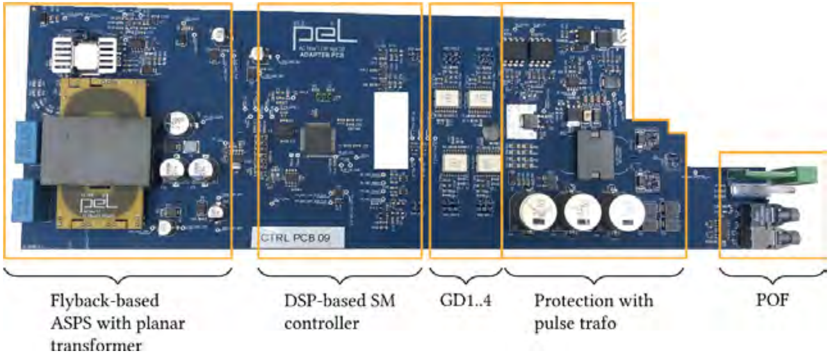

▲ Overview of the Control PCB

AUXILIARY SUB-MODULE POWER SUPPLY (I)

Possible concepts

- Externally supplied
  - Single wire loop
  - Siebel
  - Inductive power transfer
- Internally supplied
  - Tapped inductor Buck
  - Flyback

Choice [6]

- Flyback with 6 isolated secondaries
  - 1× 5 V, 4 W for the controller supply (V_{+5V}). This output is tightly regulated in closed-loop.
  - 4× 15 V, 1.5 W for the IGBT gate drivers ($V_{GD1..4}$)
  - 1× 80 V, 15 W for 15 s operation when activated for the protection circuit (V_{prot})

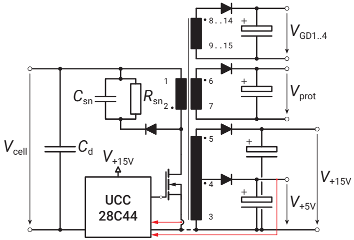

Planar trafo design

- PCB windings (isolation requirements!)
- Planar ferrite cores with custom gapping (COSMO ferrites)

Matlab design tool

- Account for flux fringing [7]
- BH curve for CF297
- Jiles-Atherton parametrization

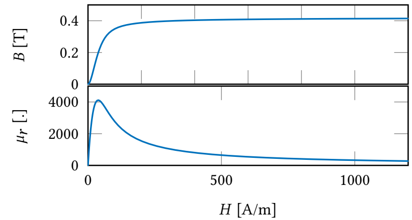

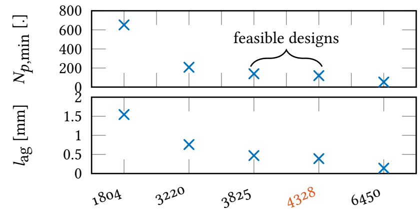

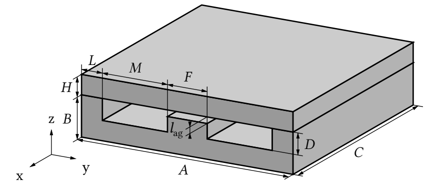

FEM

- Validate Matlab design
- 3D model for accurate leakage flux

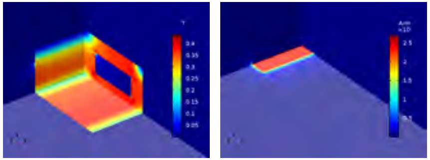

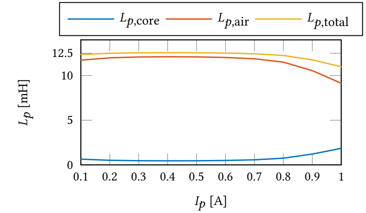

AUXILIARY SUB-MODULE POWER SUPPLY (II)

Transformer assembly

- 14 copper layers PCB
- Custom gapped ferrite E+I core

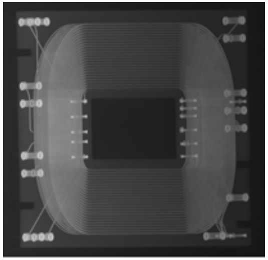

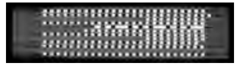

AC dielectric withstand test

- Way below threshold level of 10pC

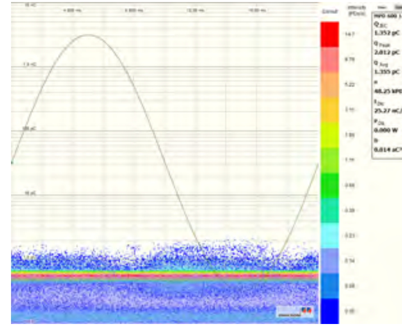

Tests

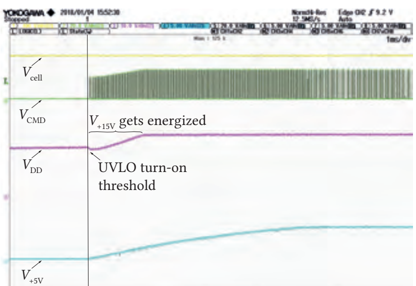

▲ Start-up

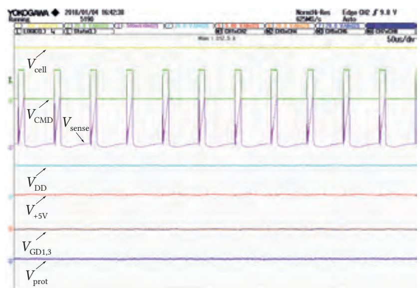

▲ Steady-state operation

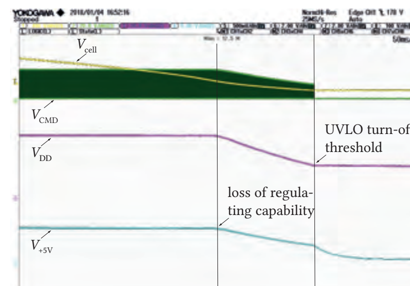

▲ Shut-down (slow dv/dt from Delta power-supply used to emulate the cell)

MMC SUB-MODULE POWER TESTS

Extensive testing has been done:

- Power tests
- Thermal heat-runs
- Over current tests
- Loss of power supply
- DC link over voltage
- Terminal over voltage
- Short-circuit tests
- ...

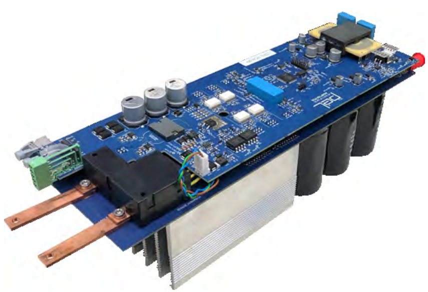

▲ Developed MMC FB sub-module

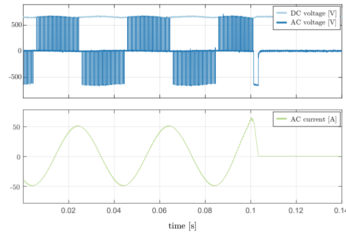

▲ MMC SM over current test

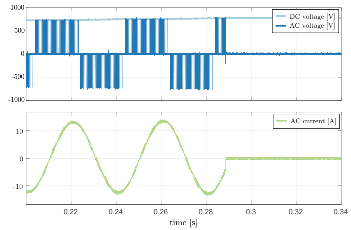

▲ MMC SM over voltage test

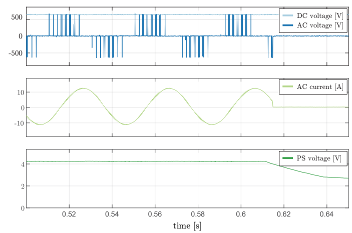

▲ Power supply under voltage detection

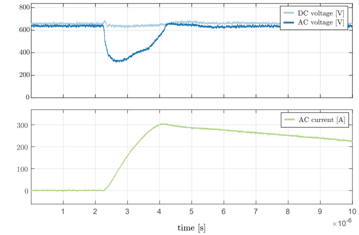

▲ Short circuit test (Desat detection)

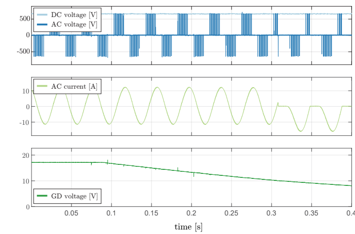

▲ Gate Driver failure

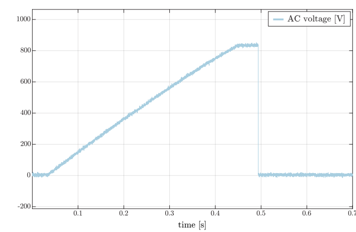

▲ AC terminals over voltage detection

MMC DIGITAL TWIN

RT-Box based distributed HIL system

MMC – RT-HIL SYSTEM (I)

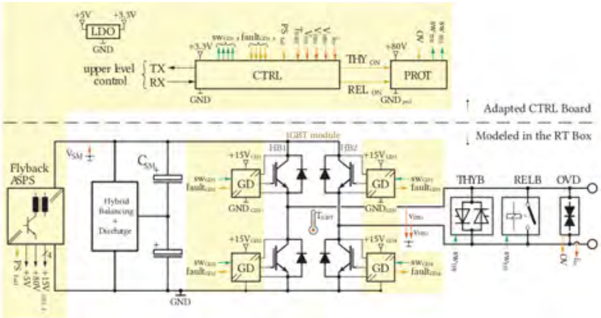

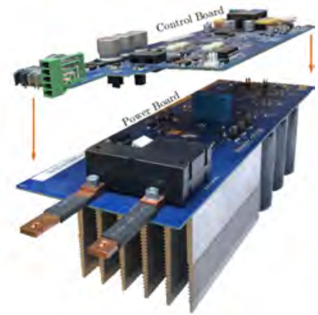

▲ Submodule layout

Submodule

- Full-Bridge IGBT module
- Capacitor bank
- Protection circuitry
- Balancing circuit
- Auxiliary power supply

ABB controller

- 2 × PEC 800 (Master/Slave config.)
- PECMI (measurements)
- COMBIO (relays, switches, etc.)
- HUB (data gateway)

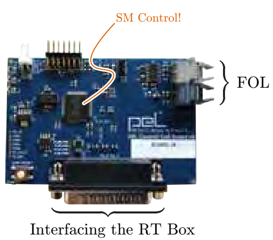

▲ SM control board adapted for HIL testing

▲ RT Boxes used to host up to eight MMC control cards

▲ Application (Grid) RT Box

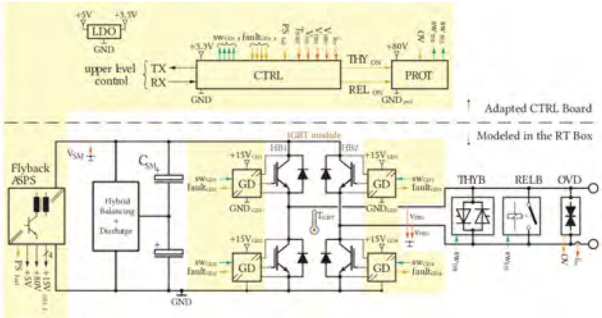

▲ Submodule layout

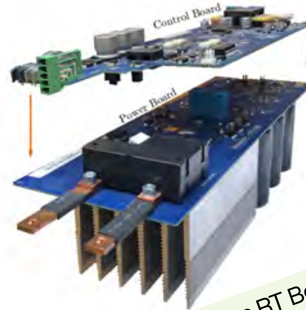

Submodule

- Full-Bridge IGBT module
- Capacitor bank
- Protection circuitry
- Balancing circuit
- Auxiliary power s

ABB contr

- 500 (Master/Slave config.)
- PECMI (measurements)
- COMBIO (relays, switches, etc.)
- HUB (data gateway)

⇒ Power part, excluding the balancing circuitry and power supply, is modeled in the RT Box ⇒ **VIRTUAL POWER PROCESSING**

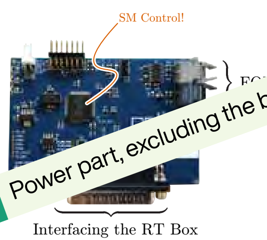

▲ SM control board adapted for HIL testing

▲ RT Boxes used to host up to eight MMC control cards

▲ Application (Grid) RT Box

MMC – RT-HIL SYSTEM (II)

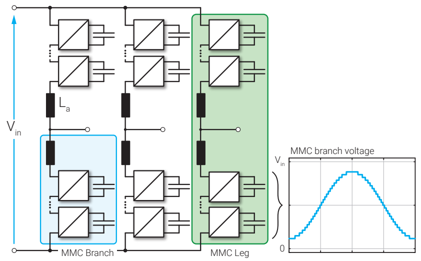

▲ Modular Multilevel Converter

▲ Channels available on the RT Box

Description	No. of channels/ connectors	Voltage range
Analog Inputs	16	$-10V \dots 10V$
Analog Output	16	$-10V \dots 10V$
Digital Inputs	**32**	3.3V or 5V
Digital Outputs	32	3.3V or 5V
SFP Connectors	4	N.A.

Limitation in the number of DIs

One RT Box hosts up to 8 SMs!

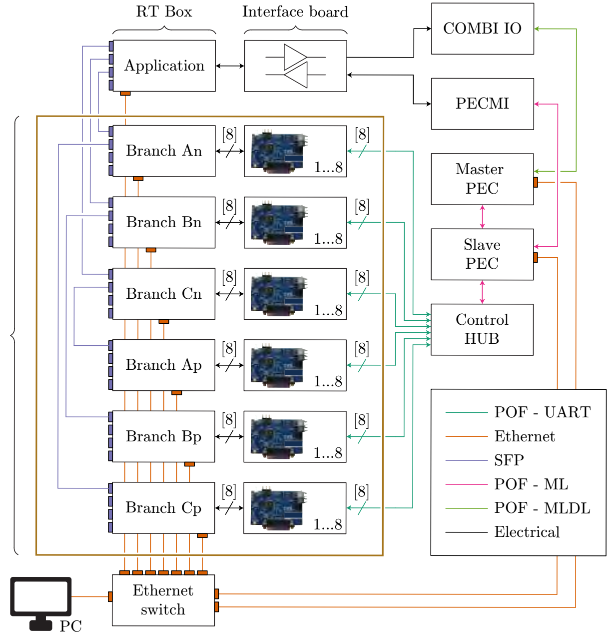

▲ Wiring communication scheme of a system comprising one MMC serving an arbitrary application

System summary

- 6 RT-Boxes - one per Branch of the MMC
- 1 RT-Box - Application (AC and DC side)
- ACS 800 PEC - ABB Industrial controller
- ABB other peripheral control boards
- Integrated into IT cabinet

▲ Application (Grid) RT Box

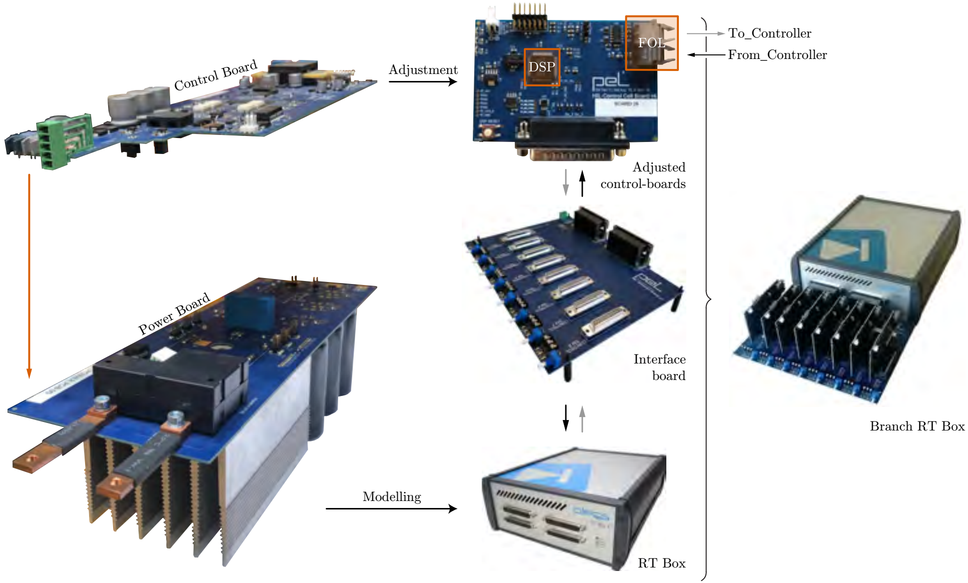

▲ Transformation of MMC cell into digital twin equivalent system

MMC – RT-HIL SYSTEM (IV)

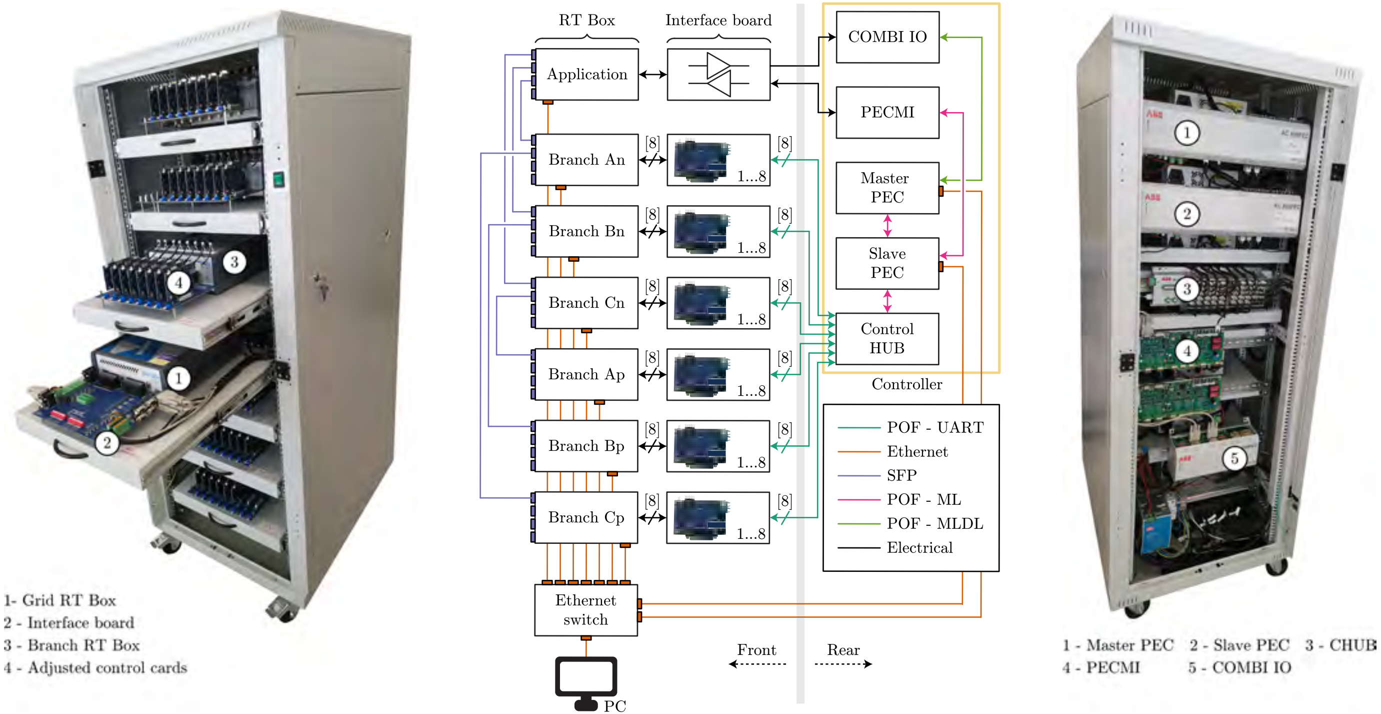

▲ Digital Twin - Realized RT-HIL system for control verification purpose: (left) front view; (middle) wiring scheme; (right) back view.

MMC RT-HIL extended version

- 4 RT-HIL cabinets - one per MMC
- 48 cells per one RT-HIL cabinet
- Various reconfigurations are possible

▲ RT Box hosting application

▲ RT Box hosting eight MMC sub-modules

▲ Digital Twins - Four RT-HIL systems allowing for various topological reconfigurations

CONTROL SW TESTING

Results recorded from the HIL platform

▲ Simulated converter param.

Rated power (S^*)	1MVar
Output voltage (V_{DC})	5kV
Grid voltage (v_g)	3.3kV
No. of SMs per branch (N)	6
SM capacitance (C_{sm})	3.36mF
Branch inductance (L_{br})	2.5mH
Brach resistance (R_{br})	60mΩ
PWM carrier frequency (f_{pwm})	1kHz
Fudamental frequency (f_o)	60Hz
Charging resistors (R_{ch})	210Ω

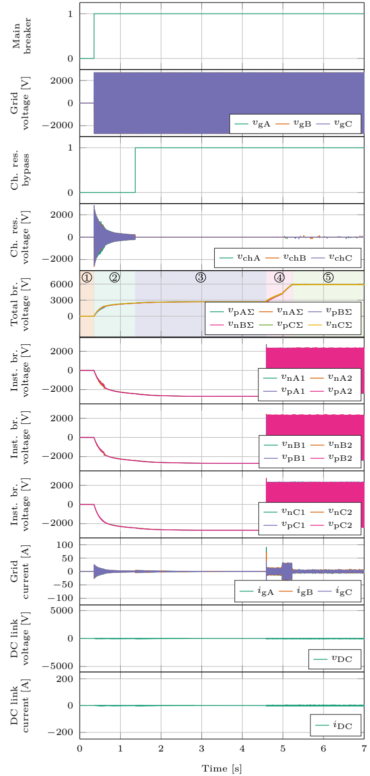

▲ Converter charging process presented through several stages

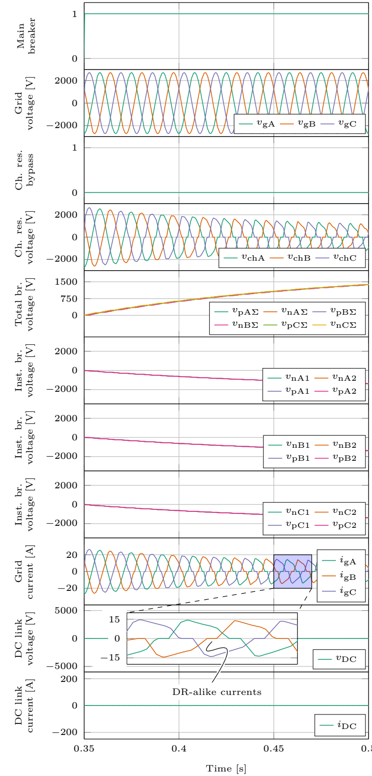

▲ A fraction of the interval referred to as the passive charging

▲ Simulated converter param.

Rated power (S^*)	1MVar
Output voltage (V_{DC})	5kV
Grid voltage (v_g)	3.3kV
No. of SMs per branch (N)	6
SM capacitance (C_{sm})	3.36mF
Branch inductance (L_{br})	2.5mH
Brach resistance (R_{br})	60mΩ
PWM carrier frequency (f_{pwm})	1kHz
Fudamental frequency (f_o)	60Hz
Charging resistors (R_{ch})	210Ω

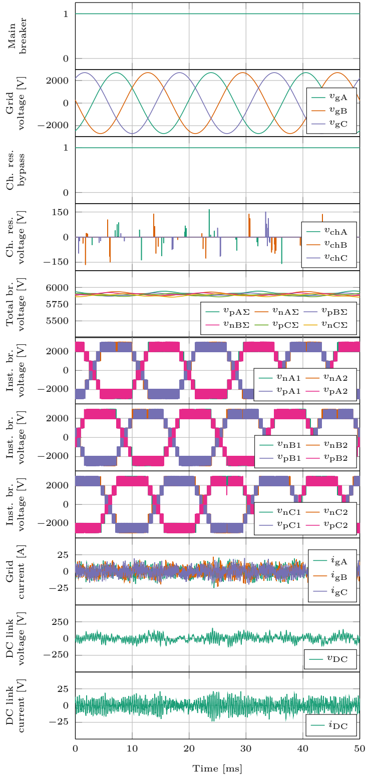

▲ Converter operation at no load ($P_{DC} = 0$)

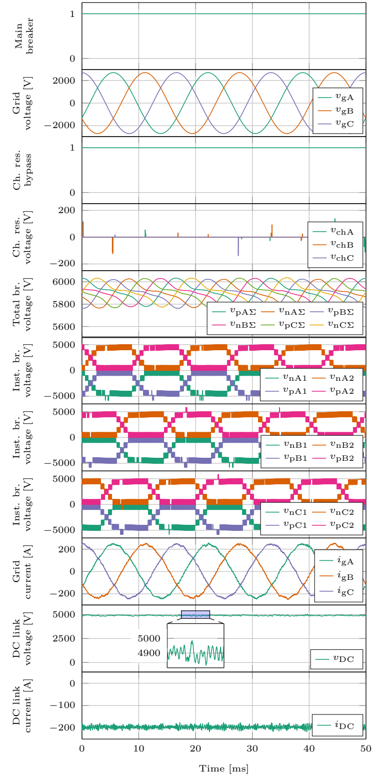

▲ Converter operation at full load ($P_{DC} = 1\text{MW}$)

RECORDED WAVEFORMS (III)

▲ Simulated converter param.

Rated power (S^*)	1MVar
Output voltage (V_{DC})	5kV
Grid voltage (v_g)	3.3kV
No. of SMs per branch (N)	6
SM capacitance (C_{sm})	3.36mF
Branch inductance (L_{br})	2.5mH
Brach resistance (R_{br})	60mΩ
PWM carrier frequency (f_{pwm})	1kHz
Fudamental frequency (f_o)	60Hz
Charging resistors (R_{ch})	210Ω

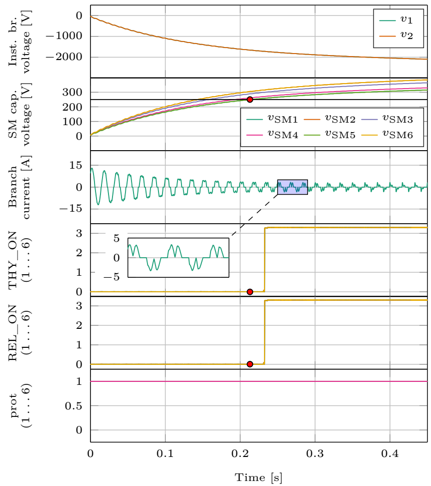

▲ Passive charging of a branch

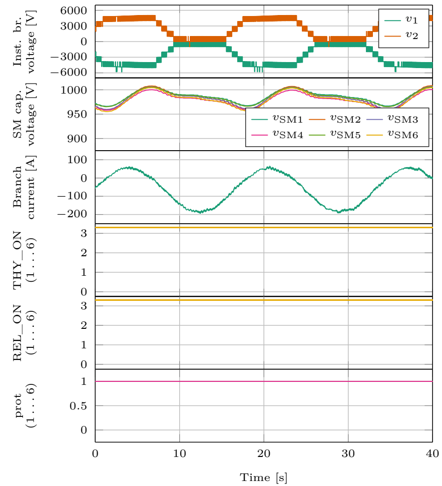

▲ Branch operation at full load

▲ Simulated converter param.

Rated power (S^*)	1MVar
Output voltage (V_{DC})	5kV
Grid voltage (v_g)	3.3kV
No. of SMs per branch (N)	6
SM capacitance (C_{sm})	3.36mF
Branch inductance (L_{br})	2.5mH
Brach resistance (R_{br})	60mΩ
PWM carrier frequency (f_{pwm})	1kHz
Fudamental frequency (f_o)	60Hz
Charging resistors (R_{ch})	210Ω

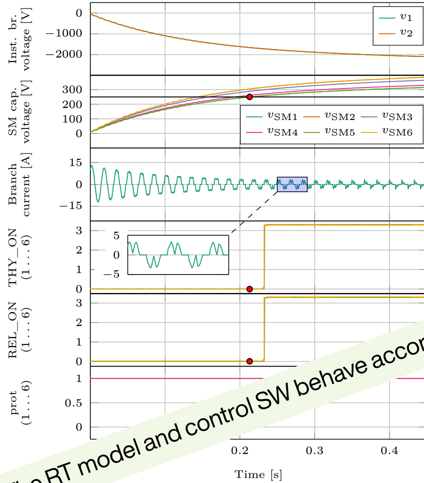

...sive charging of a branch

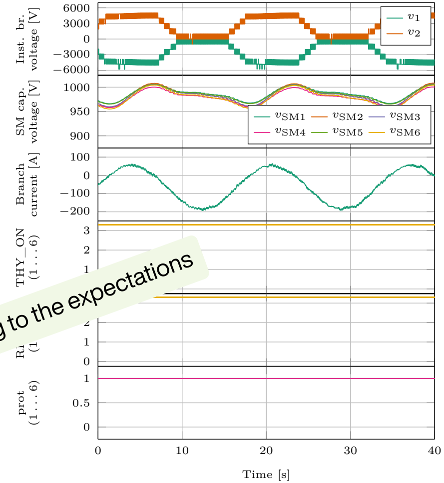

▲ Branch operation at full load

⇒ The RT model and control SW behave according to the expectations

MMC research platform

- Electrical and mechanical design
- Insulation coordination
- Control development
- Testing independently HW and SW
- RT-HIL modeling and development
- Achieving flexibility for various applications
- Supporting future research activities

▲ MMC - Actual mechanical assembly

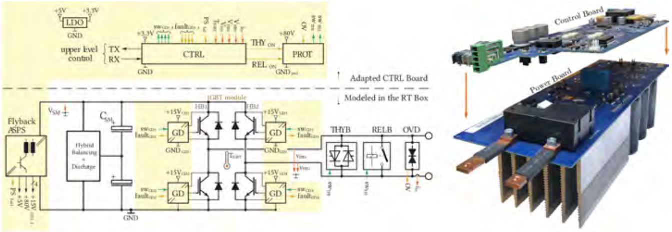

▲ PEL developed MMC sub-module

▲ Digital Twins - Four RT-HIL systems allowing for various topological reconfigurations

BIBLIOGRAPHY

[1] M. Utvić, S. Milovanović, and D. Dujić. “Flexible Medium Voltage DC Source Utilizing Series Connected Modular Multilevel Converters.” *2019 21st European Conference on Power Electronics and Applications (EPE '19 ECCE Europe)*. 2019, pp. 1–9.

[2] A. Christe and D. Dujic. “Galvanically isolated modular converter.” *IET Power Electronics* 9.12 (2016), pp. 2318–2328.

[3] A. Christe and D. Dujic. “Virtual Submodule Concept for Fast Semi-Numerical Modular Multilevel Converter Loss Estimation.” *IEEE Transactions on Industrial Electronics* 64.7 (July 2017), pp. 5286–5294.

[4] A. Christe, E. Coulinge, and D. Dujic. “Insulation coordination for a modular multilevel converter prototype.” *2016 18th European Conference on Power Electronics and Applications (EPE'16 ECCE Europe)*. Sept. 2016, pp. 1–9.

[5] I. Polanco and D. Dujic. “Thermal Study of a Modular Multilevel Converter Submodule.” *PCIM Europe digital days 2020; International Exhibition and Conference for Power Electronics, Intelligent Motion, Renewable Energy and Energy Management*. 2020, pp. 1–8.

[6] A. Christe et al. “Auxiliary submodule power supply for a medium voltage modular multilevel converter.” *CPSS Transactions on Power Electronics and Applications* 4.3 (2019), pp. 204–218.

[7] J. Muhlethaler, J. W. Kolar, and A. Ecklebe. “A novel approach for 3d air gap reluctance calculations.” *8th International Conference on Power Electronics - ECCE Asia*. May 2011, pp. 446–452.

THANK YOU FOR YOUR ATTENTION